B.R.1600A
Code No.1563
A.P.1093E(2)

Chapter 8

VALVE OSCILLATORS

List of Contents

CHAPTER 8

VALVE OSCILLATORS

INTRODUCTION

1. Uses of Valve Oscillators

Oscillators are required in radar for use in many different types of circuits, to generate at frequencies which vary from about 4 c/s in low-frequency switching circuits, to upwards of 10,000 Mc/s in certain equipments. Low frequencies are usually generated by relaxation oscillators, such as multivibrators or blocking oscillators. Radio-frequency generators, from a few kc/s to 50 Mc/s, employ tuned circuits, usually of the "lumped" L-C type, with conventional valves. For 50-500 Mc/s specially constructed triodes and pentodes are used, the tuned circuits usually taking the form of lecher lines or tuned lengths of coaxial cable; otherwise the circuit designs are essentially the same as for lower-frequency generators. Above 500 Mc/s, novel valves which succeed because of transit-time effects, such as Magnetrons and Velocity-Modulated tubes of the Klystron type, replace valves of conventional design; tuned circuits, frequently in the form of cavity resonators, are wholly or partly built into such valves.

Although this chapter considers the action of valve oscillators mainly from the aspect of CW operation, the results quoted are generally still applicable when the oscillator is used as a transmitter in a pulse radar system. The times taken for the RF pulse to build up and to die away are usually small compared with the interval during which steady oscillations are produced, so that analyses based on CW operation are justified. The shape and duration of the oscillator pulse has, however, a very important bearing on receiver design. A harmonic analysis of the pulse reveals that a certain number of frequency components must be handled adequately by the oscillator output circuits if a good pulse shape is to be produced. The bandwidth involved is termed the Frequency Spread. For example a 1 microsecond pulse would in practice have a frequency spread of at least 2 Mc/s. This would be diminished if the pulse duration were increased. (See Chap. 16 Sec. 2).

Although the modulating pulse has an important bearing on the frequency spread, other considerations, such as a poor rotating joint in the coupling circuit from transmitter to aerial, may also materially affect the output pulse shape. It is now general practice to examine the RF spectrum by means of a spectrum analyser, which is a super-heterodyne receiver whose local oscillator frequency is swept in synchronism with a CRO time base. The detected signals are fed on to the Y-plates to produce an amplitude-frequency spectrum of the components in the RF pulse.

2. Fundamental Requirements of a Valve Oscillator

Valve oscillators may generally be regarded as consisting of four component parts:-

(i) A source of energy.

(ii) A time-conscious circuit or frequency control device.

(iii) A synchronous energy-feeding device.

(iv) A load.

(i) is usually a DC power supply.

(ii) may be a resonant circuit or similar frequency-conscious device, such as a piezo-electric crystal or a phase-discriminating network. The time-conscious elements of a relaxation oscillator are of a different type, and these are dealt with in Chap. 10.

(iii) is normally a valve amplifier. The resonant circuit or other frequency-conscious device (ii) and the load (iv) dissipate energy, which must be provided for by an equivalent supply of energy from the power source (i).

Since (i) is a DC source and (ii) and (iv) constitute an AC load the power from (i) must be supplied at appropriate times, not only at the right frequency, but in the right phase with respect to successive cycles of oscillation. (This action corresponds closely to that of the escapement of a watch). The load, (iv) is an integral part of the oscillator and, in general, variations in its impedance will affect both frequency and amplitude of oscillations. Oscillators should therefore be designed so that the load is as little as possible affected by changes in the input impedance of any succeeding stage or other device. This can frequently be accomplished by inserting some form of buffer stage between the oscillator load and the output terminals. When this is done, changes in loading of the circuit as a whole affect the buffer stage only and do not disturb the loading of the oscillator to any appreciable extent. On the other hand, cases arise where the load is fed from the valve amplifier of the oscillator either directly or by coupling to the tuned circuit.

3. Conditions for Maintenance of Oscillations

The theory of oscillators is derived from that of their component parts, of which the resonant properties of tuned circuits and the amplifying properties of valves are of outstanding importance. In both cases the theory becomes complicated unless the alternating components of currents and voltages are assumed sinusoidal. For the derivation of initial conditions for self-maintenance of oscillations, these assumptions are valid; and, because of the relative simplicity of this method of analysis, useful criteria can be obtained which are serviceable in the design and adjustment of practical circuits.

For steady state conditions, however, this simple theory is unsatisfactory for the following reasons:-

(i) All valve characteristics are non-linear, and the initial conditions for the maintenance of oscillations are valid only for infinitesimal oscillations. In all practical cases the amplitude of oscillation is finite and is determined, among other things, by the curvature of the valve characteristics.

(ii) The curvature of the valve characteristics also necessarily results in distortion of the sinusoidal form of the current in the oscillatory circuit. In other words the production of harmonics is a necessary condition of self-maintained oscillations, and this affects the fundamental frequency of oscillation to some extent.

(iii) Apart from changes in the effective resistance and reactance of the valve due to non-linearity of the characteristics, the interelectrode capacitances, which are included in the total reactances of the system, are not constant with respect to either the mean electrode potentials or the amplitude of the alternating voltages.

These effects complicate accurate analysis, but overlooking them does not obscure the fundamental nature of the mechanism of oscillations.

In general, when the possibility of self-maintenance of oscillations is being considered in any circuit employing a negative-grid triode, a physical approach is often possible without detailed analysis, although this may be necessary as a last resort. To a first approximation the interelectrode capacitances C_{ga}, C_{gk} and C_{ak} of the valve may be considered as parts of the tuned circuit or circuits. The valve may then be replaced by a negative resistance, between anode and cathode. This is equivalent to assuming that anode and grid voltages are antiphase. Under these circumstances the frequency of oscillation does not depend on reactance effects of the valve current, and this is a desirable condition in most oscillators. When the valve is working in Class C, as in the case of power oscillators, the efficiency is liable to deteriorate considerably if the anti-phase relation is substantially departed from. In any case, if anode and grid potentials are separated by a phase difference of less than 90° the valve acts as a positive resistance, and not as a generator of oscillations. This effect is illustrated in Fig. 384. Vectorially, assuming sinusoidal variation,

$$\overrightarrow{i_a} = G_m \overrightarrow{v_g} + \frac{\overrightarrow{v_a}}{R_a} .$$

For the valve to act as a generator, ϕ, the angle between the current vector $\overrightarrow{i_a}$ and the voltage vector $\overrightarrow{v_a}$, must be greater than 90°. This is impossible either if $G_m v_g < \frac{v_a}{R_a}$, i.e., if $\mu v_g < v_a$, or if the phase difference between $\overrightarrow{v_a}$ and $\overrightarrow{v_g}$ is less than 90°.

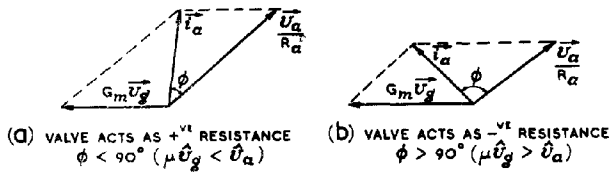

Fig. 384 - Regeneration criteria.

Valve oscillators may frequently be regarded as positive feedback amplifiers, and such circuits may be employed in non-oscillatory conditions. A common example is the reaction amplifier of Fig. 385, which has essentially the same circuit as that of the tuned grid oscillator discussed in Sec.4, but in which the coupling between anode and grid circuits is insufficient to cause self-maintenance of oscillations. The net effect is to increase the gain and selectivity (and the distortion) of the stage, without generating continuous oscillations.

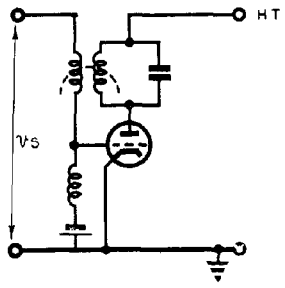

Fig. 385 - Reaction amplifier.

Another way in which the regeneration of the feedback circuit may be regarded is illustrated in Fig. 386. A damped oscillatory circuit (a) rings when a square pulse is applied, as shown at (b). If further resistance is placed in parallel with the condenser the decrement is increased; (c). If the equivalent of a negative resistance (regeneration, or positive feedback) is applied to the output terminals, the decrement is reduced; (d). If sufficient positive feedback is provided, i.e., if the magnitude of the negative resistance is small enough, stable oscillations are maintained; (e). Whilst if more than sufficient feedback is present the oscillations increase in amplitude until limited by the inherent non-linearity of the circuit; (f).

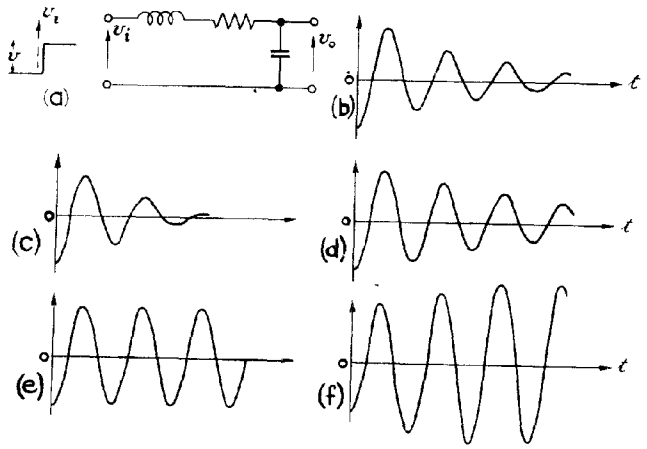

Fig. 386 - Effect of varying degrees of positive feedback on maintenance of oscillations.

OSCILLATORS EMPLOYING MUTUAL INDUCTIVE COUPLING

4. Tuned Grid Oscillator, Fig. 387

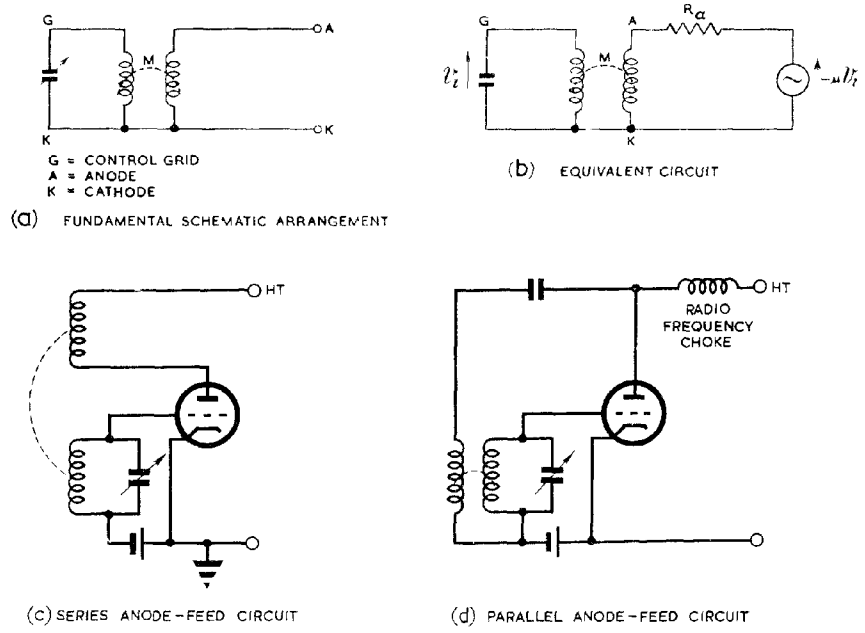

Fig. 387 - Tuned grid oscillator.

The fundamental arrangement is shown schematically at (a), and the equivalent circuit at (b). Feedback is provided by mutual inductive coupling M between anode and grid circuits. It may be shown that oscillations are maintainable at or near the resonant frequency of the tuned circuit. In this case the grid circuit is approximately resistive. If the anode circuit is also resistive, the condition for self-maintenance of oscillations is given by:-

$$M = \frac{1}{\omega_r Q G_d};$$ where Q is the selectivity-factor of the

tuned circuit, G_d the slope of the dynamic characteristic of the valve and $\omega_r = 2\pi f_r$, f_r being the resonant frequency of the tuned circuit, which is almost identical with f, the frequency of oscillations.

This relation, and those of a similar type applicable to other oscillators, are approximate only, and are based on sinusoidal oscillations of small amplitude under the simplest conditions. However, they provide an excellent guide to the modifications necessary to increase or decrease the likelihood of maintenance of oscillations.

Series and parallel anode-feeding arrangements are shown at (c) and (d).

5. Tuned Anode Oscillator, Fig. 388

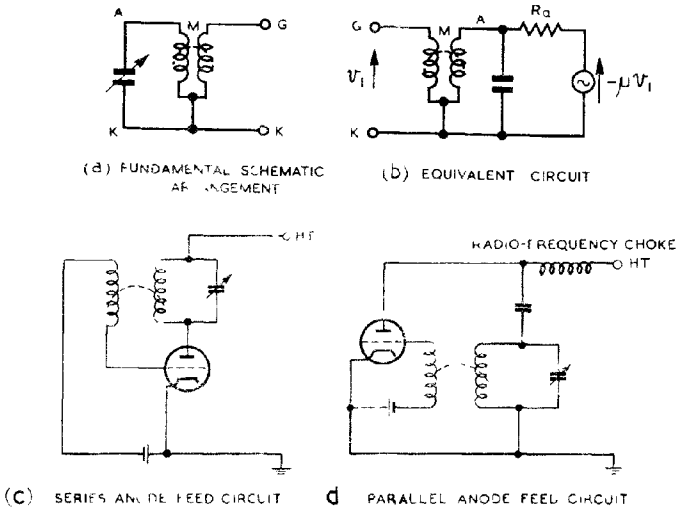

Fig. 388 - Tuned anode oscillator.

The fundamental arrangement is shown at (a) and the equivalent circuit at (b). The condition for self-maintenance of oscillations is the same as that for the tuned-grid circuit, and the modes of oscillation of the two circuits are very similar. Series and parallel anode-feeding arrangements are shown at (c) and (d).

6. Meissner Oscillator, Fig. 389

The fundamental arrangement is shown schematically at (a) and the equivalent circuit at (b). The condition for maintenance of oscillations is given approximately, in the simplest cases, by

$$\frac{M_a M_g}{L} = \frac{1}{\omega_r Q G_d}$$, where M_a, M_g, are the mutual inductances between the coil L of the oscillatory circuit and the anode and grid coils respectively, there being no other coupling between the anode and grid coils. The other symbols are the same as for the tuned grid oscillator.

As in the analysis of the other circuits employing mutual inductive coupling, it is assumed that the sense of the coupling is such as to induce at the grid a voltage in phase with the anode current.

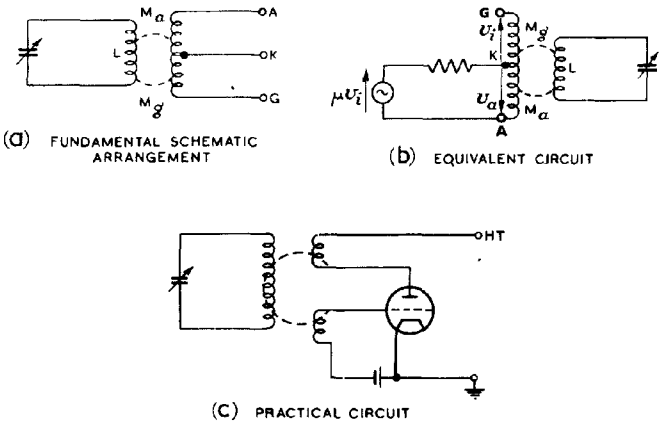

Fig. 389 - Meissner oscillator.

7. Magnetrostriction Oscillator, Fig. 390

This circuit is closely analogous to the Meissner, the tuned circuit being replaced by a mechanically resonant rod of magnetic material inserted as a core in the anode and grid coils. As the field due to the current in the coils alternates such a rod varies in length at a frequency double that of the oscillator (assuming the rod is not polarised). This variation in length sets up mechanical oscillations which have a pronounced resonance, the resonant frequencies being of the order of 5-50 Kc/s in practice. The frequency stability is very good and the oscillator serves as a low frequency equivalent of the crystal controlled oscillator for use as a frequency standard in the supersonic range.

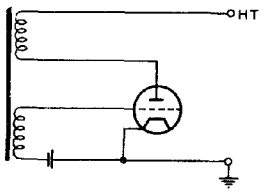

Fig. 390 - Magnetostriction oscillator.

OSCILLATORS EMPLOYING DIRECT COUPLING WITH A SINGLE TUNED CIRCUIT

8. Hartley Oscillator, Fig. 391

The fundamental arrangement is shown at (a) and the equivalent circuit at (b).

The requirement that the phase difference between anode and grid voltages should be greater than 90° is clearly met in this circuit provided high-Q components are used, and if resistances are neglected the ideal antiphase relationship is assured.

Under the simplest conditions, oscillations can be maintained provided $\frac{L_a L_g}{L_a + L_g} = \frac{1}{\omega_r^2 G_d}$, where G_d, ω_r and Q have their usual significance, and L_a and L_g are the inductances as indicated (the mutual coupling in this case is assumed to be negligible).

Because of the large impedance presented both at the grid and at the anode of the valve by the tapped-L arrangement at frequencies above resonance, this oscillator usually provides a high harmonic content.

Various series and parallel circuits are shown at (c) (d) and (e).

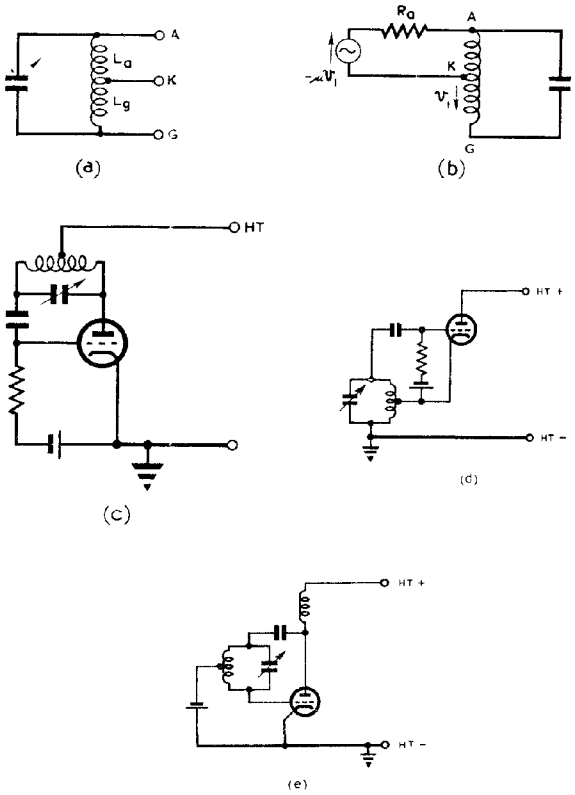

Fig. 391 - Hartley oscillator.

9. Colpitts oscillator, Fig. 392.

The fundamental arrangement is shown at (a) and the equivalent circuit at (b).

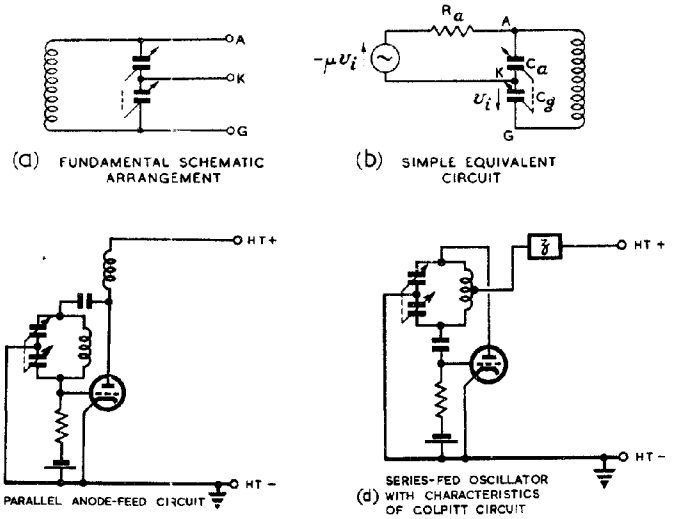

Fig. 392 - Colpitts oscillator.

This oscillator is analogous to the Hartley with the coils and condenser interchanged. It possesses good frequency stability, and is usable at higher frequencies than the Hartley circuit since stray capacitances, particularly C_{gk} and C_{ga}, are in parallel with the tuning capacitances, and thus do not upset the mode of oscillation.

Assuming the simplest circumstances, the condition for self-maintenance of oscillation may be written:-

$$G_d = \frac{\omega_r (C_a + C_g)}{Q}$$, where G_d, ω_r, Q have their usual significance and C_a and C_g are the capacitances as indicated in the figure.

The output is largely free from harmonics, since the tuned circuit presents a low impedance at both grid and anode for frequencies above the fundamental resonant frequency.

Practical circuits are shown at (c) and (d). There is no true series arrangement, but the circuit shown at (d) possesses the characteristics of a Colpitts oscillator, although the mode of oscillation is slightly more complex. The additional impedance z, usually an RF choke or small resistance, is necessary to prevent interference from the Hartley mode of oscillation. Without it oscillations may be impossible.

10. Dynatron Oscillator, Fig. 393

This is the simplest form of oscillator, requiring only two connections from the valve to the tuned circuit,(a). It relies for its mode of operation on the negatively-sloping portion of the $I_a - V_a$ characteristic of a tetrode, (b). Over this region the valve acts as a negative resistance, and, provided the magnitude of this resistance is less than the dynamic resistance of the tuned circuit in parallel with it, oscillations are maintained.

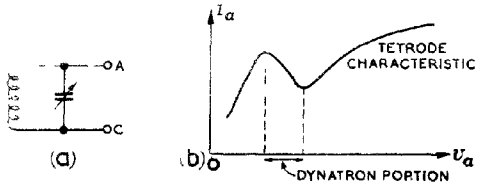

Fig. 393 - Dynatron oscillator.

11. Transitron Oscillator, Fig. 394

This type of circuit is more frequently employed as a relaxation oscillator or relay, and as such it is dealt with in Chap. 10. In essence, however, it has characteristics which are closely allied to those of the dynatron oscillator, and it may be used as a generator of sinusoidal oscillations.

The basis of operation of transitron circuits is discussed in Chap. 6 Sec. 34.

For certain values of anode and control grid potentials an increase in screen voltage gives rise to an increase in suppressor grid voltage which increases the anode current; this increase is drawn from the available space current, and, provided the mean potentials of the various electrodes are suitably chosen, is greater than the increase in space current due to the rise in screen voltage.

The net result is a decrease in screen current, so that the output resistance between screen and cathode is negative, (b). It may be convenient to use the control grid for triggering, as shown at (c). The valve oscillates while the input pulse holds the grid voltage above cut-off, the frequency being almost exactly that of the tuned circuit, assumed to incorporate the parallel stray capacitances present. After the grid potential falls below cut-off, oscillations die out, the time taken depending on the decrement of the circuit.

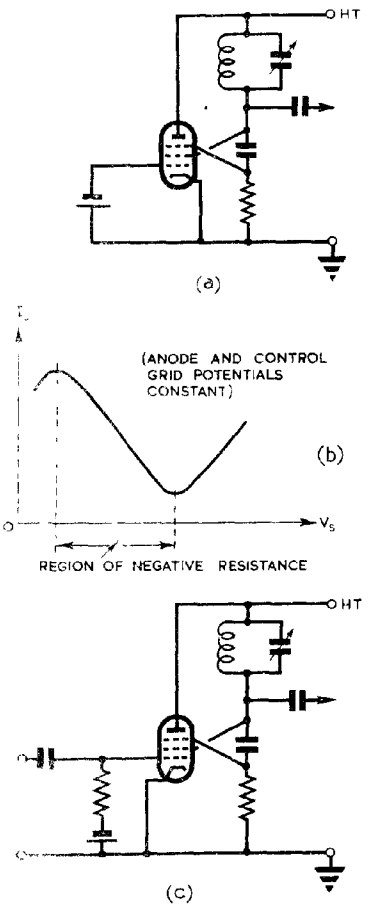

Fig. 394 - Transitron oscillator.

OSCILLATORS EMPLOYING DIRECT COUPLING WITH TWIN TUNED-CIRCUITS

12. General

The fundamental arrangement is shown schematically in Fig. 395(a). In such a circuit with loss-free components, oscillations can be generated under conditions which make the reactance of the coupling condenser C_c equal and opposite to the reactance of the two rejector circuits connected in series. For high-Q circuits any such oscillations would be damped out eventually, but would occur at substantially the same frequency as in the loss-free case.

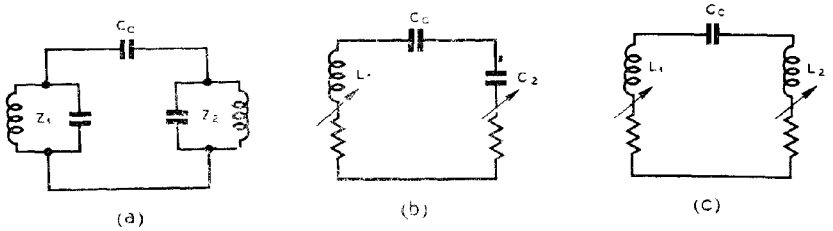

Fig. 395 - Compound oscillatory circuit.

At the oscillation frequency either one or both of the tuned circuits must be inductive, as shown at (b) and (c) respectively. The corresponding oscillation frequencies are then given sufficiently accurately by:-

(b) $f = \dfrac{1}{2\pi\sqrt{\dfrac{L_1 C_c C_2}{C_c + C_2}}}$ and (c) $f = \dfrac{1}{2\pi\sqrt{C_c\,(L_1 + L_2)}}$.

(The position of the arrows in Figs. 395(b) and (c) indicates that both of the series components of the impedance, the resistance and the reactance, are varied by adjustment of the corresponding tuned circuit of Fig. 395(a)).

By suitably connecting valve amplifiers to the networks of Fig. 395 the oscillations can be maintained. Figs. 396(a) and (b) show the types of vectorial relations one of which must apply to these circuits to permit a phase difference between anode and grid potentials relative to cathode of greater than 90°. The valve, acting as a generator between anode and cathode, makes the combined resistive component of the anode-cathode circuit negative; this is indicated in the vector diagrams by the word (Regenerative).

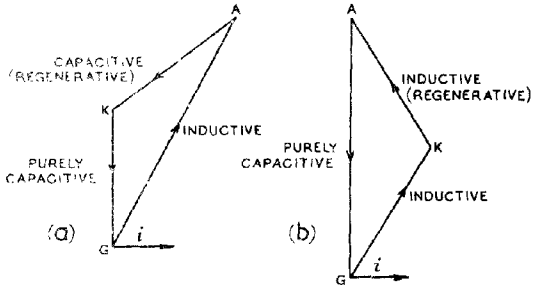

Fig. 396 - Twin circuit oscillator: vector diagram.

It follows that there are two arrangements of Fig. 395(a) which conform to Fig. 396(a) and one which conforms to Fig. 396(b); these are illustrated as equivalent circuits in Fig. 397(a), (b) and (c) respectively. They are classified as shown, according to the electrode which is common to the two tuned circuits.

The common cathode circuit is less useful than the others

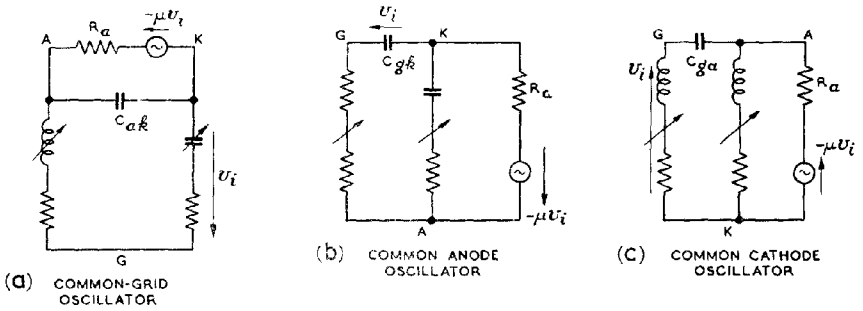

Fig. 397 - Twin circuit oscillator: equivalent circuits.

for very high frequency work because of the magnitude of the inter-electrode capacitance C_{ga}. This limits the oscillations to frequencies whose upper limit is of the order of a few hundred megacycles per second. Either of the other arrangements is capable of producing oscillations with normal triode valves up to 600 Mc/s, and with specially designed triodes up to 3000 Mc/s.

Common to all oscillators of this type is the advantage of having twin controls over the frequency and amplitude of oscillations. By suitable adjustment of the tuning controls both the amplitude and

frequency may be set to any desired values within the working range.

The mode of oscillation is similar to that of the Hartley oscillator in the circuit of Fig. 397(c) and to that of the Colpitts in circuits (a) and (b). In all cases, however, a much greater tuning range is available in the twin-circuit oscillator.

For a rejector circuit to be inductive it must be tuned to a frequency above the frequency of oscillation, and below if it is to be capacitive. Hence in the common cathode circuit the frequency of oscillation is below the resonant frequencies of both tuned circuits, whereas in the other cases it is intermediate between these two.

The behaviour of these oscillators may best be described in forms of modified circuits. Each tuned circuit is associated with certain components in parallel, the phase angle ϕ of the resultant circuit being a function of the selectivity and resonant frequency of the resultant circuit, and of the frequency of oscillation. It may be shown that, provided certain assumptions are justifiable, oscillations can be maintained at such a frequency that the resultant circuits are either both inductive or both capacitive, and the sum of these phase angles in each case is approximately 90°. Maximum amplitude occurs when both circuits are equally detuned, i.e. both phase angles are 45°. This occurs despite the fact that, as indicated in Figs. 397(a) and (b), one of the original tuned circuits may be inductive when the other is capacitive. This is because in these figures the addition of extra components for the purpose of simplifying the analysis has not been made.

13. Common-Cathode Oscillator

In this oscillator, the anode tuned circuit is associated with R_a, C_{ga} and C_{gk} in parallel, as shown in Fig. 398(a). The resonant frequency of this combined circuit is f_a and its phase angle

Fig. 398 - Common-cathode oscillator: effective tuned circuits.

when the oscillation frequency is f is ϕ_a (inductive). The grid tuned circuit is associated with C_{gk} and C_{ga} in perallel, as shown at (b). The resonant frequency of the resultant circuit is f_g and its phase angle is ϕ_g (inductive). The results

(1) $\phi_a + \phi_g \simeq 90^{\circ}$ and

(2) amplitude increases with sin $2\phi_a$ (which is equal to sin $2\phi_g$)

depend upon the condition $G_m \gg \omega C_{ga}$.

14. Common-Anode Oscillator

In this arrangement, the grid tuned circuit is associated with C_{ga} and C_{gk} in parallel, whilst the cathode tuned circuit has the additional parallel components C_{ak}, C_{gk}, R_a and the resistance $\frac{1}{G_m}$ as shown in Fig. 399(a) and (b). It follows from the diagram of Fig. 397(b) that the addition of C_{gk} to the circuit between G and A changes

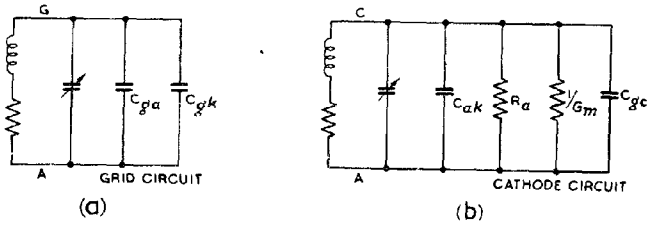

Fig. 399 - Common-anode oscillator: effective tuned circuits.

this circuit from inductive to capacitive; this gives a good indication of the frequency of oscillation. The results

(1) $\phi_g + \phi_k \fallingdotseq 90^\circ$; (both ϕ_g and ϕ_k are capacitive) and

(2) amplitude increases with sin $2\phi_g$; (which is equal to sin $2\phi_k$);

depend upon the condition $G_m \gg \omega C_{gk}$.

15. Common-Grid Oscillator

In this case the anode tuned circuit is considered in parallel with C_{ag} and C_{ak}, and the cathode tuned circuit has the additional

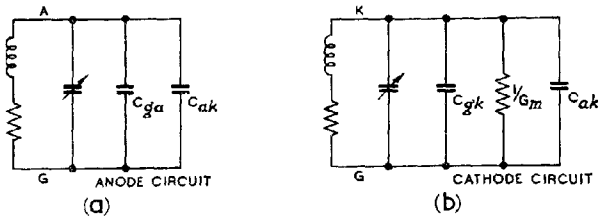

Fig. 400 - Common-grid oscillator: effective tuned circuits.

parallel components C_{ak}, C_{gk} and the resistance $\frac{1}{G_m}$, as shown in Fig. 400(a) and (b). As in the previous case, the addition of C_{ak} to the circuit between anode and grid changes the impedance from inductive to capacitive, so that the frequency of oscillation lies between the resonant frequencies of the two circuits, with and without C_{ak}.

The results (1) $\phi_a + \phi_k \fallingdotseq 90^\circ$ (both ϕ_a and ϕ_k are capacitive)

and

(2) amplitude increases with sin $2\phi_a$ (which is equal to sin $2\phi_k$);

depend on the conditions $G_m \gg \omega C_{ak} \gg 1/R_a$.

16. Earthing the Twin-Circuit Oscillators

Owing to the earth capacitance of the various electrodes, these oscillators exhibit different properties for different earthing

arrangements. The anode is usually large and the stray capacitance to earth correspondingly high. Similarly, the necessity for the heaters to be close to the cathode tends to make the cathode-earth capacitance large.

In the common-cathode circuit it is usual to earth the cathode since this has least effect on the total capacitance between anode and grid. In the common-anode circuit either the cathode or anode may be earthed, but not the grid, as this effectively increases the coupling capacitance C_{gc} and also lowers the resonant frequency of the inductively tuned circuit. Both effects tend to lower the frequency of oscillation.

In the common grid oscillator, efficient oscillations may be obtained by earthing any of the electrodes. One arrangement, known as the Lighthouse Tube circuit, is of the common-grid, earthed-cathode type, and has given satisfactory performance at centimetre wavelengths. Valves with common-grid, earthed-grid circuits have also given good results. For high-power operation, where anode dissipation is considerable so that special precautions must be taken for cooling the anode, the common-grid, earthed-anode circuit is likely to be most useful.

17. Types of Tuned Circuits Employed

When a twin circuit oscillator is employed as a radar transmitting valve or as a local oscillator at frequencies of 200 Mc/s or more, the tuned circuits usually take the form of coaxial lines, and the valve is designed to fit on to a special coaxial assembly. Such an

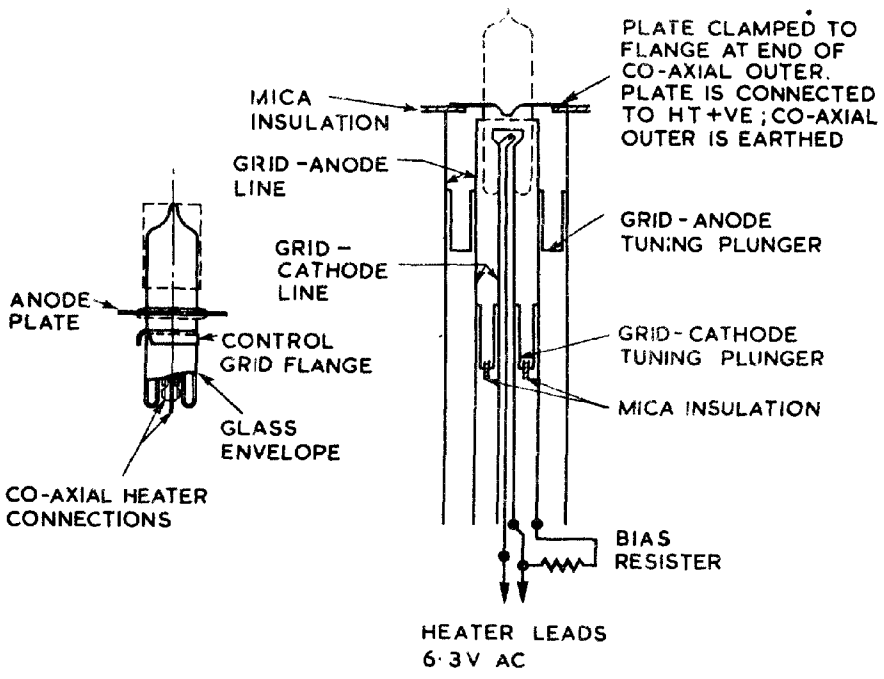

Fig. 401 - Negative-grid oscillator for centimetre wavelengths (CV 90).

arrangement is illustrated in Fig. 401. This shows a CV90 valve and the method of employing it as a common-grid oscillator. The anode is in the form of a flat plate sealed off on both faces from the glass envelope, and is suitable for clamping on to the end of a coaxial line system. The grid and heater connections are designed to fit various sections of coaxial tubing, the heater supply leads also being of coaxial construction. Anode-grid and grid-cathode lines are variable by means of plunger tuning. The anode is directly connected to the positive HT line, being insulated from the earthed outer of the coaxial line by a mica washer.

The valve, which measures 8·5 cm x 2·5 cm (neglecting the width of the anode plate) is capable of providing an RF output of 3 watts at 1000 Mc/s for an anode input of 10 watts. This output is reduced for higher frequencies, but by the use of harmonics the frequency can be raised to 5000 Mc/s, with an output of 0·1 watts. It may be used as a local oscillator or as a low-powered transmitter.

For lower frequencies conventional triodes with tuned open-wire lecher lines may be employed. (See Chap. 4 Fig.147).

18. Crystal-Controlled Oscillators, Fig. 402.

Because of their excellent frequency stability, piezo-electric crystals are often employed in place of tuned circuits in oscillators of the twin-circuit type. The frequency is limited to a few megacycles, so that the magnitudes of the interelectrode capacitances are not of any great importance in determining which of the circuits should be used. Both the common-anode and the common-cathode arrangements shown in Figs. 402(a) and (b) are employed. In either

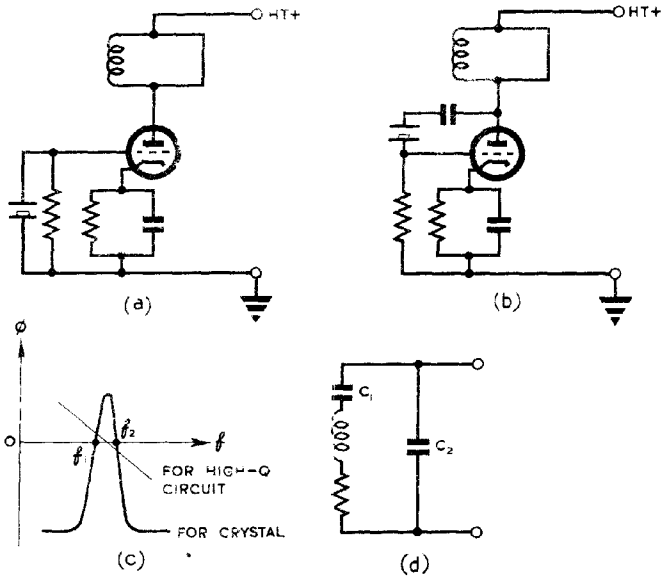

Fig. 402 - Crystal oscillator.

circuit the crystal must present an inductive impedance to the rest of the circuit for oscillations to be possible. Fig. 402(c) shows the variation of ϕ, the phase angle, for a typical piezo-electric crystal, and (d) shows the equivalent circuit. ϕ can be positive only between the frequencies f_1 and f_2; hence oscillations can occur only at a frequency greater than f_1 and less than f_2. These limiting frequencies lie very close together, due to the fact that $C_2 \gg C_1$.

As indicated in the figure, $\emptyset$ alters very little over this range for the comparable case of a high-Q L-C circuit, which must therefore be considered less desirable in maintaining frequency stability.

Again, as $C_2 \gg C_1$, the effect of the external connections on the Q of the circuit, and on f_1 and f_2 is negligible.

For accuracies of the order of one part in a million or better the crystal should be kept at a uniform temperature by enclosure in a thermostatically controlled oven.

19. PUSH-PULL CIRCUITS, Fig. 403

The use of twin valve circuits symmetrically arranged makes the design of oscillators extremely simple. The anode and grid potentials of a conventional amplifier are normally antiphase; by connecting each anode to the grid of the other valve, the output of each valve provides the input for the other, in the correct phase for oscillations to be self-maintained. This is the essence of the multivibrator circuit described in Chap.10. A similar circuit may be used to generate RF oscillations. The fundamental arrangement is shown schematically at (a) and a practical circuit at (b).

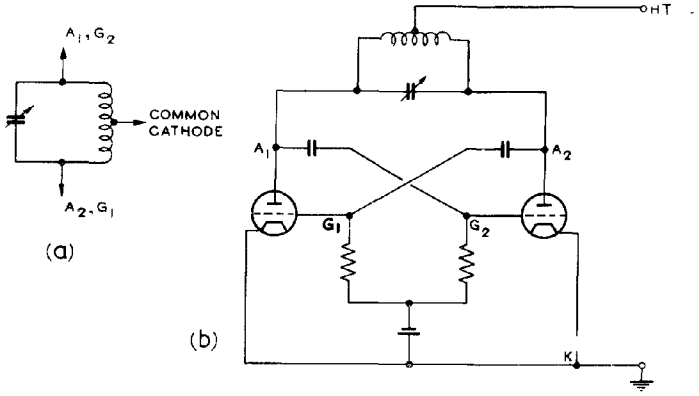

Fig. 403 - Push-pull circuit.

Push-pull circuits possess certain advantages over single-valve oscillators. Provided they are properly balanced, there are no even harmonics present in the output waveform. This conserves power and reduces interference with other transmitters. Since one electrode of each valve is connected to the corresponding electrode of the other, at least as far as radio frequencies are concerned, the interelectrode capacitances associated with this electrode and the tuned circuit are in series and the resultant effect on the tuned circuit is thereby halved. In the circuit shown at (b), for instance, the effective capacitance in parallel with the tuned circuit between the two grids is $\frac{C_{gk}}{2}$ where C_{gk} is the interelectrode capacitance between grid and cathode for either valve. This effect is nullified at very high frequencies, where the inductance of the cathode leads becomes of equal importance to the interelectrode capacitances. The doubling of this inductance in the push-pull circuit then destroys the advantage obtained by halving the capacitance.

20. RESISTANCE-CAPACITANCE OSCILLATORS, Fig. 404

A resistance-loaded, capacitance-coupled amplifier (a)

normally operates over the flat portion of its gain-frequency characteristic, where the phase difference between input and output is 180°. Over this region, neither gain nor phase is frequency-conscious. At low frequencies where the reactance of the coupling condenser is large enough, the gain falls off, and the phase of the output is advanced as illustrated in the vector diagram at (b). A similar falling-off of gain, accompanied by a phase lag, occurs at high frequencies due to the shunt reactance of the input capacitance of the succeeding stage and sundry strays. This is illustrated at (c).

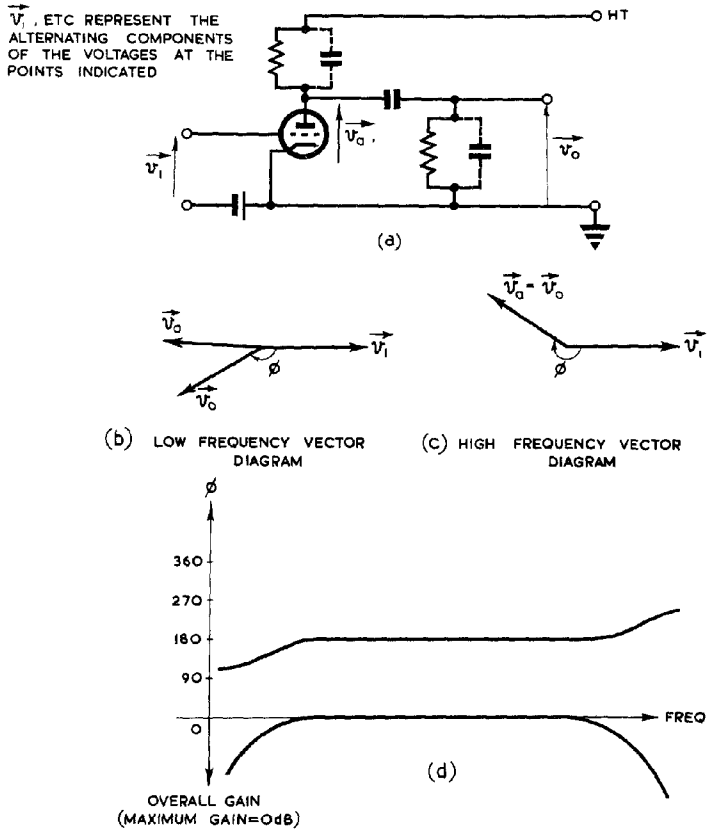

Fig. 404 - R-C oscillator.

The overall gain-frequency and phase-frequency characteristics of a typical R-C amplifier are shown in Fig.404(d).

If two or more such amplifiers are used in cascade, the total phase shift is obtained by adding the individual phase shifts for the separate circuits. For example, if f_{120} is the frequency at which the input of each valve leads the output by 120°, the total phase-shift for three identical stages in cascade would be 360°. The output of the third stage would then be in phase with the input of the first, and if the output were coupled to the input a 3-valve oscillator of frequency f_{120} would be formed.

The corresponding two-valve circuit is not frequency discriminating over the linear portion of the valve characteristics, since the phase-shift of 180° per stage occurs over the flat portion of Fig. 404(d). Such a circuit usually works as a multivibrator, described in Chap. 10, and not as a generator of sinusoidal oscillations.

The number of valves required for sinusoidal R-C oscillator may be reduced by the insertion of additional phase-shift meshes. Since the frequencies involved are usually low, it is normal to employ R-C rather than L-C networks, because of the prohibitive size of the latter when designed for use at these frequencies. A three-stage network such as that shown in Fig. 405(a) could be designed to operate with an amplifier providing 180° phase-shift. For oscillations to be maintained, the network would have to provide an additional 180° phase shift, whilst not introducing more attenuation than the available amplification.

The relative magnitudes of the components may be obtained by solution of the mesh equations for the circuit of Fig. 405 (b).

Let G_m = mutual conductance of valve

R_a = anode slope resistance of valve

$R = \dfrac{R_a R_L}{R_a + R_L}$

Then one condition for maintenance of oscillation is :-

$$G_m \geqslant \frac{23}{R} + \frac{29}{R_1} + 4\,\frac{R_1}{R^2}$$

and the frequency of oscillation f is :-

$$f = \frac{1}{2\pi\, CR\, \sqrt{6 + 4\,\frac{R_1}{R}}}$$

If a high-slope pentode is used the following simplifying assumptions may be made:

$$R_a \gg R_L \quad , \quad R \gg R_L,$$

and the above formulae reduce to

$$G_m \geqslant \frac{29}{R_L}$$

$$f = \frac{1}{2\,CR\sqrt{6}}$$

The attenuation of the phase-shifting network is 29, hence the available amplification will need to be at least 29.

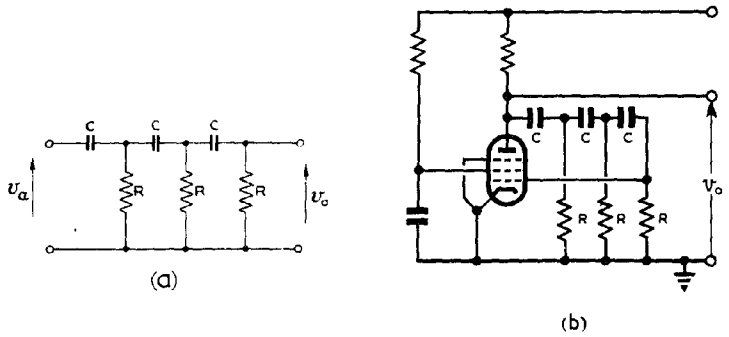

Fig.405 - Single valve, three-mesh oscillator.

The three-mesh network may be replaced by a four-mesh circuit. This reduces the network attenuation and enables a lower gain amplifier to be used. Either C or R of one or more of the meshes may be made variable for the oscillator to be tunable.

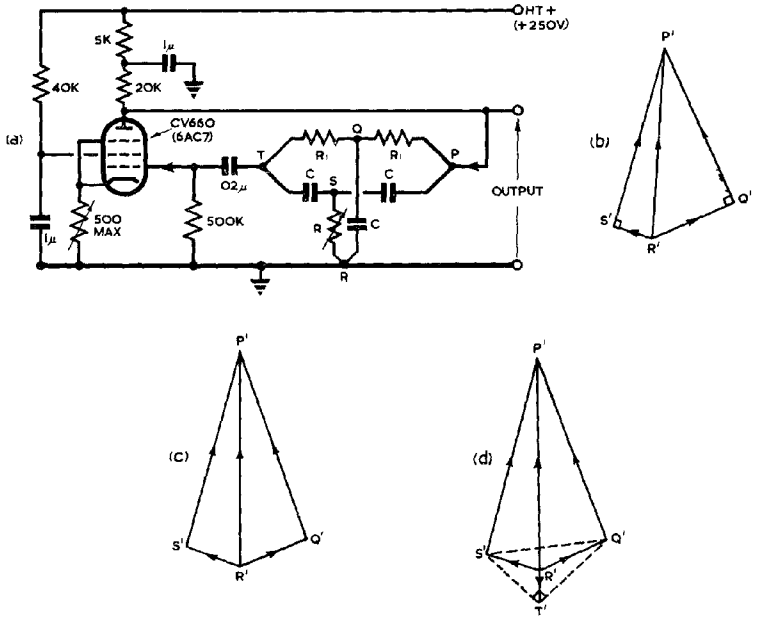

Fig.406 - Wien bridge oscillator

Such a resistance-capacitance oscillator must operate in Class A for the output voltage to be reasonable sinusoidal. The bias is therefore usually provided by a cathode self-biasing network, since the disadvantages of this method of biasing do not arise under Class A working conditions.

A second form of R-C oscillator is shown in Fig. 406(a). The phase-discriminating feedback circuit takes the form of a Parallel-T (Twin-T) network which is very sensitive to frequency changes. The vector diagrams of Figs.406(b) - (d) illustrate the action. If the series arms QT, TS of the T's are omitted the voltages for the remaining four elements are as shown at (b). The insertion of QT and TS distorts the right angles as shown at (c). The complete voltage distribution is given by (d) and the frequency of operation is such that T'R' and R'P' are collinear; i.e. that the anode and grid potentials are antiphase (with respect to cathode).

Typical component values for an 800 c/s oscillator are:-

R_1 = 100 K Ω

R_2 = 25 K Ω variable

C = 0.003 μF

Frequency is conveniently controlled by varying R_2 whilst amplitude may be preset by varying the cathode feedback resistor.

A third type of R-C oscillator, known as the Willan's Oscillator, is shown in Fig. 407. This is sometimes known as the Wien Bridge Oscillator on account of the resemblance of the phase-discriminating circuit PQR to the adjacent arms of a Wien Bridge. If the phase angle of the impedances between PQ and QR are equal, the voltage across QR will be in phase with that across PR. The condition for equality of phase angle is

$$\frac{1}{\omega C_1 R_1} = \omega C_2 R_2$$

which gives f the oscillation frequency as

$$f = \frac{1}{2\pi\sqrt{C_1 C_2 R_1 R_2}}$$

Since the output voltage from the phase discriminating network is in phase with the input a two-stage amplifier is needed to maintain oscillations.

The frequency may be varied either by making R_1 and R_2 variable and ganging them, or by a similar ganging of C_1 and C_2.

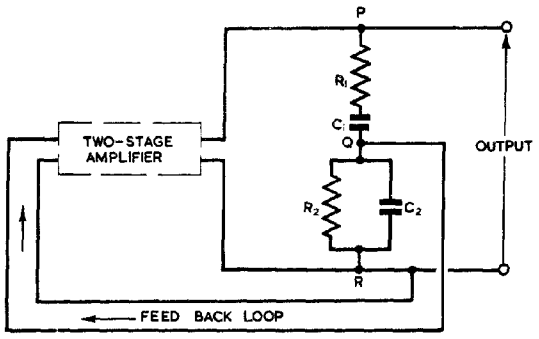

Fig.407 - Principle of Willan's Oscillator

VELOCITY MODULATED OSCILLATORS

21. General

Conventional valves are limited in their uses at UHF by the effects of transit time, reactance of electrodes and electrode leads, etc. (see Chap. 7 Secs. 25 and 26). While considerable success in minimising them has been achieved with specially constructed triodes,

having small electrodes very closely spaced, other types of valves which have utilised some of these effects have come into common usage. These depend for their mode of operation on variation of the velocities of the electrons (Velocity Modulation), instead of the total valve current (Density Modulation), as in conventional valves. Tubes employing this principle of velocity modulation must be hard, high-voltage tubes, so that the transit time for the passage of an electron through the modulating region is small enough to be comparable with the period of oscillations. The modulation depth is normally small, so that fluctuations at the high voltage end do not appreciably affect the initial velocity. This is analogous to the operation of a screened-grid valve, where variations in anode potential have little effect on grid modulation. Such a circuit is necessarily inefficient, since the tube current is largely DC, and the "anode" voltage is approximately constant, so that the power generated by the small AC components is at best only a few per cent of the total power dissipated. High efficiencies are obtainable only by modes of operation which are relatively complex, the description of which is beyond the scope of this work.

In practical velocity-modulated tubes the tuned circuits are normally of the resonant-cavity type, and are partly or wholly built into the valve envelopes. For simplicity they will be represented in the following sections as lumped circuits, and practical designs will be dealt with later.

22. Velocity Modulated Amplifier

Fig. 408 shows the basic velocity modulation circuit. An electron gun similar to that of a CRT projects a high velocity electron beam through an aperture in the plates of a condenser across which is developed an alternating field. The distance between the plates is assumed, in the first instance, to be small, so that the transit time between them is negligible; this will be considered in further detail later. When the resultant field is in one direction the beam is accelerated, and when in the opposite direction, retarded. Thus, after passing through the aperture of the first tuned circuit, or Buncher, the velocity of the beam is modulated, and the faster moving electrons tend to overtake the slower ones, so that Bunching occurs in the Drift Space; (Fig. 408).

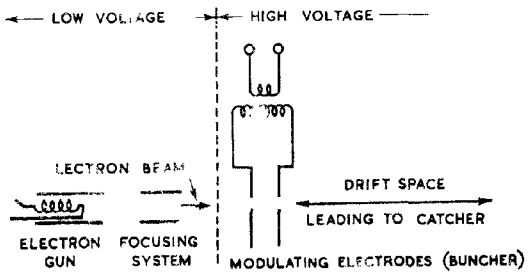

Fig. 408 - Velocity modulated circuit; schematic diagram.

The effect is illustrated in Fig. 409. For simplicity it is assumed that the modulation of velocity is sinusoidal, the field of the buncher imparting to the steady velocity u_o a deviation velocity $u_d = \hat{u}_d \sin 2\pi ft$. $100\,\frac{\hat{u}_d}{u_o}$ is the percentage modulation depth. The resultant velocity $u = u_o + u_d$ will be referred to as the Drift-Space Entry Velocity, or simply the Entry Velocity. The instant at which a "snapshot" of the electron beam distribution is taken is denoted by t, and t_o is the instant at which the electron under consideration entered the drift space. At (a), u is plotted against $t - t_o$ for the case where $\sin 2\pi ft = 0$; i.e., $t = 0 + nT$ where $T = \frac{1}{f}$. At (b) the distance s which the electrons have travelled into the drift space is plotted against $t - t_o$. Thus (a) gives the entry velocity and (b) the shapshot distribution at the instant t, the

interval $t - t_o$ being the time spent in the drift space by the electron considered.

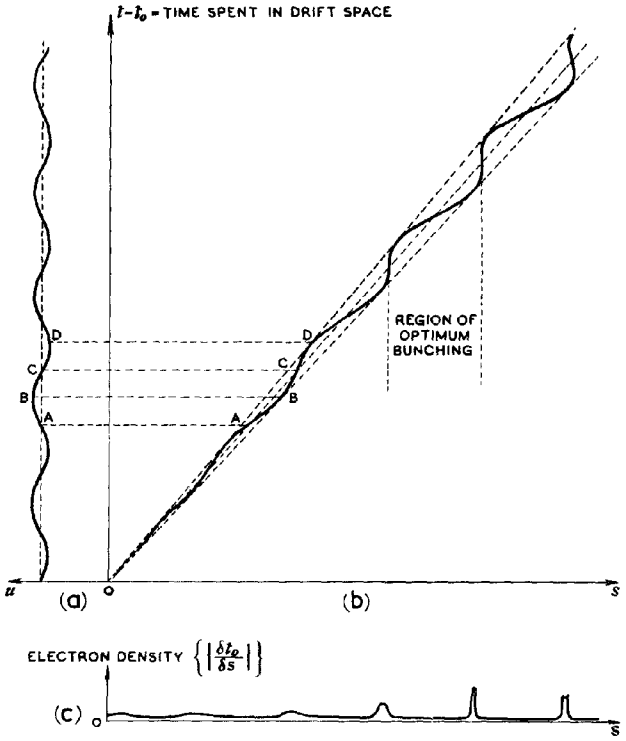

Fig. 409 - Drift space entry velocity and charge distribution ($t = nT + 0$).

The entry velocity of electrons emerging at instants A and C of Fig. 409(a) is u_o, corresponding to the line OAC $[s' = u(t - t_o)]$ in Fig. 409(b). At B the entry velocity has a maximum value, $u_o + u_d$, corresponding to the line OB $[s = (u_o + \hat{u}_d)(t - t_o)]$, whilst at D the entry velocity is a minimum, corresponding to OD $[s = (u_o - \hat{u}_d)(t - t_o)]$. The position of an electron entering the drift space at any instant t_o for which $\sin 2\pi f(t)$ has any value other than 0 or ± 1 may be found by sinusoidal interpolation between the three constant-velocity lines OB, OA, OD. It is assumed that the electron distribution along the axis $t - t_o$ is uniform, i.e. that equal numbers of electrons are emitted in equal intervals of time. The dispositions of these electrons are given by graph (b) for $\sin 2\pi ft = 0$, and the ratio $\left|\frac{\delta t_o}{\delta s}\right|$ (Fig. 409(c)) gives the mean electron density for the region of length δs. In the figure, δt_o is taken as one twelfth of the period T.

Curves similar to those of Fig. 409(b) may be plotted for the instants $t = \frac{T}{4}, \frac{T}{2}, \frac{3T}{4}$, and these are shown in Fig. 410(a). The corresponding line distributions are at (b), (c) and (d). These figures show how the bunches are formed by the faster-moving electrons overtaking the slower ones, the bunches moving at approximately the mean beam velocity u_o, so that they are separated by a distance $s \simeq u_o T$.

The regions in Fig. 410(a) where $\frac{\delta s}{\delta t_o} = 0$ are sometimes called Bunching Planes. These corresponding to maximum peaking effect in the line distribution diagrams (b), (c) and (d). It should

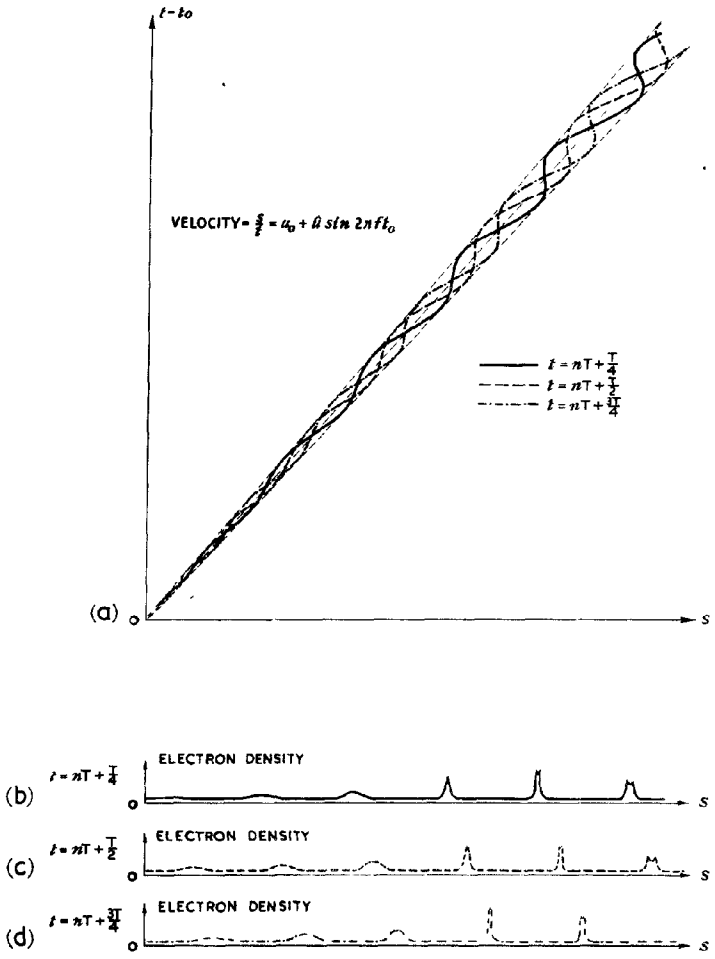

Fig. 410 - Drift space charge distribution for different values of t.

be obvious, however, that bunching is not confined to these particular regions, but occurs in varying degrees at all points of the drift space.

The effects illustrated are modified in practice by the following considerations which have been ignored in the simple diagramatic treatment.

(i) The entry velocity does not vary sinusoidally with time. This does not affect the principle of the method, as the sinusoidal form of Fig. 409(a) may be replaced by any other, and the process applied in the same way.

(ii) Acceleration is not instantaneous, occurring at a point, but takes place over a period of time comparable with T; one effect of this is that there may be some density modulation present which cannot be accounted for by velocity modulation only.

(iii) There is mutual repulsion between the electrons of the beam. This is usually a second order effect.

The manner in which modulation occurs merits further detailed

consideration, as it is fundamental in many centimetre-wave generators. An idealised modulating element is shown in Fig. 411 illustrating the instantaneous distribution of the electric field; the corresponding distribution of axial potential is shown in Fig. 412(a). It has been assumed that the region outside the plates is devoid of alternating fields; this is signified by the O - O lines within which these fields must be confined. Accordingly, whatever rise in potential occurs along the axis at any instant must be offset by a corresponding fall before the outside is reached. From energy considerations, it follows that an electron which instantaneously passes axially through this field meets with no net acceleration or retardation.

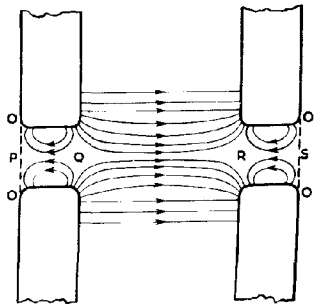

Fig. 411 - Instantaneous field distribution within the buncher gap.

Suppose, on the other hand, that the time of transit of the electron is comparable with the periodic time of the modulating voltage. Some electrons enter the region with the potential distribution as at (a), being accelerated from P to Q. By the time they pass Q, the direction of the field may have changed to that shown at (b), so that the electrons are further accelerated for the journey Q - R. Provided the distance QR is approximately $\frac{u_o}{2f}$, the field will again reverse when the electrons are in the region of R, so that the final stage of the motion, from R to S, is again accelerating.

Electrons which are a quarter-period ahead of these reach Q when the potential there is a maximum, and encounter a retarding field as they approach the centre. At this point the field everywhere is zero, and the electron velocity is again u_o. The second half of the transit is a repetition of the first half, the electrons being accelerated until they reach R, at which point the potential is a maximum, and retarded from R to S, being ejected with velocity u_o.

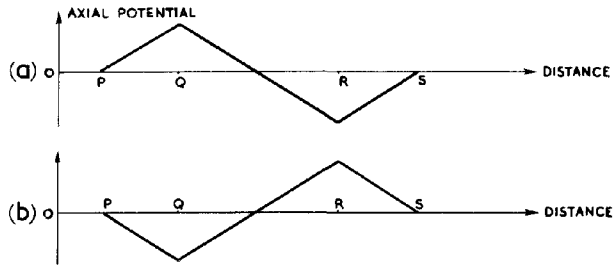

Fig. 412 - Instantaneous potential within the buncher.

Electrons which are a half-cycle ahead of the first are correspondingly retarded throughout the motion. The behaviour of other electrons may be estimated by interpolation.

An accelerated electron is supplied with energy from the source which feeds the buncher. A retarded electron supplies this source with energy; so that the net energy lost by the buncher in this manner is, to a first approximation only, zero.

If the electrons after modulation are collected at an anode, or Catcher, to which is attached a parallel tuned circuit, as shown in Fig. 413, oscillations are set up in the latter in the same way as they are in a Class C amplifier with tuned circuit load. At the anode it is the density modulation, due to the bunching, which is important, and not the difference in velocity itself. If the current variation of Fig. 414 is compared with that of a Class C amplifier, the closeness of the analogy will be apparent.

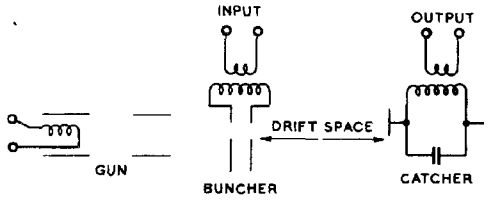

Fig. 413 - Extracting energy from velocity modulated circuit.

The mechanism thus described in schematic form constitutes an amplifier of sorts, since, to a first approximation, the input supplies no net power, whereas useful power is available at the output. Unfortunately, the amplification obtainable from such a system is not independent of input amplitude, i.e. of the modulation depth. If the depth of modulation is doubled the output amplitude is not correspondingly doubled, and may be diminished. In fact the variation of amplification with modulation depth is extremely complex, depending on the length of the drift space, mean velocity and frequency. Although amplifiers employing the principles described are in use, they are very limited in their application and are inherently noisy. These disadvantages are not important when the methods are applied to the design of a constant frequency oscillator, and it is in this respect that they are commonly employed.

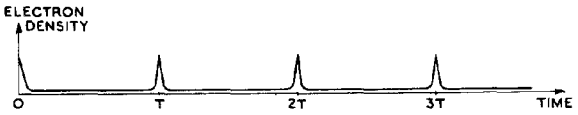

Fig. 414 - Variation of electron density with time in the region of optimum bunching.

It is not essential for the bunched electrons to impinge on an electrode connected directly to a tuned circuit in order that energy may be transferred to the latter from the valve current. The modulated beam may be directed through the aperture of a second pair of electrodes similar to the modulating set, connected to a circuit

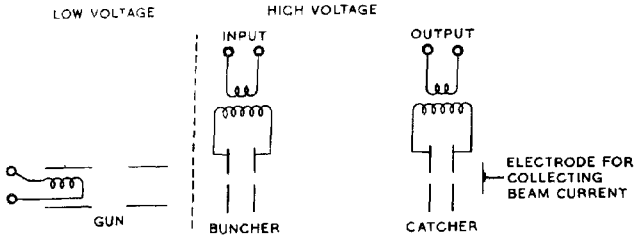

Fig. 415 - Alternative method of extracting energy.

tuned to the operating frequency (Fig. 415). Each bunch of electrons passing through the aperture will induce currents to flow in the circuit, and successive bunches will, because of the resonance of the circuit, arrive at the correct instants to reinforce oscillations already present there. In other words, the electron beam may be made to augment the alternating displacement current between the condenser plates without actually impinging on either of them. In practice it is probable that both effects occur.

To convert the double-tuned circuit amplifier into an oscillator all that is required is a feedback circuit from catcher to the buncher. This is indicated in Fig. 416. The phase of the feedback must correspond to the length of the drift space and the mean velocity of the beam for regeneration of positive feedback to occur at the desired frequency. This means that the feedback loop must be of the right length, since a difference in length of $\frac{\lambda}{2}$ would change this feedback from positive to negative or vice versa.

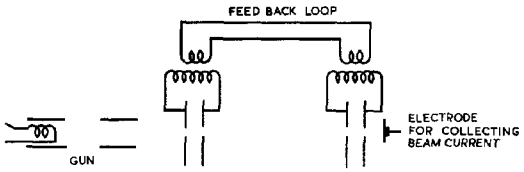

Fig. 416 - Adaptation of velocity modulated amplifier as oscillator.

The foregoing description has been limited to theoretical circuits without considering the practical forms which these circuits may take. Common forms of practical velocity-modulated tubes will be described in the following paragraphs.

23. Velocity Modulated Oscillators in Common Use

Heil Tube, Fig. 417

This oscillator is a low-powered generator possessing moderately good frequency stability. Its main advantage is that it may be tuned over a wide frequency range. The combined tuned-circuit and feedback link are formed of a short length of coaxial line with a hollow inner conductor. Apertures are cut at opposite ends of a diameter, the first to permit the entry of the electron beam, thus forming the buncher; the second allows the modulated beam to emerge, and constitutes the catcher, currents being induced in the inside walls of the coaxial line by the pulses of current in the beam. The drift space consists of the region in the neighbourhood of the diameter joining the two apertures. The transit time across this space must be such as to ensure that the currents induced at the output are in phase with the currents at the input. The emerging electrons are collected at an anode beyond the second aperture.

The resonant frequency of the circuit depends on the effective length of the coaxial line. This line is usually terminated in a variable length of short-circuited lecher line. As this length is varied, the voltage difference between cathode and accelerating electrode must be changed correspondingly to maintain the phase equality at input and output.

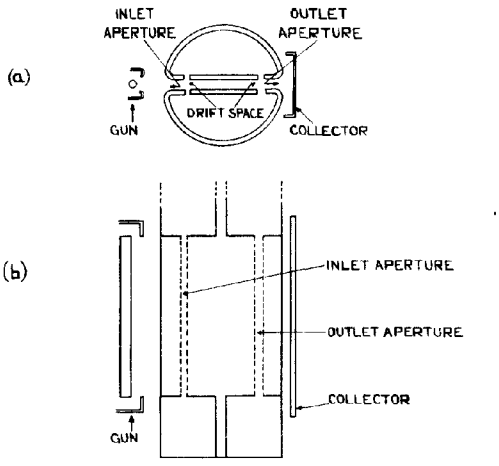

Fig. 417 - Heil tube.

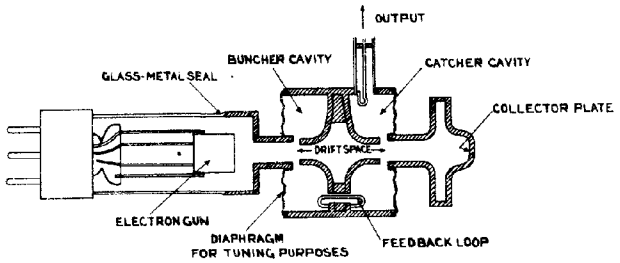

Fig. 418 - Double rhumbatron klystron.

In this tube the two tuned circuits are of the resonant cavity type, the rhumbatron shape being particularly suited to the aperture method of feeding and extracting energy. The term Klystron is usually applied to a velocity modulated oscillator using a

cavity resonator. Feedback is provided by a coaxial cable, terminated at both ends by loops which are inductively coupled to the cavities. The length of this cable must correspond to the length of the drift space between the apertures of the two rhumbatrons. Owing to the finite size of the loops and the variation of their input impedance with frequency, the optimum cable length will not be independent of frequency.

A major difficulty encountered in this oscillator is the necessity for the two circuits to have the same resonant frequency. The high selectivity of the rhumbatrons used permits only the smallest deviation from resonance before the maintenance of oscillations becomes impossible.

Reflex klystron

In the reflex klystron, instead of a second tuned circuit and aperture being employed, the electron beam is reflected and made to return to the modulating aperture at the correct phase for the maintenance of oscillations. This is done by the insertion of a reflecting plate at a potential negative to cathode (Fig. 419). Because of the considerable retardation and subsequent concentration of electrons between rhumbatron and reflector, the inaccuracies of neglecting interaction between electrons are greatly increased; but the simplified explanation which follows, although it neglects this, is sufficient to indicate the general mode of operation.

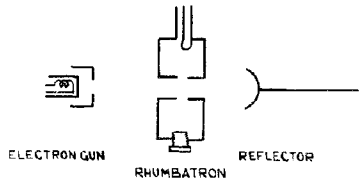

Fig. 419 - Schematic diagram of reflex klystron.

It is assumed as a first approximation that an electron after emerging from the aperture is subject to a constant retarding force E. This force brings the electron to rest and causes it to return to the aperture with the same velocity as that with which it emerged. The method by which bunching occurs under these conditions is illustrated in Fig. 420. The notation used in this diagram is the same as that of Fig. 409. The velocity u of the returning electrons varies throughout the drift space as shown at (a).

Because of the constant retarding force, the straight lines OB, OA, OC, of Fig. 409(b) become the parabolas shown in Fig. 420(b). The line distribution of electrons for different values of t is given by the four curves for $t = 0, \frac{T}{4}, \frac{T}{2}, \frac{3T}{4}$. The diagram shows that at the instant $t = 0$ the electron density $\frac{\delta t_0}{\delta s}$, at the aperture (where $s = 0$) due to the reflected beam, is large, whereas at all other instants $\frac{\delta t_0}{\delta s}$ is small. Approximately half the electrons pass through the aperture in a "bunch" whilst the passage of the remainder is spread over the rest of each cycle.

If e is the charge, and m the mass of an electron, the retardation r due to the field E is $r = \frac{Ee}{m}$. The time for an electron to be brought to rest and to return again to the aperture

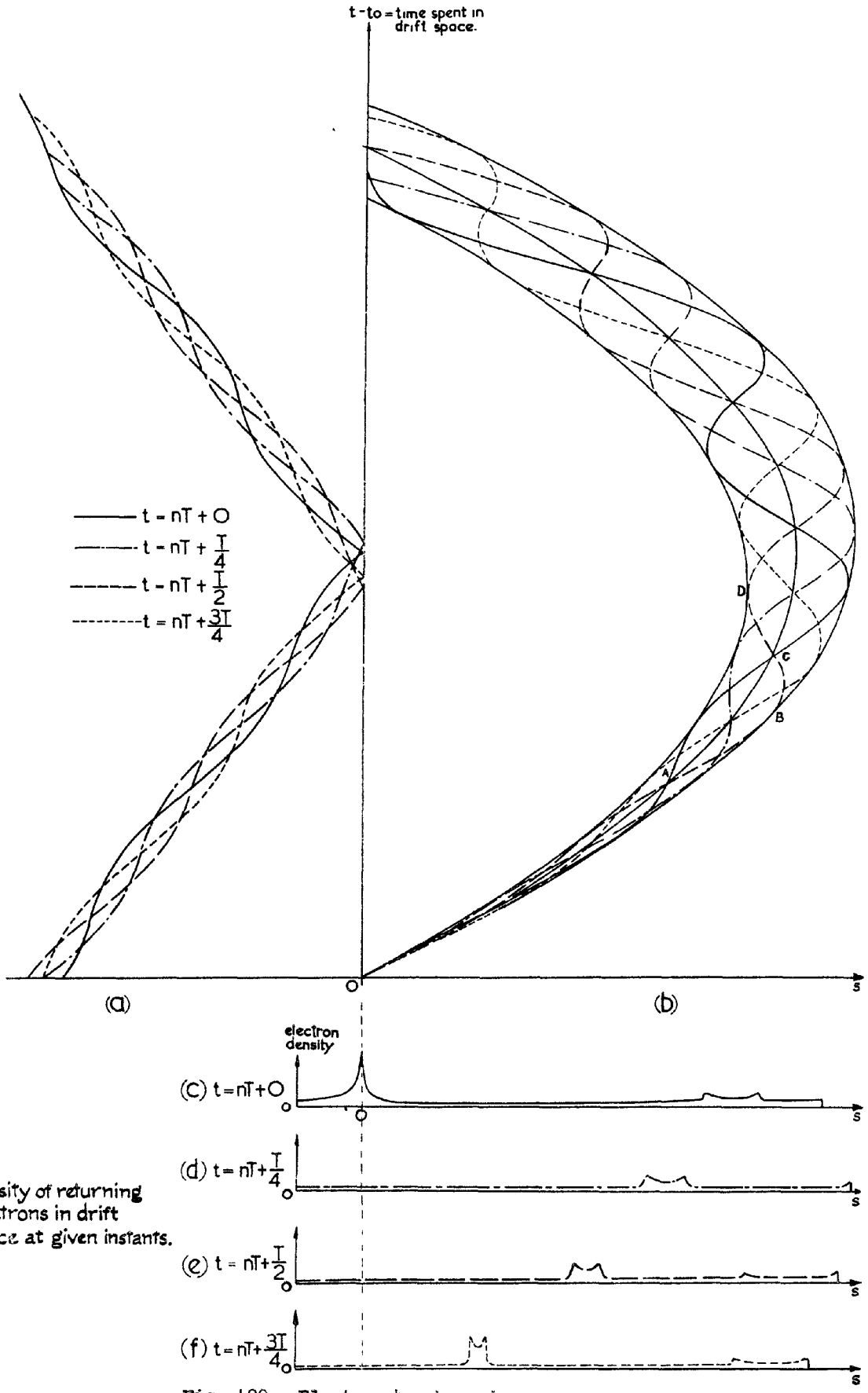

Density of returning electrons in drift space at given instants.

Fig. 420 - Electron bunching in a reflex klystron.

is $t = \frac{2u}{r}$. The mean time is therefore $\bar{t} = \frac{2u_o}{r} = \frac{2mu_o}{Ee}$.

For oscillations to be maintained there must be a suitable phase relationship between the return of the bunches to the aperture and the oscillatory field which causes the bunching; i.e., $\bar{t}$ must have a suitable value, dependent on the manner in which energy is fed into the cavity.

Further, for optimum bunching the difference between the times spent in the drift space by the fastest and the slowest electrons should be approximately an odd multiple of $\frac{T}{2}$. The time taken to bring to rest an electron which enters the drift space with velocity u is $\frac{u}{r}$; the total time it spends in the drift space is therefore $2\frac{u}{r}$. Hence the time-difference for the fastest and slowest electrons is

$$2\frac{\hat{u}}{r} - 2\frac{\check{u}}{r} = 2\frac{u_o + \hat{u}_d}{r} - 2\frac{u_o - \hat{u}_d}{r}$$

$$= 4\frac{\hat{u}_d}{r}.$$

Hence $4\frac{\hat{u}_d}{r} = (2p + 1)\frac{T}{2}$ where p is an integer

$$= \frac{(2p + 1)}{2f}$$

$$\text{or } \hat{u}_d = \frac{2p + 1}{8f} \cdot \frac{Ee}{m}.$$

In order to set up the oscillator at a given frequency so as to produce the maximum amplitude it is necessary to adjust both $\bar{t}$ and $\hat{u}_d$; i.e., both u_o and E. Thus both resonator-cathode and resonator-reflector voltages must be variable.

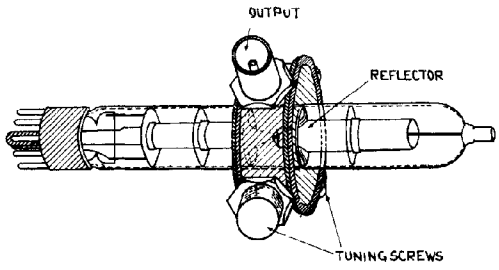

Fig.421 - Reflex klystron (CV 35).

Klystrons are still undergoing development, and details of design are not standardised. A type of tube in common use is shown in Fig. 421.

THE MAGNETRON

24. Description

The magnetron is a valve used for generating UHF oscillations. It has two electrodes; a cylindrical cathode surrounded by, and coaxial with, a cylindrical anode. The original magnetron had an undivided anode, but practical modern magnetrons have anodes split into a number of parallel

segments, equal in size, and separated by gaps. An electric field is established between anode and cathode. A magnetic field is applied parallel to the axis of the electrodes, and is as uniform as conditions will permit over the whole space between them. Because of the magnetic field, the electrons do not move directly from cathode to anode, as in a simple diode, but are constrained to move in curved orbits, as described below. In virtue of this, electrons can be made to arrive at desired segments of the anode in such a manner as to give rise to and sustain high-frequency oscillations in tuned circuits suitably connected to the anode segments.

Practical magnetrons are of three main types:-

(i) The split-anode magnetron operating in the Dynatron (or Habann) mode.

(ii) The split-anode magnetron developed by Megaw.

(iii) The resonant cavity centimetric magnetron, as widely used in radar.

(i) The Habann oscillator works with relatively high efficiency (30 - 70%) up to about 600 Mc/s. It is not at present in use in service equipments, but a brief description of it is given as an example of how negative resistance effects can arise due to changes in field distributron and in consequence of the electron orbits. (Sec. 26).

(ii) This valve is a low-power magnetron, enclosed in a glass envelope of normal size and shape. In contrast to the Habann oscillator, it is a microwave generator. It is not used in British Radar equipments, and it is not dealt with in these notes.

(iii) The resonant cavity centimetric magnetron is the only centimetre-wave oscillator so far produced capable of giving pulse powers of the order of megawatts with high efficiency. For operation on centimetre wavelengths the tuned circuits are so small that they are embodied in the anode block of the valve and are not, in general, variable. Fig. 422 illustrates the essential features of this type of magnetron.

25. Electron Orbits

The operation of any kind of magnetron is determined largely by the motion of the electrons in the anode-cathode space. The orbits of the electrons depend upon three factors, namely:-

(i) the electric field due to the anode-cathode potential difference,

(ii) the applied magnetic field, and

(iii) the space charge effect, i.e., the forces which the electrons exert on one another.

Early simple theories of magnetron operation which ignored (iii) were based on the calculation of the orbit of a single electron as follows:-

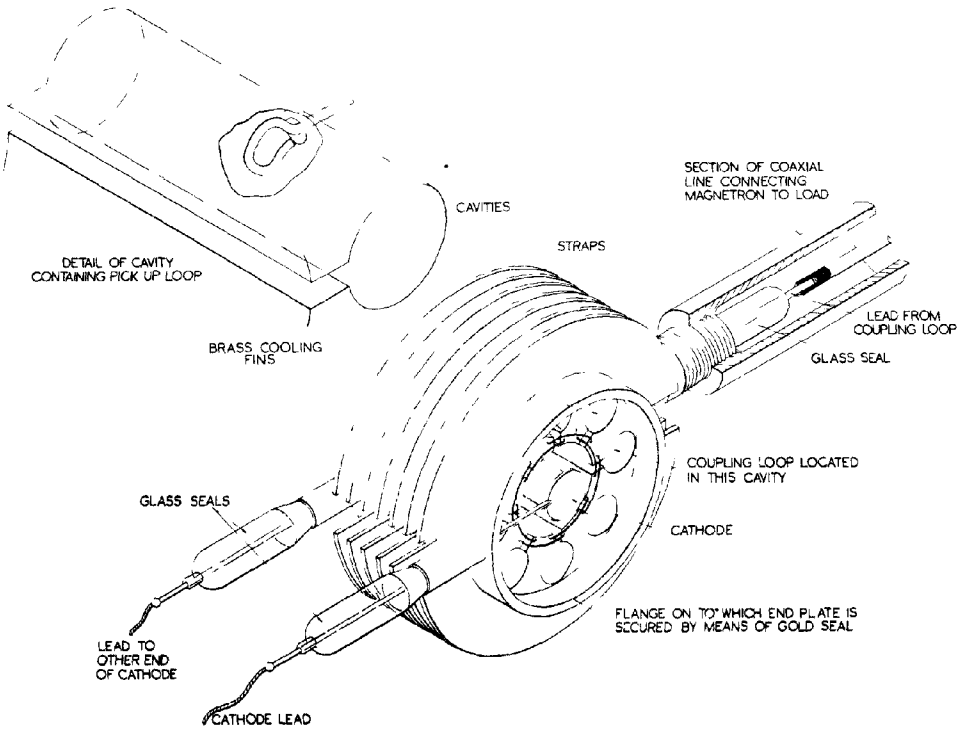

Fig. 422 - Typical hole and slot type magnetron with end plate removed.

Assume that the anode is a uniform cylinder.

Let V be the potential difference between the cathode and any point distant r from the axis.

Let u be the velocity acquired by a electron due to the accelerating effect of the potential difference V.

Denote by suffixes a, k the values of V, u, and r at anode and cathode respectively.

Let m be the mass and e the magnitude of the charge of an electron.

It can be shown that

$$V = V_a \frac{\log r/r_k}{\log r_a/r_k} \quad \ldots\ldots\ldots\ldots\ldots\ldots\ldots\ldots(1).$$

Fig. 423 shows how V varies with r for the case where $r_k \ll r_a$.

Since the kinetic energy acquired by the electron is $\frac{1}{2} m u^2$, and the work done on the electrons is e V,

$\frac{1}{2} m u^2 = e V$, so that

$$u = \sqrt{\frac{2 e V}{m}} \ .$$

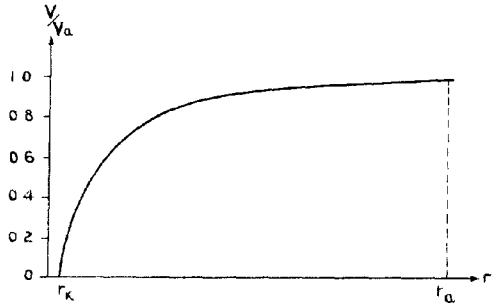

Fig. 423 - Potential distribution in the anode-cathode space.

In particular,

$$u_a = \sqrt{\frac{2 e V_a}{m}} \quad \ldots\ldots\ldots\ldots\ldots\ldots\ldots\ldots\ldots\ldots(2).$$

Fig. 423 shows that, for $r_k \ll r_a$, the potential gradient is steep near the cathode so that $V \fallingdotseq V_a$ and hence $u \fallingdotseq u_a$ except within a short distance of the cathode.

So far, only one factor influencing the electron orbit has been discussed, namely the effect of the electric field between anode and cathode. Due to it the electron would move along a radius from cathode to anode, with a velocity which increases at first rapidly and thereafter, very slowly (Fig. 424(a)).

Now if an electron moving with velocity u is subjected to a force F due to a magnetic field, of flux density B, perpendicular to the plane of its motion

$$F = Beu,$$

and is mutually perpendicular to B and to u. This causes the electron to move in a circular orbit, of radius ρ, given by

$$Beu = \frac{mu^2}{\rho} \quad \ldots\ldots\ldots\ldots\ldots\ldots\ldots\ldots(3).$$

Since, except within the region close to the cathode, u is

approximately constant and equal to u_a, it is valid, as a first approximation, to equate the value of u obtained from equation (3) to that for u_a in equation (2).

This gives

$$B = \sqrt{\frac{2m V_a}{e\rho^2}} \quad ; \quad \text{or} \quad \rho = \sqrt{\frac{2m V_a}{e B^2}} .$$

Thus every electron leaving the cathode region commences to describe a path which is approximately circular. Whether or not the path is completed depends upon the values of V_a and B. Fig. 424(b) shows the case where ρ is very large; Fig. 424(c) where, by increasing B, ρ has been reduced to $\frac{r_a}{2}$, so that the electron just skims the anode, and Fig. 424(d) shows ρ made small, by suitably increasing B. For the case of Fig. 424(b), all electrons would reach the anode; whereas for that of Fig. 424(d) none would do so; i.e., the valve current would be cut off. Fig. 424(c) represents the case where B is just large enough to prevent the electrons from reaching the anode; i.e., the magnetron current is just cut off. The value of B required to achieve this is called the cut-off value B_c and is obtained by putting $\rho = \frac{r_a}{2}$ in the expression for B above. This gives

$$B_c = \sqrt{\frac{8m V_a}{e r_a^2}} \qquad \ldots\ldots\ldots\ldots\ldots\ldots\ldots\ldots\ldots\ldots (4).$$

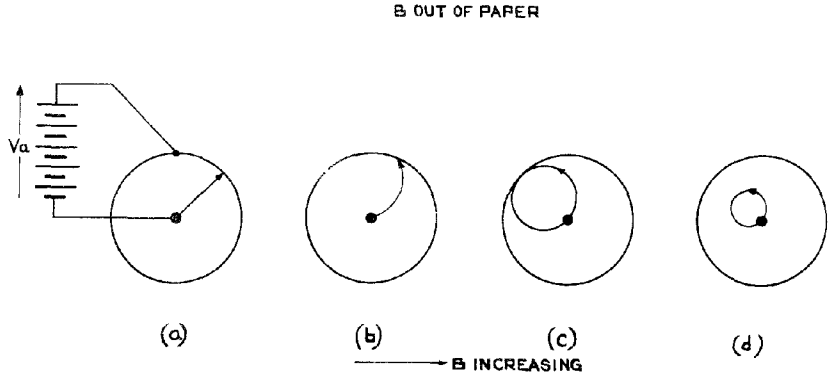

Fig. 424 - Single electron orbits with fixed V_a and varying B.

(Actually, the orbits cannot be true circles, for the assumption that u is constant is only an approximation. The true orbit curves more sharply near to the cathode, and is roughly epicycloidal in shape).

Fig. 425 indicates the circular orbits of electrons, for V_a and B constant. It is seen that their centres lie on an equipotential surface coaxial with the cathode; and that a similar coaxial surface marks the space charge boundary.

The existence of the space charge modifies the above theory. Electrons on their way out from the cathode are repelled by those nearer the anode, and are unable to execute the orbits so far described. Also, electrons which are attempting to return to the cathode are prevented from so doing by those nearer the cathode. It is more probable that these outer electrons, since they cannot fall back into the cathode, move in circular orbits around it.

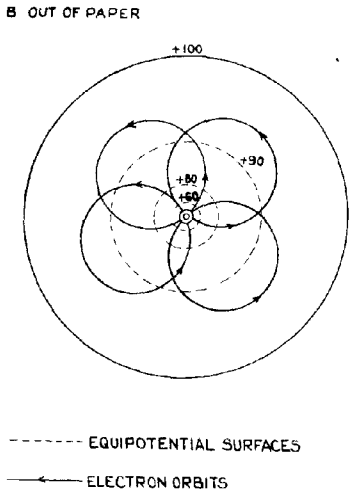

Fig. 425 - Electron orbits for a cut-off magnetron with V_a and B constant and uniform.

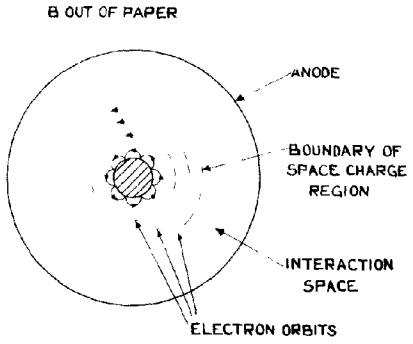

Fig. 426 - Electron orbits as modified by the space charge.

Fig. 426 indicates the electron paths obtaining when a steady anode voltage has been established, B being larger than the cut-off value. It is useful to regard the space charge region as composed of a number of thin coaxial cylindrical shells each containing a large number of electrons which revolve with the same angular velocity. The angular velocity depends upon V_a, B and the radius r of the shell. The greater r, the larger is the angular velocity of the electrons.

Up to the present, only the ortital conditions obtaining when V_a is fixed have been considered, Figs. 424 and 425 indicating the orbits when space-charge effects are ignored and Fig. 426 when they are not. It may be shown that whichever orbit is assumed, much the same result is obtained, this result according well with the practical performance of the Habann oscillator. This oscillator will be examined from both points of view and thus the effect upon the orbits of varying V_a will be introduced.

26. The Split-Anode Magnetron Operating in the Dynatron Mode (Habann Oscillator)

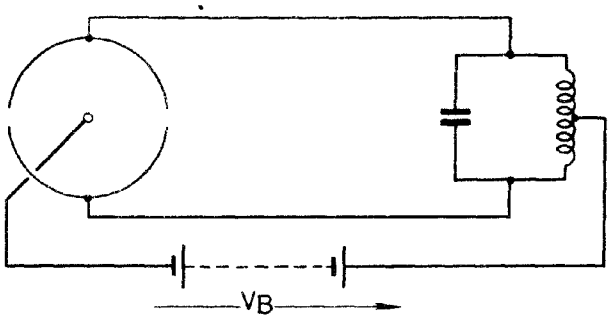

Fig. 427 - The two-segment magnetron.

This mode occurs at frequencies such that the period of oscillation is long compared with the time of transit of an electron from cathode to anode, and normally arises for waves longer than about 50 cms. In such circumstances it is valid to assume that, during their passage from cathode to anode, the electrons are in a field that is approximately steady.

Consider a two-segment magnetron, connected as shown in Fig. 427. Suppose that initially each segment is at a potential V_o above that of the cathode, B being larger than B_c for this particular value of the anode voltage. Then Fig. 428(a) shows the equipotential lines and electron orbits under this circumstance, space-charge effects being ignored. Fig. 428(b) gives similar information, but shows the concentric circular orbits which appear reasonable if the space charge is taken into account. In this latter case, the orbits follow the equipotential lines, whilst in the former, the orbit centres lie on an equipotential line.

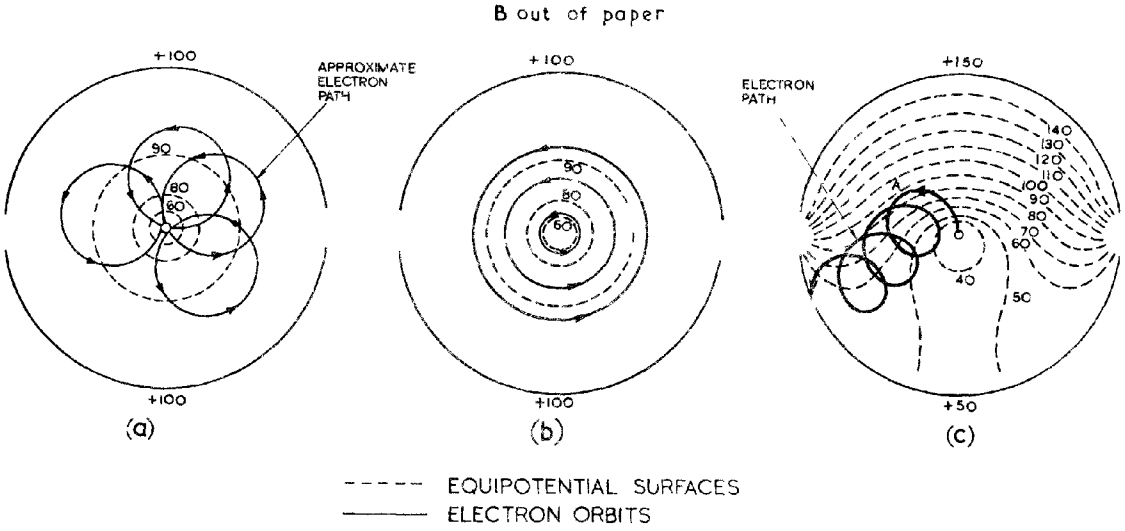

Fig. 428 - Orbits of a single electron in a split-anode magnetron.

Now let the potential of the upper segment be raised to $(V_o + V_1)$, whilst that of the lower segment is reduced to $(V_o - V_1)$. The field configurations and equipotential distributions are consequently changed as indicated in Fig. 428(c). In the absence of space charge effects, the electrons still move in such a manner that the orbit "centre line" is always approximately at right angles to the electric field; i.e., this line still corresponds to an equipotential line. Fig. 428(c) shows an electron orbit for such a case, and if the similar orbits of many electrons, leaving the cathode at all parts of its surface, be considered, it is readily seen that more electrons will arrive at the lower segment than at the upper.

If now the effect of space charge be considered, an electron at A (Fig. 428(c)) will be prevented from moving in towards the cathode by other electrons and will therefore be constrained to move on a path approximating to the envelope of the orbit such as that shown

in the figure; i.e., the orbit itself tends to follow an equipotential line. Electrons in other portions of the anode-cathode space similarly tend to follow equipotential lines. Hence the introduction of the effect of the space charge, whilst it modifies considerably the individual electron orbits, in no way alters the conclusion, viz, that more electrons arrive at the lower potential segment than at the higher. Further, it can be shown that if the circular orbits assumed in the presence of space charge (and fixed V_a) be postulated, the cut-off value of B is given by

$$B_c = \sqrt{\frac{8m\ V_a}{e\left(r_a - \frac{r_k^2}{r_a}\right)^2}} \quad :$$

and if $r_a \gg r_k$ this reduces to equation (4), which was obtained on the assumption of an entirely different orbit. This fortuitous agreement has been largely responsible for the continued neglect of consideration of space-charge effects as in the early magnetron theories, but, although such omission leads to negligible errors, except in the orbit concept, for the Habann oscillator, it gives erroneous results for the resonant cavity magnetron considered in Secs. 27 - 42.

Before proceeding to this case, it is instructive to consider how, in the Habann oscillator, the conditions required for the maintenance of oscillation are fulfilled. We have seen that more electrons arrive at the lower potential segment than at the higher. That is, referring to Fig. 427, the existing negative charge on the lower condenser plate is increased because of this, by an amount (say) ΔQ. If the instantaneous value of the RF voltage on the condenser is v, its RF energy is thus increased by $\frac{1}{2} v.\Delta Q$. By arranging that most electrons arrive at the lower segment when C is fully charged (i.e. when v has its maximum value) the greatest possible increment of energy is given to the tuned circuit. Half a periodic time later the upper plate of the condenser will be negative with respect to the lower; and at this instant the majority of the electrons will be arriving at the upper plate. Thus the oscillatory circuit receives increments of energy due to the arrival of electrons at the right time. Hence dissipation in the tuned circuit (or in whatever load is coupled to this circuit) may be made up by the magnetron. Since the current through each segment is antiphase to its RF voltage, the magnetron behaves as a negative resistance element; this accounts for the name "Dynatron mode" often used to describe this kind of magnetron operation. This mode can be efficient only if the electron cathode-to-anode transit time is negligible compared with the periodic time, for only then will each increment of charge be received when the corresponding segment voltage is at a minimum.

27. The Resonant Cavity Centimetric Magnetron

The construction of a typical magnetron of this type is indicated in Fig. 422. The tuned circuits are holes and slots cut in a solid beryllium-copper block; Fig. 429 illustrates some common anode block constructions. Considering one hole and slot apart from the remainder, we may regard the slot as a condenser, since most of the electric field is located at it, and the hole as, roughly, a single turn coil. Thus a single hole and slot constitute a resonant circuit. The equivalent circuit of the magnetron as a whole is more complicated than this, not only because there are many cavities, but also because they are coupled one to another in a complicated manner. Firstly there is mutual induction between the holes, since magnetic flux emerging from the top of one hole passes through an adjacent one to form a closed loop, (see Fig. 430(a)). Also, there

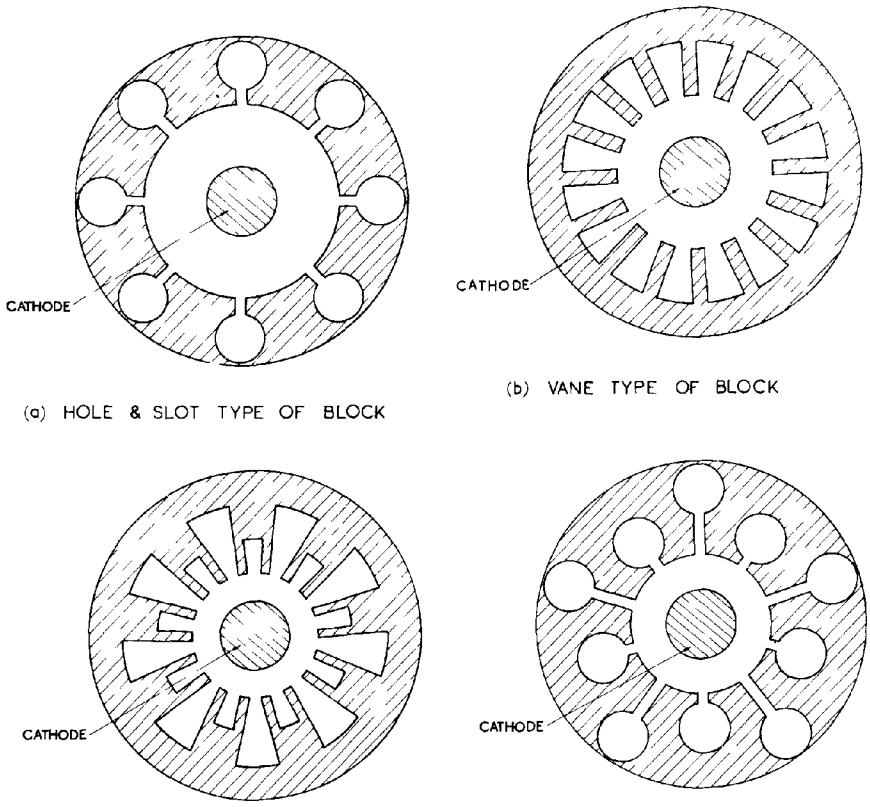

(a) HOLE & SLOT TYPE OF BLOCK

(b) VANE TYPE OF BLOCK

(c) 'RISING SUN' VANE TYPE OF BLOCK

(d) RISING SUN HOLE & SLOT TYPE OF BLOCK

Fig. 429 - Types of anode block construction in use.

are capacitances to the end plates and to the cathode, giving rise to capacitive coupling between the cavities. Coupling also occurs through the medium of the space charge itself. Since an N-segment magnetron may be regarded as having a simple equivalent circuit given roughly by placing the N-segments in parallel, the resultant equivalent lumped circuit has a capacitance N times and an inductance

$\frac{1}{N}$ th of that of a single cavity. Thus the operating frequency would appear to be that of a single cavity. In practice, whilst the cavity dimensions are the most important single factor in determining the frequency of operation, they are influenced materially by the space-charge cloud, as well as by the values of the applied voltage and the magnetic flux density. Hence it is necessary to consider in some detail the behaviour of the space charge.

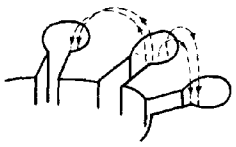

(a) MAGNETIC (INDUCTIVE) COUPLING BETWEEN HOLE AND ITS NEIGHBOURS

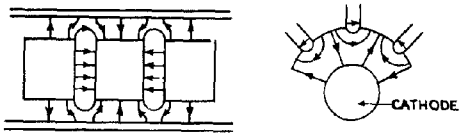

ELECTRIC (CAPACITIVE) COUPLING BETWEEN SEGMENTS AND END-PLATES (LEFT-HAND SKETCH) OR BETWEEN SEGMENTS AND CATHODE (RIGHT-HAND SKETCH)

(b) COUPLING BETWEEN SEGMENTS.

Fig. 430 - Coupling between segments.

28. The Single Stream Steady State

The following account is now generally accepted as describing what occurs in the anode-cathode space of a resonant cavity magnetron. It is based on the concept of the Single Stream Steady State. Each electron is assumed, if V_a is constant, to be moving in a circular orbit about a point on the axis as centre. If V_a is varied the electronschange their orbital radii accordingly. It is assumed that the changes of anode voltage occur so relatively slowly that the electrons immediately move into the orbit corresponding to the new value of V_a, so that any instantaneous condition is virtually a "steady state", i.e. one obtaining with fixed V_a. Since magnetrons are pulse-operated, the validity of this assumption might appear doubtful; but present pulse technique cannot produce modulating pulses rising to their full value in less than about $0{\cdot}02\mu S$. Electron orbits can automatically adapt themselves to changes of this order, so that a succession of "steady" states occurs as the pulse is applied. Hence at any point in the space-charge region the electrons are, at any instant during the change, either all going towards or all going away from the cathode. This is the distinction between Single Stream and Double Stream steady states, for under the double stream condition some electrons may be moving through the point towards the anode and others towards the cathode. Analysis has shown that the latter condition would obtain if the pulse rise were instantaneous. Since we have not yet approached sufficiently near to this condition for the single stream state to be invalidated, the possibility of a double stream steady state will hereafter be disregarded. (It may be noted that the early concept of electrons hurtling among one another in an interweaving of epicycloids implied a double stream state). Also, with the rates of rise of the modulating pulse encountered in practice, it is not necessary to differentiate between CW and pulse operation.

29. Behaviour of the Space-Charge Cloud when the Anode Voltage Varies

So far, discussion has been limited to the operation of the magnetron with V_a fixed. The next step is to consider what happens

to the space-charge cloud when oscillations of the tuned circuits (cavities) cause the anode voltage to vary.

Any disturbances at the anode, resulting in oscillations, sets up a voltage pattern upon it. This pattern can be analysed into component waves revolving at different angular rates around the anode surface.

One of these component waves roughly in step with a particular "electron shell" (see Sec. 25) may cause considerable distortion of its cylindrical form. This distortion in turn affects the motion of other electrons. It can be shown that electrons between this shell and the anode, and which, with constant V_a, move faster than those in it, are slowed up when the space charge cloud is deformed, and that those nearer the cathode have their angular velocities increased. Thus the electrons outside the "in-step" shell give up energy whilst those inside gain energy. If the outer electrons give up more energy than is acquired by those nearer the catnode there will be a net loss of energy by the space charge, and if this energy can be taken up by the tuned circuits a means of sustaining oscillations is provided. This condition, although necessary, is not sufficient, for the energy of the space charge must be replenished from the DC source. This can be achieved only if the deformation of the space-charge cloud is sufficiently great to cause electrons, in sufficient numbers, actually to reach the anode, and this clearly depends upon the value of V_a. (It depends also upon the nature of the voltage pattern around the anode.)

Before considering the factors mentioned above in greater detail, a rough picture of the part played by the space charge, and of the operation of the magnetron generally, may be obtained with the aid of the following analogy.

30. The Electrometer Analogy

Consider a light paddle-shaped vane (Fig. 431(a)) supported by a torsion head and deflected by the charged surfaces ABCD. The vane takes up a position of equilibrium determined by the deflecting torque due to the system of charges, and the restoring torque due to the suspension. (This is a form of what is generally known as a quadrant electometer).

If the constraint on the vane is removed and the cylindrical outer surface rotated, the vane will keep step with the rotation. Alternatively, the same result could be achieved by the use of a commutator in the leads to the segments, arranged so as to reverse the charges periodically. Such a system can be regarded as an elementary motor and could be made to perform work.

Conversely if the rotary vane in the arrangement shown in Fig. 431(b) were driven by an external motor, charges would be induced on the segments as indicated, and would vary periodically. The resulting voltages would cause currents to flow in the external circuit. Such a system is clearly a simple generator, and could be made to supply power to a load.

In the magnetron there is a state of affairs resembling this in several respects. The segments of the electrometer correspond to the anode segments of the magnetron, and the charged vane to the rotating space charge. Figs. 432(a) and (b) show the space charge distorted due to the segment potentials, for the 4-segment and 8-segment cases. It will be noted that in neither case shown could oscillation be maintained, for no electrons reach the anode, and

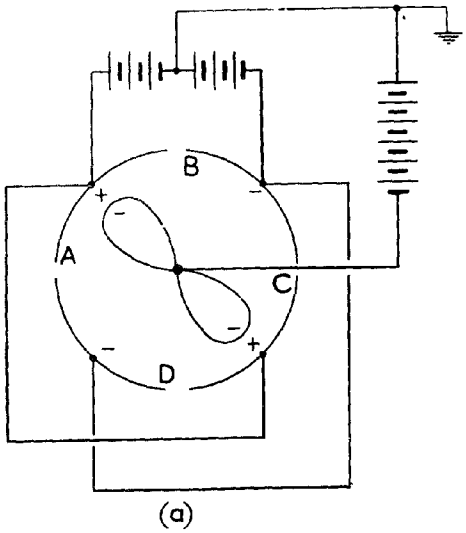

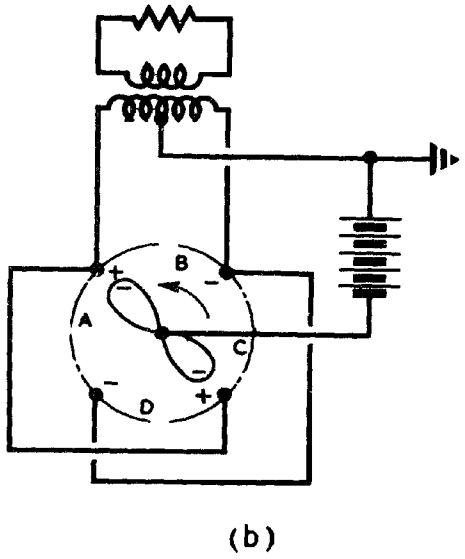

Fig. 431 - The electrometer analogy.

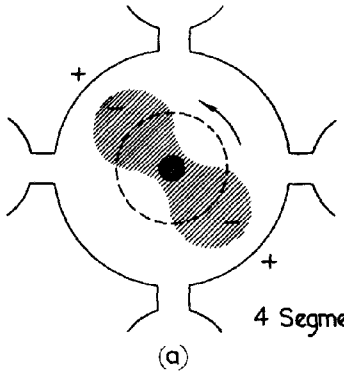

B out of paper

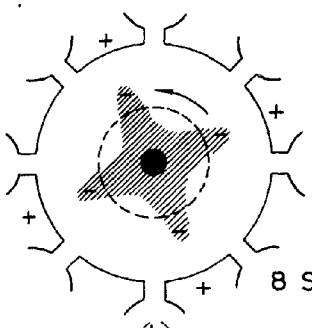

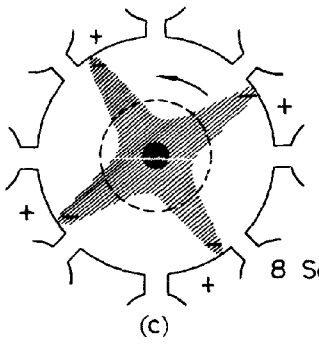

Fig. 432 - Space charge deformation in the magnetron.

and hence no energy is being supplied to the space charge. Fig. 432(c) shows the cloud sufficiently distorted for this to occur. Under this condition there will be an inwards radial flow of current in the magnetron (corresponding to the outward flow of electrons). This current flows under the influence of an external magnetic field, and the space charge is accordingly constrained to to revolve. (In the case shown, the magnetic flux is out of the paper, and the consequent motion is counterclockwise). Thus we have an effect equivalent to the driving motor in the analogy.

31. Modes of Oscillation

It is next necessary to consider in further detail the voltage pattern on the anode referred to in Sec. 29. Common anode block arrangements have been shown in Fig. 429. Consider that of Fig. 429 (a). If a slot, regarded as the condenser of the equivalent tuned circuit, be charged up in some way, the cavity will oscillate at its natural frequency. Now such a cavity has many possible modes of oscillation, and in a magnetron the existence of other cavities all coupled by magnetic and electric fields and by the space charge, complicates the problem considerably.

The simplest and commonest mode is one in which at any instant alternate segments are at equal and opposite RF potentials, i.e. there is a phase difference of 180° (π radians) between adjacent segments. This mode is commonly called the π - mode. The instantaneous potential of any segment varies sinusoidally with time. Fig. 433(a) shows the instantaneous voltage distribution around the anode at intervals of one eighth of a periodic time T, for an eight-segment magnetron, the segments being drawn for convenience in a straight line. Whereas the time variation of voltage at any point on the anode is sinusoidal, the voltage distribution plotted against distance round the anode is not. That is, the voltage pattern is a sinusoidal time variation, of amplitude varying periodically with the angular distance; i.e., it is a standing wave. Further this standing wave can be analysed into a series of spatial harmonic components, each of which can be regarded as consisting of two identical travelling waves moving round the anode in opposite directions. Thus, if we take the π - mode here considered, and restrict our attention to the travelling waves comprising the primary or fundamental spatial harmonic only, we shall obtain the results shown in Fig. 434(a). If all the spatial harmonics were included, the waveforms of Fig. 433(a) would result.

The primary component in the standing wave so far considered would have 4 complete repeats around the anode. This is known as its mode number, n. Thus the π - mode in an 8 segment magnetron is also the mode for which n = 4; whereas in a 10-segment magnetron the π - mode would be the one for which n = 5, since there would then be 5 complete repeats around the anode.

n may have any value, i.e., any phase difference may exist between adjacent segments, provided only that the total phase change round the block is a multiple of 360°. Then each component travelling wave will have a number of repeats n_1 given by $n_1 = mN + n$ where N is the number of segments and m any integer (positive or negative, a negative answer corresponding to a component in the opposite direction). Thus if we take the case so far considered, where n = 4 and N = 8, n_1 = 4 (for m = 0), 8 (for m = 1), 12, 16, etc., also n_1 = -4, -8, -12 etc. for negative values of m. The component for which n_1 = -4 is called the primary reverse component, and by combining this with the primary forward component (n_1 = 4) we have obtained the resultant curve of Fig. 434(a). Adding in also all the other travelling components would have produced Fig. 434(a).

In a similar manner the Figs. 434(b), (c) and (d) have been produced, for the cases n = 3, n = 2, n = 1 respectively. For putting n = 3, N = 8, m = -1 we obtain n_1 = -5 for the primary reverse component. These are shown in Fig. 434(b), which leads to Fig. 434(b) if these and all the other travelling components are added. The reader is left to confirm for himself that the correct values for the primary reverse modes have been taken in Fig. 434(c) and 434(d), and that these results would lead to the anode waveforms shown in Figs. 434(c) and 434(d).

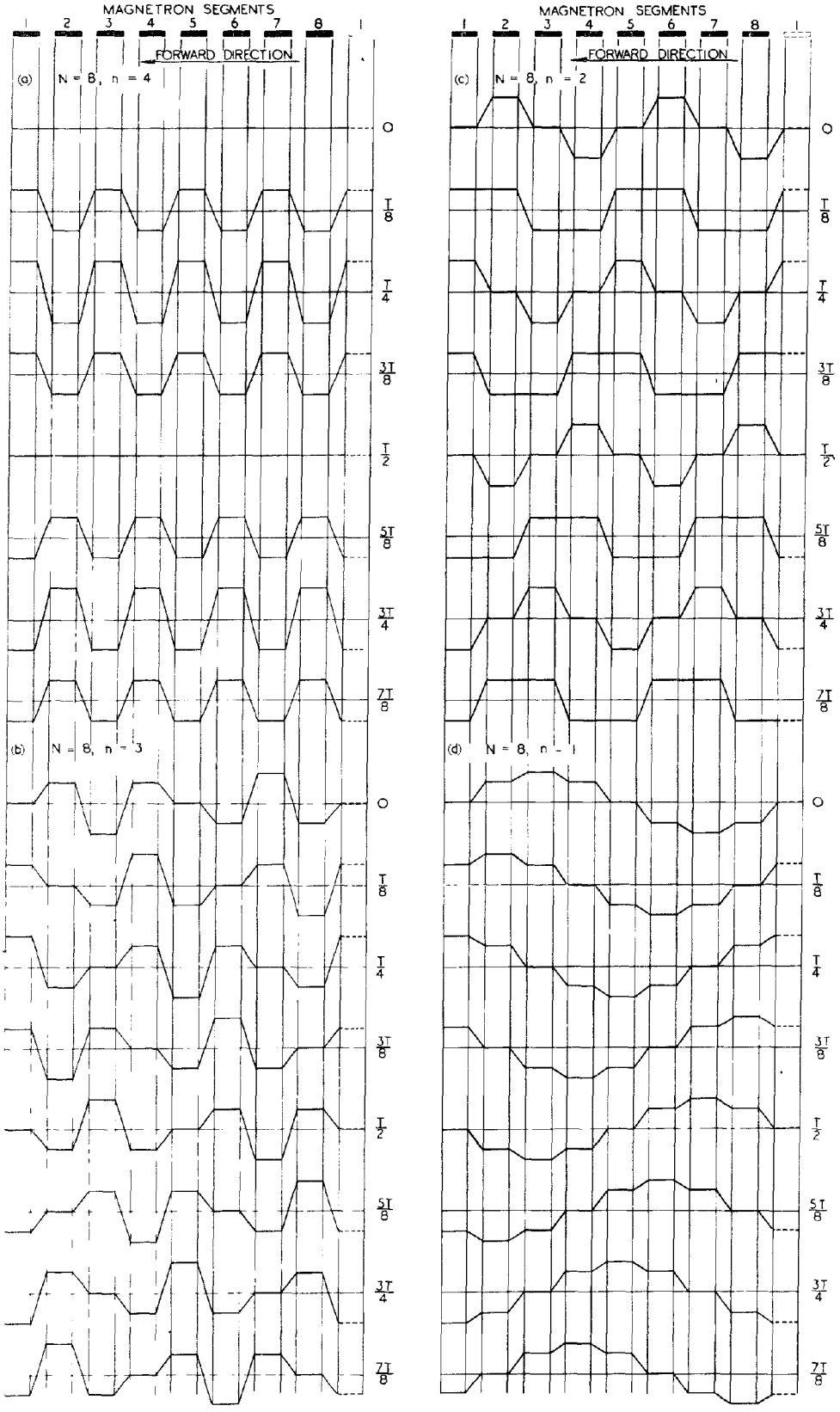

Fig. 433 - Standing waves of voltage on a magnetron anode.

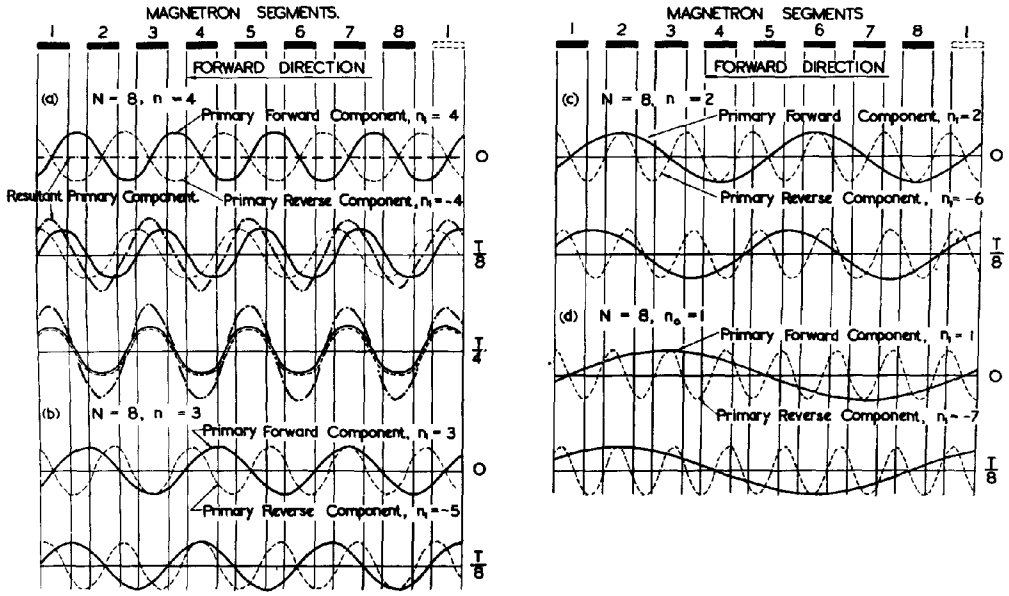

Fig. 434 - Primary components of standing waves of voltage on an 8-segment magnetron anode.

Since an apparently infinite number of modes appears, from the foregoing, to be possible, it is next necessary to consider how it is that a given magnetron can be made to operate in (say) the π-mode, as is most usual.

32. Initiation of Oscillation - The Energy Transfer Criterion

It has already been stated (Section 29) that variations in the anode potential cause the electrons in the space-charge cloud to be distorted in their orbits, and that an electron shell roughly in step with a component of the anode waveform is markedly affected. Now, since the farther the electrons are away from the cathode, the faster they move in their circular (constant V_a) orbits, a sudden "pulling-out" towards the anode of some electrons will cause those nearer the anode to pile up on those drawn out towards it. Thus, not only will this lead to the "star-fish" shape of the space-charge cloud indicated in Fig. 432(b), but it will cause a retardation of the outer electrons, which will tend to assume approximately the same angular velocity as the component of the anode waveform considered. Thus these outer electrons will give up energy. Electrons nearer the cathode than those in the shell most affected will increase in angular velocity, and hence acquire additional energy. For oscillations to be initiated the energy given up by the space-charge must exceed that taken from it. This requires that an adequate proportion of the space charge must lie outside the shell which is in synchronism with the anode waveform component. It can be shown that whereas the distribution of the space charge clearly depends on V_a (assumed constant) the radius of an electron shell in which the electrons travel with a definite velocity does not. For a mode of oscillation with frequency f and mode-number n the synchronous velocity is a

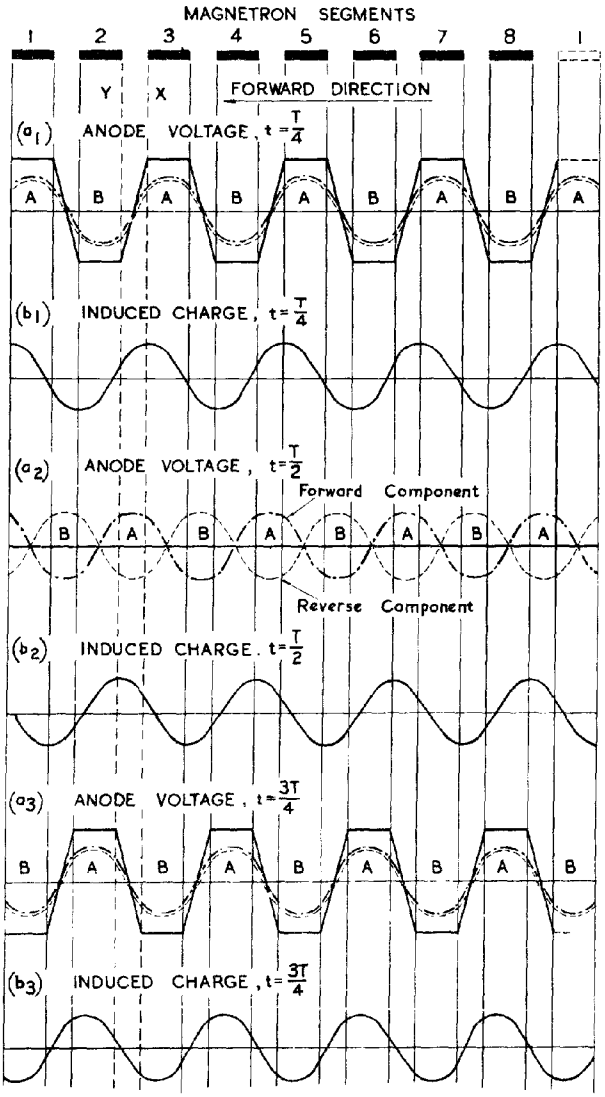

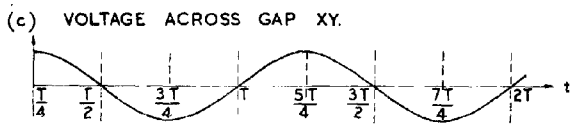

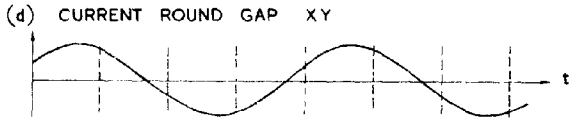

Fig. 435 - Distribution of anode voltage and charge under oscillatory conditions.

function of f/n. The radius of the shell moving with this velocity depends on B and r_k but not on V_a. Also, the larger n, the smaller is this radius.

The magnetron must therefore be operated with V_a large enough so that the radius of the space-charge cloud is greater than the radius of the synchronous shell by an amount sufficient to ensure the transfer of energy from the space charge to the cavities. This condition will be termed the Energy Transfer Criterion. The value of V_a required to satisfy this criterion will be called the "Energy Transfer Potential". Since the radius of the critical shell is smaller the larger the value of n, to operate the magnetron in a high order mode necessitates a smaller anode voltage than operating it in a low order mode: also, if V_a be steadily increased, the energy transfer criterion is satisfied successively for lower and lower order modes.

All components of the anode waveform affect the electron cloud to some extent. But only a forward component, i.e. one moving in the same direction as the space charge as a whole, can be in synchronism with an electron shell. Reverse components have little effect on the general motion of the space charge as a whole. Further, it can be shown that the potential V_1 due to a wave component n_1, at a point within the space charge, distant r from the axis, increases with $\left(\frac{r}{r_a}\right)^{n_1}$ so that, except near to the anode, the contributions to V made by low values of n_1 will be larger than those made by high values of n_1. Hence it appears that, from these considerations alone, the primary forward mode would cause the greatest distortion of the space-charge cloud.

It remains to be shown that the energy available when the energy transfer criterion is satisfied can actually enter the cavities; i.e., that the power flux is directed into them. In order to see this, consider again the 8-segment magnetron, operating in the n = 4 mode. We shall again take only the primary components, as shown in Fig. 435, in which the components of Fig. 434(a) are repeated. Also we shall assume that the primary forward component is the major effective component for the initiation of oscillation. In Fig. 436, the conditions in the magnetron at time $t = \frac{\pi}{4}$ are illustrated. The line OA is drawn through the instantaneous crest of the primary forward component of the anode waveform: OB through the trough. It is shown in the full mathematical theory of the magnetron that the aggregation of electrons takes place in such a manner that the bulges in the distorted space-charge cloud are always ahead of crest lines such as OA. At points on the anode opposite to each bulge there will be, by induction, a local increase in the positive charge on the anode, and, correspondingly, there will be a local reduction in the

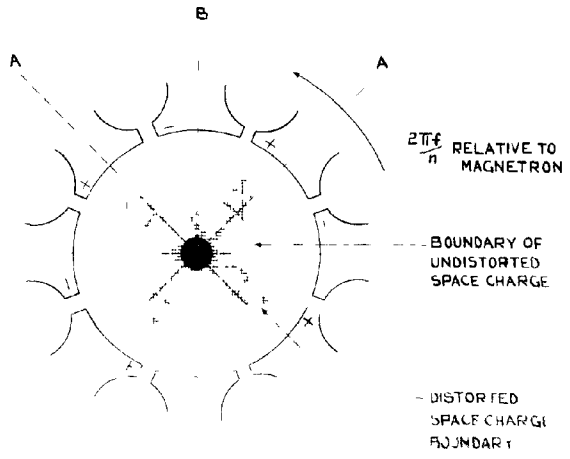

INDUCTION OF CHARGES ON THE ANODE BY ROTATING SPACE CHARGE

Fig. 436 - Induction of charges on the anode by rotating space charge.

charge on the anode opposite each trough in the space-charge cloud. Thus, superposed upon the positive charge on the anode due to the applied voltage, there will be a variation of charge corresponding to the deformation of the space charge. This variation is indicated on Fig. 436 by plus and minus signs.

The spatial distribution of induced charges on the anode must be periodic, and in the case taken will have four periods round the anode. In the diagram (Fig. 435) only the fundamental component of this distribution is shown, as this is the only component which contributes appreciably to the output power. As the primary forward component of voltage moves round the anode, the space charge deformation, and therefore the variation of charge on the anode, moves with it. The distribution of charge at later instants is shown in Figs. 435(b2) and (b3).

Consider a particular gap XY. The spatial distribution of the anode voltage at successive instants is shown in Figs. 435(a1), (a2) and (a3), and the corresponding time-variation of the voltage across the gap XY is shown in Fig. 435(c). The relation between the component of the charge distribution and the potential of X relative to Y may now be deduced. Since the charge distribution is moving round the anode in an anticlockwise direction, there is a component of current flow at every point on the anode, proportional to the corresponding component of instantaneous charge density at the point. Hence the graphs of Fig. 435(b1), (b2) and (b3) may be interpreted as current distribution round the anode, instant by instant, a current flowing in an anticlockwise direction being reckoned as positive. The manner in which the current flowing from X to Y, i.e. around a cavity, varies with time may be deduced from these graphs, and is plotted in Fig. 435(d).

Fig. 437 shows the particular cavity considered. When X is positive with respect to Y the direction of the electric field across the slot is as shown by the arrow E. Hence if electric field strength is regarded as positive in the direction of the arrow, Fig. 435(c) may be usefully taken as a graph of electric field intensity. When the current round the cavity (Fig. 437) is positive the direction of the magnetic field is as shown by H (out of the paper). Hence if magnetic field intensity is regarded as positive in this direction, Fig. 435(d) may be taken as a graph of magnetic field intensity.

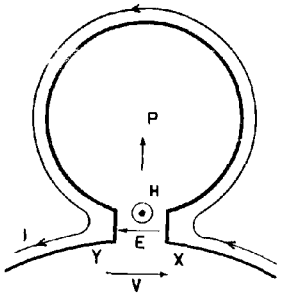

Fig. 437 - Power flux into cavity.

If the cavity were resonating without gain or loss of energy, the time-phase relation between E and H would be a quadrature one. But superposed on the magnetic field due to resonance of the cavity, there is in the magnetron an additional magnetic field produced by the mechanism described above. Comparison of the graphs of Figs. 435(c) and (d) shows that the phase of H differs from that of E by a phase angle less than $\pi/2$, so that H has components both in quadrature and in phase with E. The former indicates that the electronic mechanism of the magnetron modifies the resonating field in the cavity and hence affects the frequency of oscillation. It is one reason why resonant frequencies measured

with the cold clock differ appreciably from those obtained when the magnetron is actually in use. It is also a reason why the magnetron frequency is sensitive to changes in anode voltage.

The in-phase component indicates that there is a flow of energy, and the direction of the power flux P is obtained from the usual consideration, i.e. that E, H and P form a right handed system. (see Fig. 438). Thus, in Fig. 437, the power flux is directed into the cavity. It is thus possible, provided V_a has the required value, with due regard to n, for energy to be transferred from the space charge to the resonating cavities.

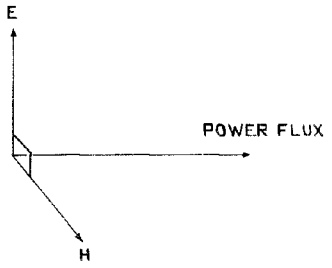

Fig. 438 - Relative dispositions of the electric, magnetic and power flux vectors.

It should be stated that the precise behaviour of the electrons in the shell most affected by the anode waveform, and also the exact location of this shell, is not yet firmly established. There are some differences in the views held by various research workers. It is, however, agreed that, although a certain shell (or shells) may have greater importance than others in the operation of the magnetron, the essential factor is the behaviour of the space-charge cloud as a whole. Oscillations are possible only if the cloud gives up more energy than it gains: and this condition can be achieved, in a particular mode, only if V_a has sufficiently high value; that is, if the energy transfer potential is exceeded.

33. Maintenance of Oscillation; The Energy Supply Criterion

As already observed, oscillations can be maintained only if the energy transferred from the space-charge cloud to the cavity is replenished from the HT supply; i.e. some electrons in the space-charge cloud must have sufficient energy to reach the anode.

This condition, which will be termed the Energy Supply Criterion, may be determined mathematically, and it is found that, as in the case of the energy transfer criterion, V_a must be greater than a critical value, called the Energy Supply Potential (or Threshold Potential). This potential also increases with the ratio $\frac{f}{n}$, so that as V_a is increased from zero the energy supply criterion is satisfied first for the higher order modes and successively for those of lower order. For given values of f, n and B the energy transfer and supply potentials are not the same.

34. The Two Criteria Combined

It follows from Secs. 32 and 33 that for a magnetron to oscillate continuously in a given mode its anode supply voltage must exceed both the energy transfer and the energy supply potentials.

It has been previously stated (Sec. 26) that B_c, the cut-off value of B for a given V_a, is given by

$$B_c = \sqrt{\frac{8m V_a}{e\left(r_a - \frac{r_k^2}{r_a}\cdot\right)^2}},$$

so that $V_a \propto B_c^2$. Hence the curve showing the variation of B_c with V_a is a parabola, indicated by OS, Fig. 439. Further, it has been mentioned already that the energy supply potential depends upon both B and n. It can be shown that for given values of n the graphs of the energy supply potential against B yield straight lines which are tangential to the cut-off parabola, as shown. (The points of contact are calculable, and are nearer the origin the larger is the value of n). Corresponding graphs showing how the energy transfer potential varies with n are shown by the dotted lines in Fig. 439.

For a given V_a and B, a point may be plotted on the composite graph representing the operating conditions. For example, Fig. 439 shows that, for the point P,

(i) V_a is insufficient to cause all electrons to reach the anode; V_a would have to be increased to the ordinate of S for this to happen.

(ii) that the energy transfer potential for n = 5 is exceeded

(iii) that the energy supply potential for n = 5 is exceeded also.

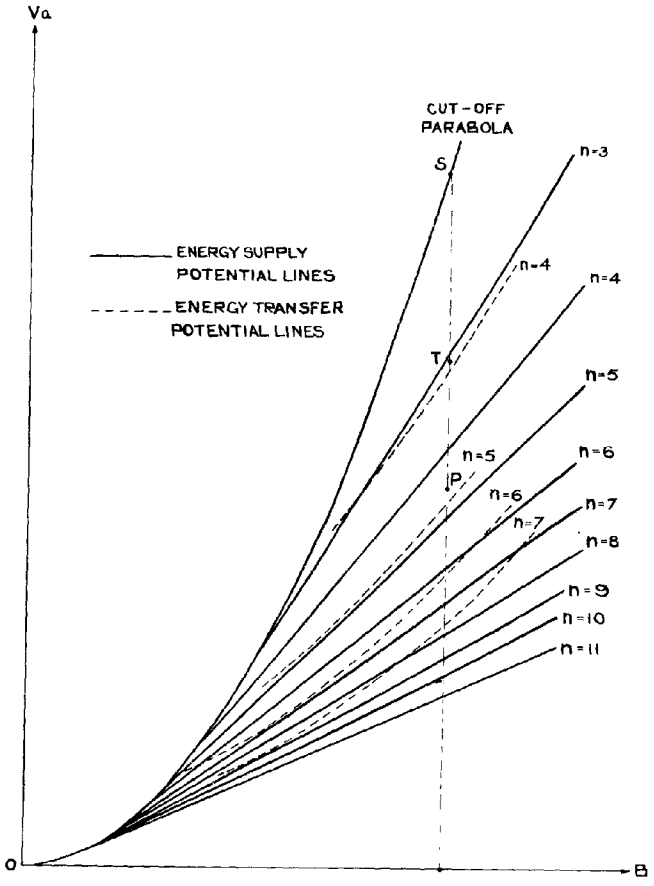

Fig. 439 - Operating conditions for an unstrapped magnetron.

(ii) and (iii) combined given the information that oscillation in the n = 5 mode is possible. The diagram also shows that oscillation in any lower order mode is not. With the working point at P, however, not only are the conditions for oscillation in the mode n = 5 fulfilled, but so also are those for all higher order modes. Thus the coexistence of several modes appears possible. Actually this does happen, and has a deleterious effect which has to be minimised; (see Sec. 35). However, the deformation of the space charge is greater the smaller the value of n so that, although other modes might well be present, the mode n = 5 would predominate in the case indicated.

To operate the magnetron in the n = 4 mode with fixed B would involve raising V_a so that the working point was (say) T. It is possible to show, however, that for efficient operation V_a should be as near as possible to the energy supply potential. In any mode for which the energy transfer potential considerably exceeds the energy supply potential, as with the n = 4 mode here shown, working would be inefficient. It would be better in the case shown to work in the mode n = 5 or n = 6.

Consider V_a raised quickly, but not instantaneously, from zero to its working value. Then V_a rapidly passes through the conditions for oscillation in the modes given by n = 10, 9, 8, 7 etc., operation in these modes becoming more inefficient, and in some case ceasing altogether as V_a rises. These different modes will, in general, cause the magnetron to operate at different frequencies, so that operation at the desired frequency may not take place until some short time after the pulse has been initially applied. The ensuing delay between the application of the modulating pulse and the transmission of the RF pulse at the correct frequency might lead to Range errors if not allowed for in the timing system.

The coexistence of several modes, operating at slightly different frequencies is undesirable, and is minimised by Strapping.

35. Strapping

The purpose of strapping is to minimise the coexisting modes, both in number and in magnitude of oscillation. It is done by connecting short conductors between pairs of segments, the segments so connected being separated by a third. In a general way it is easily seen that joining segments in this manner will tend to favour some modes rather than others. For example, if an 8-segment magnetron be taken and alternate segments joined as in Fig. 440, the π-mode (n = 4) is favoured, since this implies a phase difference between the strapped segments of 2π. For the mode n = 5 the phase difference would be $\frac{5\pi}{2}$, a condition impossible if the segments are short-circuited. Strapping is, however, not as simple as is here implied, since the straps cannot be regarded as simple short-circuits. For each strap, being a conductor, has inductance, and since it passes over the separating segment, capacitance exists between it and this segment. Thus the presence of the strap alters the frequency at which a particular mode operates. In the π - mode the strapped segments are at the same potential, and hence the strap carries negligible current; so its inductive effect can be ignored. Its capacitive effect cannot; hence the frequency corresponding to the π-mode is lower when the magnetron is strapped than when it is not, by an amount largely determined by the strap position relative to the block. If the mode n = 5 arose there would be current through the strap; so its inductive effect would be important, as would its capacitive effect also. Hence although the general effect of strapping is to change the frequencies at which modes arise, such changes will usually be

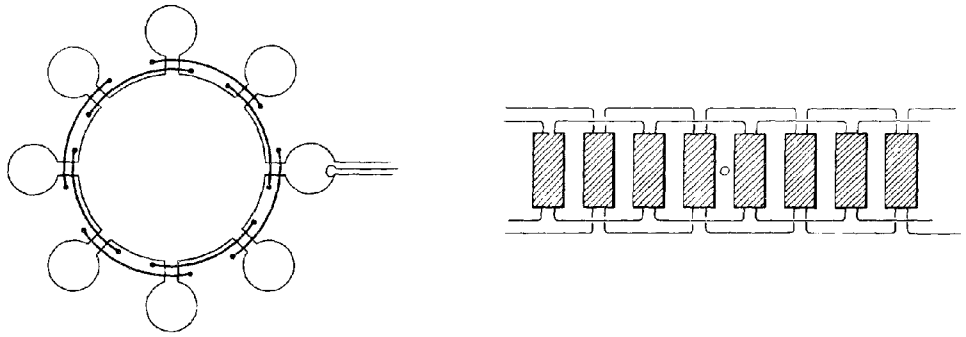

(a) DOUBLE RING STRAPPING (SINGLE RING STRAPPING OMITS THE OUTER STRAPS AT ONE END AND THE INNER STRAPS AT THE OTHER END)

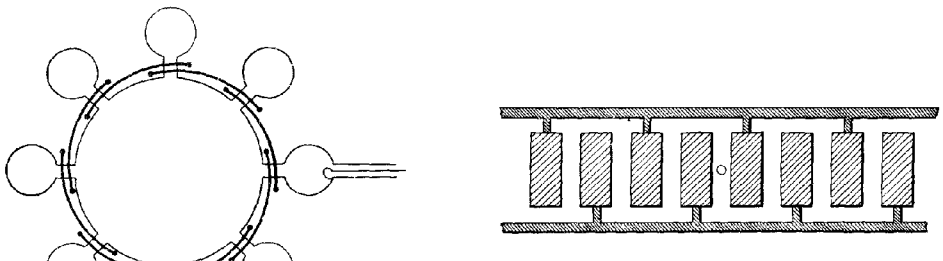

(b) ECHELON STRAPPING BOTH ENDS

(c) STRIP STRAPPING

(d) INCOMPLETE RING STRAPPING

(e) Y - B STRAPPING

Fig. 440 - Strapping systems.

different for the several modes. Thus the different modes are separated in frequency by strapping; and the conditions in the magnetron system as a whole, and in particular the selectivity of the load, may then be adjusted so that matching is achieved at the frequency of the required mode; (normally of the lowest order possible, and most commonly the π-mode).

The suppression (or minimisation) of all but the wanted mode markedly increases the efficiency. For example, it has been explained that, if Va is such that the operating point is almost on the n = 5 energy supply potential line of Fig. 439, any n = 6 (or higher mode) output must be inefficiently produced. Hence its contribution to the total magnetron output must reduce the overall efficiency. Since strapping, by diminishing the unwanted modes and separating

them in frequency, tends to make the output consist almost entirely of the required efficient modes, its introduction results in a very considerable increase in the overall efficiency of this type of magnetron.

Referring again to Fig. 439, it has been stated that working in the n = 4 mode (at point T) would be less efficient than working in the n = 5 mode at point P. Whilst this is true for the unstrapped magnetron, it is not true for the strapped magnetron, to which Fig. 439 would not apply. This is because the value of the energy supply potential for a given B and n depends upon frequency, and hence changes with strapping.

Some common forms of strapping in practical use are shown in Fig. 440.

Strapping also provides a means of pre-tuning, i.e. setting up the magnetron on a spot frequency before it is sealed off. The lid is kept off and CW from a klystron oscillator at the desired frequency is injected into the magnetron through the coupling loop. The straps are then bent until the magnetron resonates at the required frequency, this condition being determined by the use of a resonance indicator in the coaxial line from the klystron to the magnetron. (Allowance has to be made for the difference in frequency occasioned by the presence of the lid and the space charge, in the operating magnetron: but empirical rules enable this to be done with the required accuracy).

The omission of one or more straps from an otherwise symmetrical system, or introducing a break in a strap (or straps) can have a marked effect on the response of a magnetron at some particular mode or modes. Strap omission is sometimes made necessary by such practical factors as the position of cathode leads etc.

36. Effect of Anode Length, and of End-Plate Distance

The length of the anode and the distance between it and the end plates influence the frequency of the various modes; Figs. 441 and 442 indicate the extent of this effect. The fact that the anode-to-end-plate distance affects the frequency of operation is made use of in tunable magnetrons, one form of which has a thin lid the centre of which may be depressed and the frequency thus changed. In this way a change of about 150 Mc/s in 3000 Mc/s can be achieved. Another form of tunable magnetron has metal rods which can move in and out of the anode block, thus altering both its effective length and the anode-to-end-plate separation.

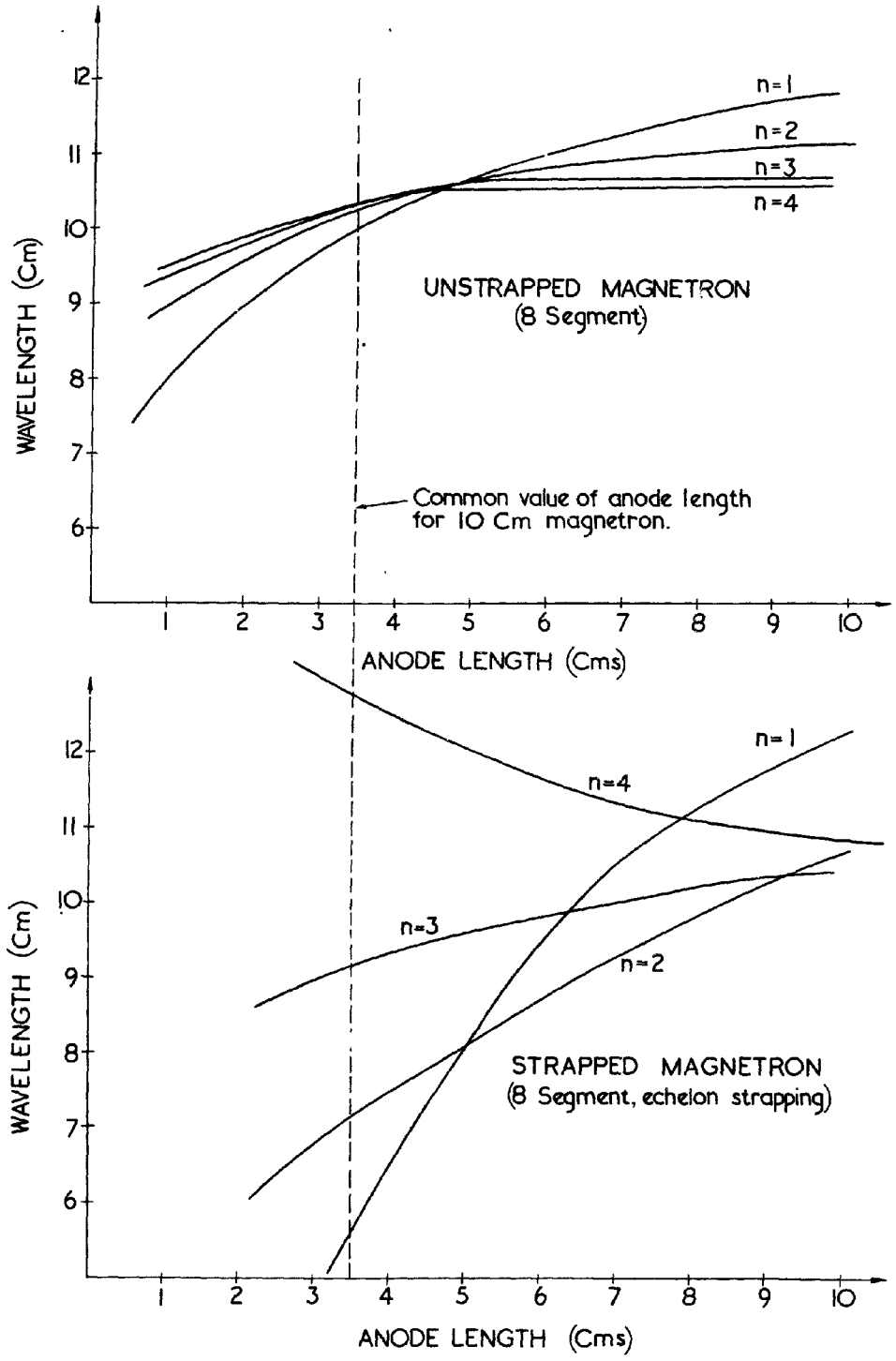

Fig. 441 - Wavelength v. anode length for strapped and unstrapped magnetrons.

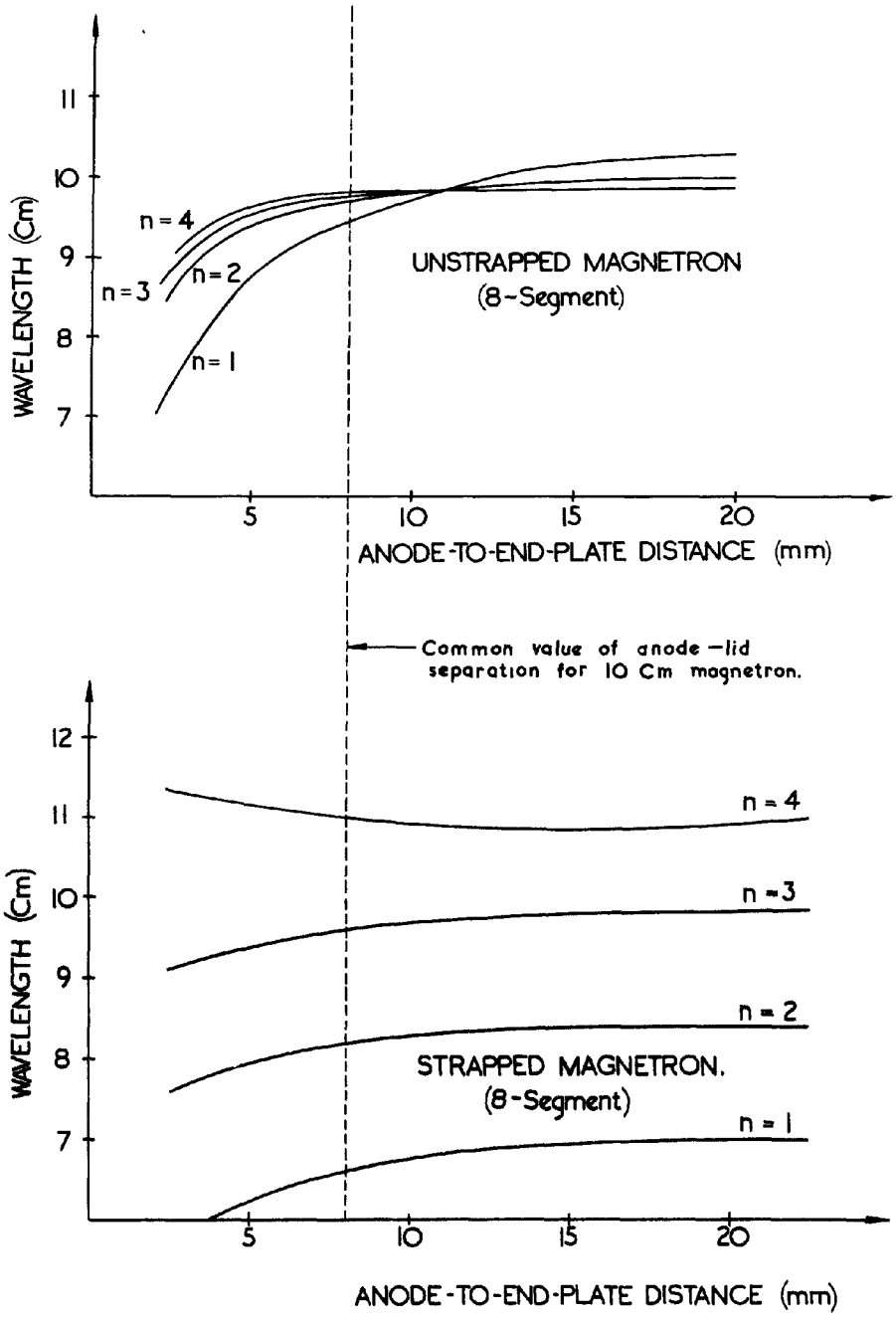

Fig. 442 - Wavelength v. anode-to-end plate distance for strapped and unstrapped magnetrons.

37. Output Couplings

The output is commonly taken from a magnetron by means of a coupling loop, made by bending round the inner of the coaxial output line and soldering it on to the outer (see Fig. 422). The output can then be adjusted by turning the loop, thus varying the magnetic flux linkage.

At 3 cm. and shorter wavelengths it is not practicable to make loops small enough to be located within the cavity in this manner, and the methods indicated in Fig. 443 are used. (a) shows a loop inductively coupled to the cavity; in (b) the output conductor is attached to the upper surface of one of the segments of the anode block; and in (c) to one of the ring straps commonly used at these wavelengths.,

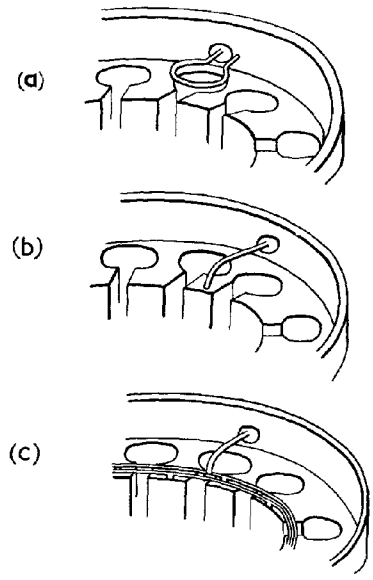

3 Cm OUTPUT COUPLINGS

Fig. 443 - 3 cm. output coupling.

38. Cathode Features

The turbulence of the electron cloud in an operating magnetron is vigorous enough to force a proportion of electrons back to the cathode with increased energy. There is consequently additional heat dissipated at the cathode and a possibility of cathode disintegration. The energy dissipated in this way is sometimes so large that, after an initial warming-up period, it is possible to reduce the magnetron heater supply, or even switch it off entirely. The cathode must be robust to withstand the bombardment, and is commonly made by using a nickel mesh as a foundation and filling this with emissive oxide.

39. Pulse Operation of Magnetrons

In most radar applications magnetrons are required to produce high power RF pulses of short duration, this being normally achieved by applying to the cathode approximately rectangular negative-going pulses, of the required duration. This is preferable to applying positive going pulses to the anode, which it is usually convenient to earth. The pulses should be steep-fronted and have a rapid die-away, to minimise the effect of unwanted modes set up when V_a is changing. (See Sec. 34). They should also have a flat top, since changes in V_a during the oscillating period can seriously affect frequency, efficiency and output power.

40. Magnetron Characteristics and Rieke Diagrams

Two methods are in common use for presenting magnetron performance, namely, Magnetron Characteristics and Rieke Diagrams. Magnetron Characteristics are drawn in Cartesian Coordinates, the modulating voltage applied to the magnetron in pulsed operation being graphed against the value of the valve current I_a during the pulse. Contours of constant flux density B and contours of constant RF output power are drawn. Sometimes efficiency contours are also included.

An example of a set of magnetron characteristics is given in Fig. 444. It is seen from this that to obtain high efficiency it is necessary to have a high value of applied voltage and magnetic flux density. For constant B there is an optimum value for V_a beyond which the efficiency begins to fall.

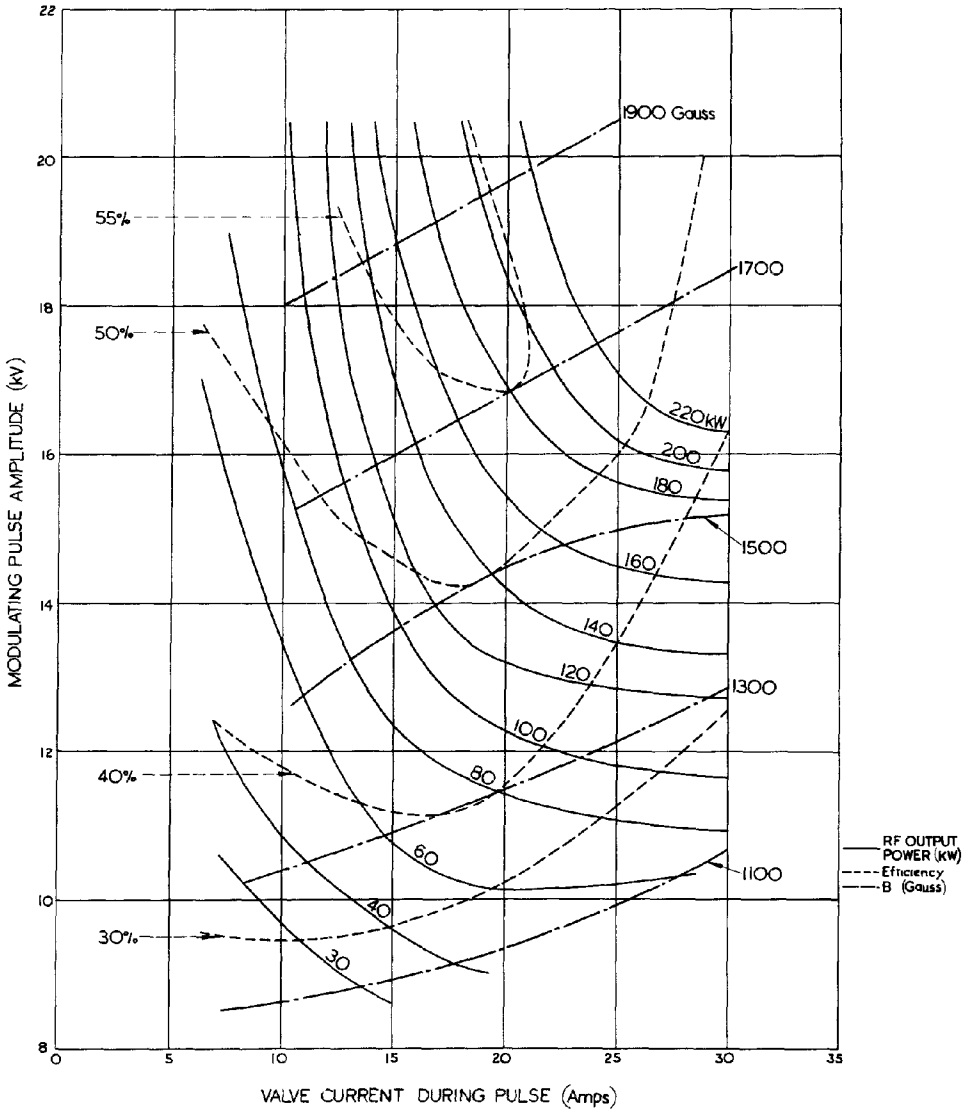

Fig. 444 - Magnetron characteristics.

Whereas Magnetron Characteristics indicate magnetron performance under conditions of varying V_a and B, the load being always adjusted for maximum output power, Rieke Diagrams show performance for fixed I_a (or V_a) and fixed B for variations of load impedance.

xxx Rieke Diagrams

Consider the magnetic field strength and pulse amplitude to be constant. Then variation of load impedance over all possible values of resistance and reactance will cause changes in valve current, peak power output, efficiency, frequency of operation, and frequency stability. Corresponding changes occur if the current is fixed and the voltage varied. It would be possible to plot these variations as contours on Cartesian axes representing values of resistance and of positive and negative reactance; but it is more convenient to plot them on a Polar Circle Diagram as shown in Fig. 445. This has the advantage that the effect of a loaded output line or waveguide can be taken into account on the same diagram when performance is being deduced in a particular case. The normal circle diagram technique is then employed to transform the impedance to the output loop so that the corresponding performance can be read off.

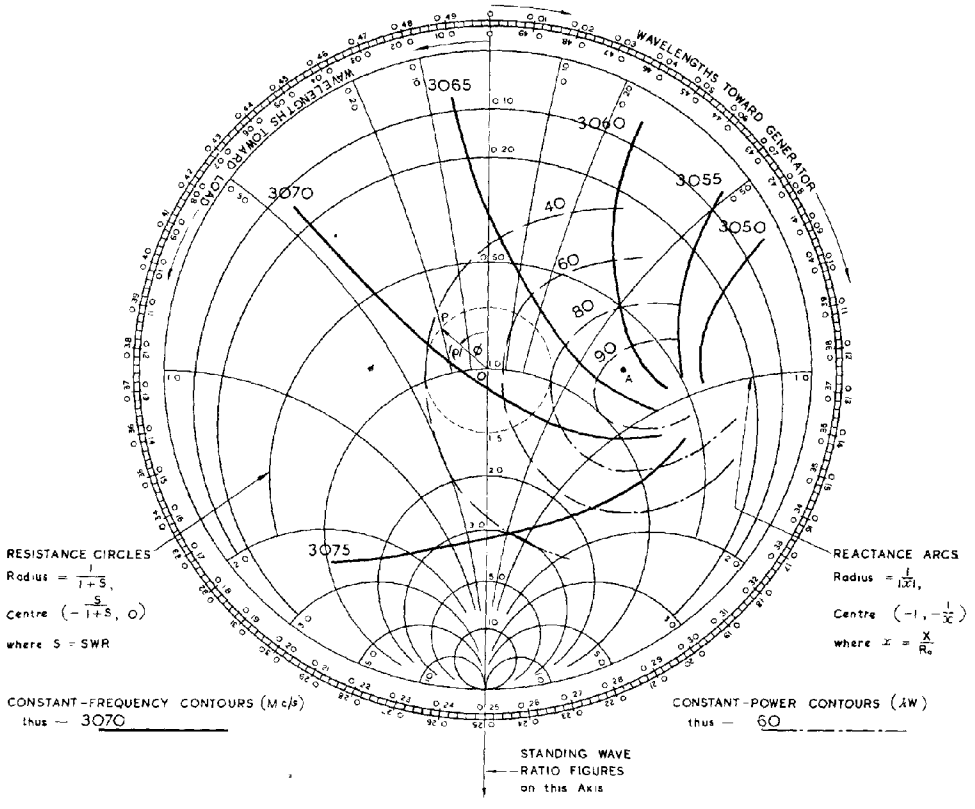

Fig. 445 - Rieke diagram.

In the Polar Circle Diagram, the complete circles represent circles of constant resistance and the arcs orthogonal to these circles, constant reactance. An important property of this circle diagram is that when the line is terminated in a load represented by the point P, the magnitude of the reflection coefficient ρ of the load is represented by OP, and the phase change on reflection is given by ϕ (see Fig. 444).

Hence circles centred at O are circles of constant ρ. These are also circles of constant standing wave ratio since reflection coefficient and standing wave ratio are interrelated (SWR. = $\frac{1 - \rho}{1 + \rho}$). The vertical axis is scaled in terms of the standing wave ratio.

The following important points arise from the diagram. In the example taken, the region of highest power lies at A. Following the constant-ρ circle from A to the vertical axis reveals that the corresponding standing wave ratio is not unity. This implies that the line or waveguide is mismatched; and this is due to the fact that the optimum load for the magnetron at the output loop is different from the characteristic resistance of the line or waveguide. In order to match the magnetron output impedance to the line or waveguide, many modern magnetrons have a built-in matching device at the output loop. In the region of A the frequency stability is poor because the frequency contours converge, so that a small change in loading causes a comparatively large change in frequency. Hence operating the magnetron to obtain maximum output power makes good frequency stability impossible.

The operating conditions of the magnetron and the maximum efficiency at which it can be operated depend upon the characteristics of the magnetron and its load; i.e. the radar system of which the magnetron is part. The particular features of the radar system that are important are the modulating voltage and pulse shape, the type of receiver employed (e.g. whether there is Automatic Frequency Control or not), and the maximum standing wave ratio that may be set up in the feeder system due to joints, spacers, and variations in loading originating at the aerial array.

Suppose, for example, that the standing wave ratio on the line or guide is subject to variation between 1 and 1·5, due, perhaps, to a variable termination of the line caused by a faulty scanning system. This variation of the SWR of necessity causes fluctuations in the magnetron frequency. If automatic frequency control (see Sec. 49 - 53) is not employed at the receiver this may seriously affect the performance of the radar system. Suppose that a frequency change of 10 Mc/s is permissible. Then, since a SWR of 1·5 corresponds to $\rho = 0{\cdot}2$, the magnetron can be operated under such conditions that the constant-ρ circle of radius 0·2 does not cover more than 10 Mc/s change in frequency contours.

41. Frequency Stability and Pulling Figure

Frequency changes in an operating magnetron can be traced to several causes. As has already been pointed out, variation in input conditions produces a change in frequency. As this variation also results in a change of anode current, the effect is called Current Pulling and is of the order of 0·1 to 1 Mc/s per ampère for 10 and 3 cm. magnetrons. Variation in anode block temperature also causes a frequency change because of the expansion of the block. The change is roughly proportional to the change in temperature and the coefficient of linear expansion of copper. Load variations are the

most important causes of frequency changes. The term Pulling Figure is defined as the difference between the highest and lowest frequencies obtained as the load is varied in any manner which does not cause the standing wave ratio to exceed its maximum permissible value. Normal values of pulling figure are of the order of 10 to 15 Mc/s.

If a long transmission line or waveguide is employed between the magnetron and the aerial system operation at more than one frequency may be possible, and the magnetron frequency may jump from one value to another more or less at random. This is commonly known as Frequency Splitting. It is avoided by keeping transmission systems as short as possible or by avoiding standing waves on long lines or guides.

Use of Rieke Diagrams to Illustrate Frequency Pulling and Frequency Splitting

In the example already quoted in Sec. 40, referring to Fig. 445, the standing wave ratio was assumed to be 1·5, so that $\rho = 0{\cdot}2$. The frequency variation over the region covered by the circle $\rho = 0{\cdot}2$ may be determined by interpolation between the frequency contours already drawn. The pulling figure may thus be shown to be about 6·5 Mc/s.

The Rieke diagram also illustrates how a short line is preferable to a long one. Suppose that the line (or guide) is of length ℓ and that the standing wave ratio is 1·5. If the frequency is varied the electrical length $\frac{\ell}{\lambda}$ of the line changes, but to a first approximation the standing wave ratio may be taken as constant. The working point on the Rieke diagram correspondingly traverses a constant-ρ circle as shown in Fig. 445. For any given position of the point on the circle the corresponding angle ϕ is, in fact, the phase angle between the direct and reflected waves on the line at the input terminals, and hence the relation between f and ϕ is given by

$$\phi = \frac{4\pi\ell}{\lambda} + \phi_r,$$

where ϕ_r is the phase change on reflection at the load. (In the case of a waveguide λ_g should be read for λ in the preceding expressions). We may thus deduce that

$$\phi = \frac{4\pi\ell f}{u} + \phi_r \quad \ldots\ldots\ldots\ldots\ldots\ldots (5),$$

where u is the velocity of propagation on the line (or the phase velocity in the guide). In Fig. 446, f is plotted against ϕ, giving the line XY.

Suppose now that the line is energised by the magnetron. Then there is the fundamental relation between f and ϕ already plotted in Fig. 446, obtained direct from the Rieke Diagram. The working conditions are therefore given by the intersections of the two curves. In the example taken there are three intersections, suggesting that there are three possible operating frequencies. However, only two are possible, because although the three points of intersection give three conditions of equilibrium, the one at A is unstable. For if some small change in the system were to occur, resulting in a small increase in f, then, from equation (5) ϕ is increased; as shown by the frequency pulling curve, this would result in a further increase in f. On the other hand, at B and C

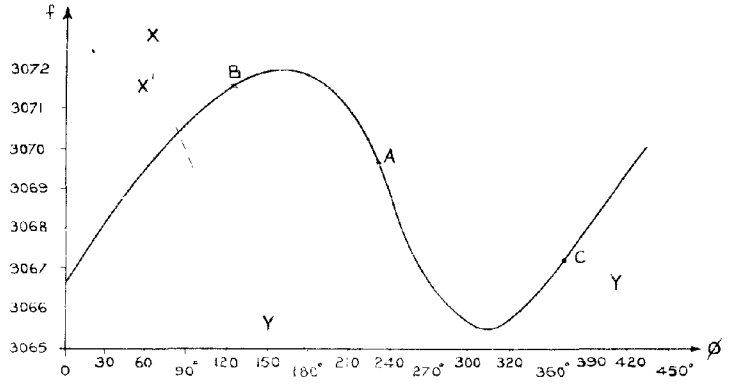

Fig. 446 - Frequency pulling curve (full line).

an increase in f causes a decrease in ϕ , which tends to pull the frequency back. Since these two frequencies are equally possible the magnetron may jump from one to the other, causing frequency splitting. If this is to be avoided the line XY must be sufficiently steep for the curves to intersect at one value of f only as indicated by X'Y'. The slope of the line XY is $\frac{u}{4\pi\ell}$; hence, to make XY steep enough to avoid frequency splitting, ℓ must be sufficiently small.

For a certain critical length of line or guide the slope of XY will be equal to the maximum slope of the frequency pulling curve; and it is then possible, with one value of ϕr, for XY to be tangential to the frequency pulling curve at its steepest part. This leads to very considerable frequency instability, and is termed Broad Spectrum operation.

Further, a long line or guide is troublesome because the impedance as seen by the magnetron changes at time intervals corresponding to twice the transit time of the line or guide, due to reflections from the load back to the magnetron; these cause varying load impedance at the magnetron output loop and corresponding frequency changes. (The importance of this effect will depend upon the extent of the mismatch at the termination).

The longer the line, the more stringent must be the magnetron specification in regard to frequency stability; i.e. the smaller must be the pulling figure. An improvement in stability may be obtained even for long lines by putting a stub tuner close to the magnetron to adjust the region of operation so that it covers a fairly flat portion of the frequency characteristic.

42. Pre-plumbing of Magnetrons

Pre-plumbing is a process whereby magnetrons, complete with such devices as stubs, common T/R, and other switching apparatus, etc., can be so accurately manufactured that subsequent adjustment is unnecessary. This precludes any possibility of the introduction of instability due to maladjustment.

CONTROL OF NEGATIVE-GRID OSCILLATORS

43. Stabilisation of Oscillators

Oscillators may be divided into two classes, Master Oscillators and Power Oscillators. The former are usually required as frequency standards and are protected from variations in loading which would tend to upset the frequency stability. Power oscillators, on the other hand, must maintain an adequate frequency stability and a high degree of efficiency whilst undergoing various changes in loading conditions. Both types are used in radar. For various reasons, among which conservation of power, bulk and weight predominate, it is usual to employ power oscillators in transmitters rather than master oscillators followed by power amplifiers. At UHF there is no choice, since the problem of satisfactory amplification has not been solved. For calibrators, where accuracy is of primary importance, a frequency-stabilised oscillator is often used, followed by amplifying stages. Crystal-controlled oscillators are commonly employed, being superior to other types in this respect.

Oscillators should be protected from such fluctuations in supply voltage as produce variations in output frequency.

Control of the amplitude of the output voltage of an oscillator commonly takes the form of an automatic volume control circuit, controlling the bias of the valve. The use of automatic bias by grid leak and condenser, described in Chap. 7 Sec. 4, is a particular case. Frequency stabilisation may be provided by the use of a large-valued resistance in the feedback circuit. This resistance is in series with the slope resistance of the valve and its large value masks variations in R_a which might otherwise affect the oscillation frequency.

In some radio-frequency oscillators commonly used in superheterodyne receivers and signal generators, the dual functions of master oscillator and power amplifier are performed by the same multi-electrode valve. A pentode, for example, may be employed, with control grid, screen and cathode acting as a triode oscillator, whilst the output is taken from the anode, screened from the oscillatory circuit by the suppressor grid. By this means variations in loading are substantially prevented from affecting the oscillation frequency. This type of circuit is usually referred to as an electron-coupled oscillator.

It is frequently found that a rise in mean anode potential affects the frequency in one direction, whereas a rise in screen potential has a reverse effect. When this occurs a suitable potentiometer arrangement for supplying screen and anode from the same supply may be chosen so that these two effects cancel each other, leaving the frequency of oscillations relatively independent of supply voltage.

In general it is possible to improve frequency stability by causing the circuit to oscillate at, or very close to, the resonant frequency of the tuned circuit employed. The effect of a high-Q circuit is largely nullified if it is used as a reactance. By inserting various compensating reactances in one or more of the electrode leads it is often possible to allow for interelectrode capacitances and other stray reactances so that the tuned circuit is used at the peak of its resonance curve. This is not practicable at very high frequencies when lead inductances introduce further complications.

44. Steady State Conditions

The performance of oscillators often depends fundamentally on the values of the supply voltages, and by suitable control of these an oscillator may be given various characteristics. To show how this is done it is first necessary to examine what factors determine the steady-state conditions of an oscillator.

Fig. 447(a) shows the schematic arrangement of the four oscillator components listed in Sec. 1. For purposes of description it is convenient to divide these into two parts, the "amplifier" and "network" sections respectively, as indicated at (b). Each of these parts may be considered separately, provided it is correctly terminated; i.e., when considering the behaviour of the amplifier section, it must be terminated by the input impedance of the network, and vice versa.

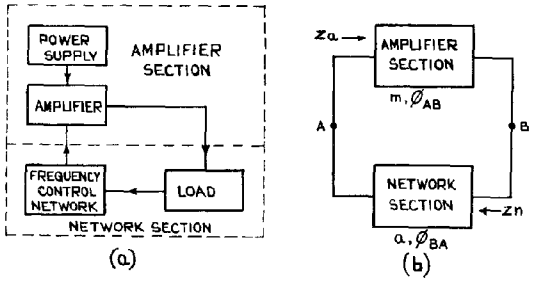

Fig. 447 - Schematic arrangement of fundamental oscillator components.

It is convenient to include the effect of grid current as extra damping in the network; this effect is of considerable importance in limiting the amplitude of oscillations in conventional oscillators.

It will be assumed that oscillatory voltages are sinusoidal. This is approximately true even for Class C operation, with non-sinusoidal currents, provided the tuned circuits are highly selective.

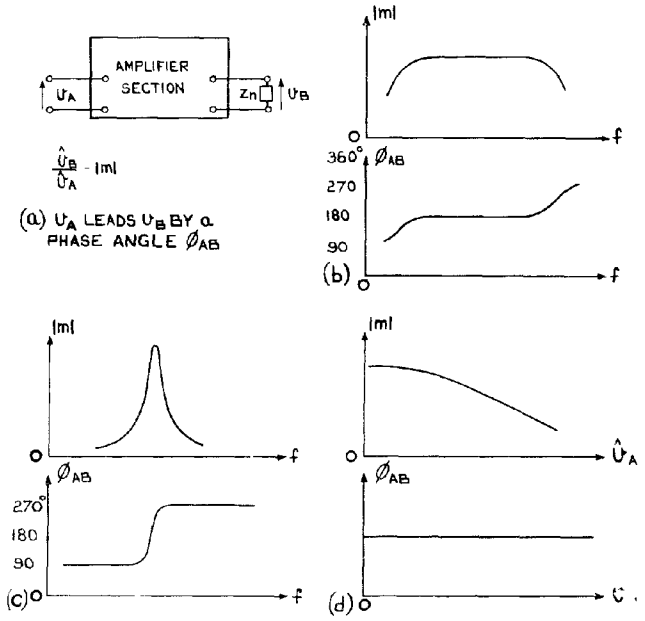

Fig. 448 - Amplifier section.

The behaviour of the amplifier section, terminated in z_n (Fig. 448(a)) may be described in terms of its amplification $|m| = \frac{\hat{v}_B}{\hat{v}_A}$ and phase shift ϕ_{AB}. Both of these vary with frequency. If z_n is resistive, as in a video amplifier, the normal variations of $|m|$ and ϕ_{AB} with frequency are as shown at (b), whilst if z_n is the impedance of a parallel tuned circuit, Fig. 448(c) shows typical variations.

As the amplitude of oscillation varies, the non-linearity of the characteristics causes changes in the value of $|m|$. To a first approximation ϕ_{AB} is not affected. These effects are illustrated at (d).

Similarly, the behaviour of the network section is illustrated in Fig. 449. If it is linear there will be no change in phase ϕ_{AB} or in attenuation $|a|$ as the amplitude is altered. ($|a| = \frac{\hat{v}_B}{\hat{v}_A}$).

There will be considerable variation as the frequency changes, depending on the nature of the network. Fig. 449(a) shows a typical high-Q circuit which might form the network, and (b) and (c) show the attenuation and phase variations with frequency.

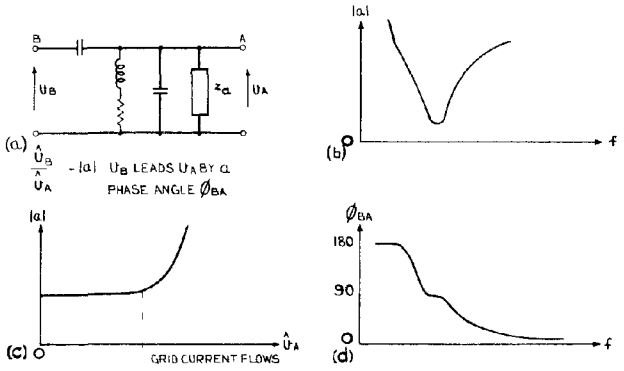

Fig. 449 - Network section (typical case).

When the effect of grid current damping is included in the attenuation $|a|$, this is not linear, but increases considerably when the amplitude of oscillations becomes large enough to raise the grid above cathode potential. This effect is illustrated at (d).

When the two sections, amplifier and network, are joined together to form the complete oscillator, steady oscillations can be maintained only if two conditions are fulfilled; the amplification of the amplifier must be just sufficient to compensate for the attenuation of the network; also the phase shift for the combined circuit must be a whole number of complete cycles; i.e. $|m| = |a|$, and $\phi_{AB} + \phi_{BA} = n.360^o$, where n is an integer.

Together these relations determine the frequency and amplitude at which oscillations may be maintained. In theory there may be several values of each which satisfy the steady state conditions, but in practical circuits one mode of oscillation usually predominates to the exclusion of others.

45. Effect of supply potentials on steady state conditions

In practical oscillators the frequency is seldom appreciably affected by variations in mean anode or grid potentials (save in the case of relaxation oscillators, not considered here.) But since such changes affect the amplifier gain they have considerable effect on the amplitude of oscillations. Maximum amplification is available under Class A working, but not necessarily maximum amplitude. This is because oscillations usually build up until the flow of grid current has increased the damping to the point at which attenuation is equal to amplification. An increase in bias in the first instance increases amplitude but decreases the values of both |a| and |m| in the steady state. If the bias is maintained at a steady level and the HT supply raised, amplitude is usually increased and also |a| and |m| .

In most triode oscillators it is the effect of grid current rather than curvature of valve characteristics which predominates in determining the amplitude at which oscillations will be maintained.

With Class C bias, oscillations are not self-starting since initially the angle of flow of anode current (Chap. 7 Sec. 4) is zero, and therefore |m| = o. When an input signal is applied causing anode current to flow, |m| increases with amplitude as illustrated in Fig. 450(a), Curve III. The effect of increasing bias is to delay the point at which amplification commences and also to reduce the gain for a given amplitude. A similar result follows a reduction in HT potential, the reduced angle of flow causing a reduction in |m| . This similarity is illustrated at (b).

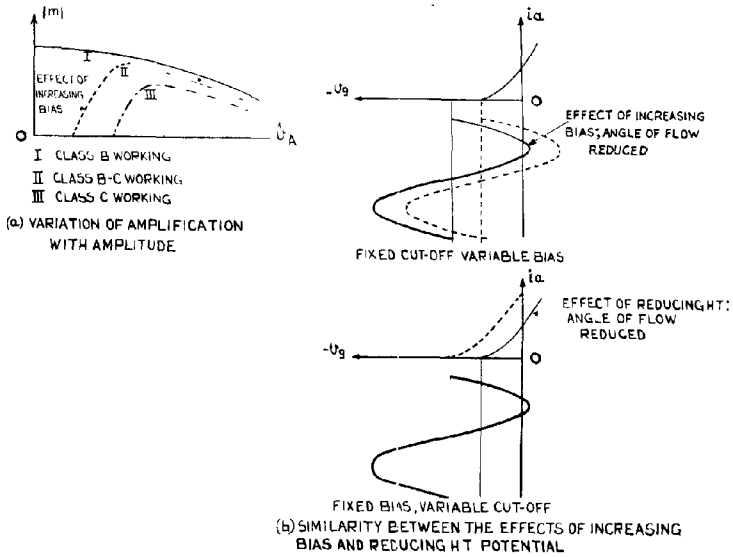

Fig. 450 - Effects of bias and HT potential on Class C operation.

The damping effect of grid current must be compared with the other damping factors of the network. Although the network may have a high Q, excessive grid-current damping will effectively reduce both the selectivity and the dynamic resistance of the network, assuming that it acts as a parallel tuned circuit.

In general, for a given HT supply, there is a unique value of bias necessary to maintain oscillations at a given amplitude. If a large amplitude is required this may be provided by an increase in bias. There is clearly a limit to this process, since as $|m|$ is reduced to a point at which it is less than the minimum attenuation $|\check{a}|$ oscillations cannot be self-maintained under any circumstances.

Similarly if the bias is held constant and the HT reduced, a point will be reached at which oscillations cease altogether, owing to the steady reduction of the angle of flow until $|m| < |\check{a}|$ for all values of $\hat{v}_A$.

46. Biasing circuits

As pointed out in Sec. 45, the effect on an oscillator of varying the bias is chiefly to change the amplitude of oscillations, and appreciable changes of frequency do not usually occur. If it is important that the amplitude should be constant, the steady supply potentials should not be allowed to vary, and the circuit should be designed as a master oscillator, so that changes in loading do not affect the operation. Under these circumstances, a constant bias can often be provided by a conventional cathode resistor with a by-pass condenser of sufficiently large capacitance, or by a suitable potentiometer arrangement.

If a valve oscillator is not otherwise protected from noticeable changes in loading, it should be provided with an automatic regulating device which increases the available power as the power demanded by the load increases. It will be shown that in common oscillator circuits such a requirement is not met by a cathode biasing circuit, and that for Class B or C working the reverse is true; viz. as the load increases due to a diminishing load resistance, which increases the damping of the circuit, the corresponding bias increases so that the available power is also diminished. In the circuit of Fig. 451(a) the valve current for Class B working is as shown at (b). Increased damping of the tuned circuit diminishes its dynamic resistance so that the amplitude of the anode alternating voltage is diminished; (c). This raises the anode voltage during the conducting period of each cycle, and thus increases the valve current; (b). This increases the bias. The same argument holds for Class C conditions.

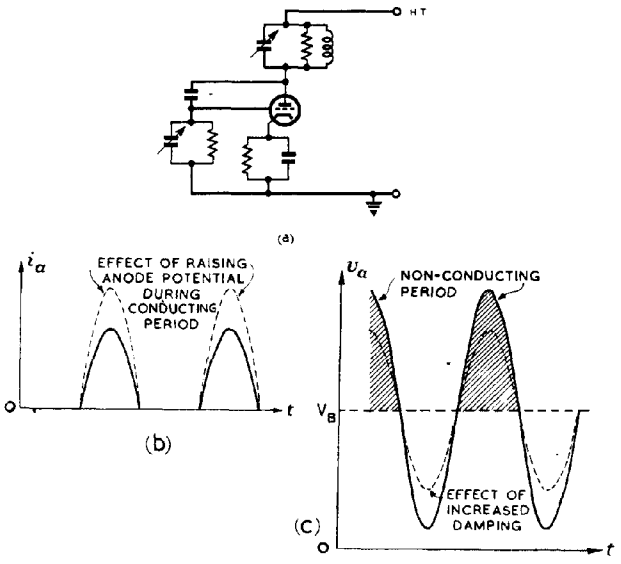

Fig. 451 - Non-self-compensatory effect of cathode bias.

The use of self-bias by grid leak and condenser provides automatic regulation approaching the form desired to compensate for variations in loading. In the circuit of Fig. 452(a) a decrease in amplitude of the alternating anode voltage decreases the amplitude of the grid voltage so that the condition for steady bias, viz, "charge accumulated on C during each cycle = charge which leaks away through R during each cycle" is no longer maintained, through the reduction in the angle of flow of grid current. More charge leaks away, diminishing the bias and increasing the angle of flow until a new stable condition is reached with a smaller bias. This increases the available power.

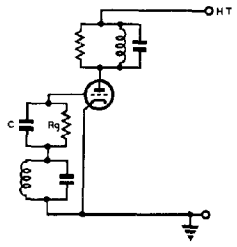

Fig. 452 - Biasing circuit using grid leak and condenser.

47. Self-quenching oscillators

The fundamental requirement for a pulse radar transmitter is the production of bursts of RF oscillations recurring at a suitable repetition frequency. This requirement can be met by suitable design of the power oscillator. Instead of maintaining continuous oscillations, an oscillator can be modified to allow oscillations to build up, reach a maximum, and decay, the valve remaining quiescent for a period, and the cycle then repeating automatically. This process is known as Self-Quenching, and when it arises from an auto-biasing arrangement in the grid circuits, the oscillator is very commonly known as a "Squegger", or Squegging oscillator. This term is also applied somewhat loosely to oscillators where the self-quenching circuit is in the anode or cathode lead.

In all cases the action arises from a gradual reduction in $|m|$ by an increase in the bias or a reduction of available HT potential, until $|m|$ becomes less than $|a|$. Under these temporary conditions oscillations cannot be maintained and usually cease altogether.

During the subsequent interval no valve current flows and the bias or HT potential returns to the value at which oscillations become possible, and the cycle repeats.

Squegging Oscillators

The actual oscillator circuit chosen to describe this behaviour is not important, and subsequent remarks apply equally to most types other than the common-cathode circuit drawn in Fig. 452.

The squegging action is illustrated in Fig. 453(a). Oscillations build up and the bias increases due to the accumulation of charge on C. Provided certain conditions are satisfied, which will be considered below, a point is reached at which the bias becomes greater than the value at which oscillations can be maintained, when the RF oscillations begin to be damped out. The charge on C leaks away through R_g and the bias is reduced until cut-off is reached. At this point $|m|$ is greater than $|a|$, and oscillations recommence. When grid current flows the bias increases and the cycle repeats.

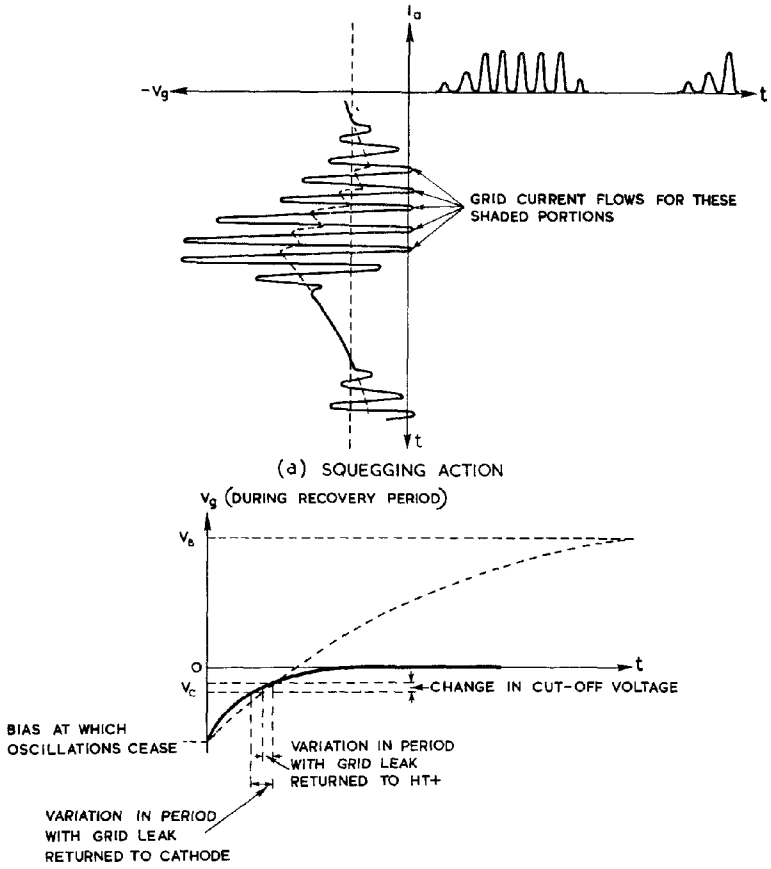

Fig. 453 - Effect of returning grid leak to a source of high potential.

The pulse width depends on the charging time-constant CR_i, where R_i is the mean DC resistance of the grid-cathode circuit when grid current flows. The recurrence frequency depends chiefly on CR_g, since it is usual for R_g to be much greater than R_i.

The circuit may be modified by returning the grid leak either to cathode or to HT potential. In the first case the action is the same except that the voltage developed across the grid leak is alternating instead of approximately constant. The connection of the resistor to a source of high potential, together with a suitable adjustment in time-constant so that the recurrence period is not altered, makes the onset of oscillations more definite and the recurrence frequency correspondingly more constant. This is illustrated at (b). A fluctuation in HT supply, for example, causing a variation in the cut-off voltage, would have much less effect on the periodicity in the modified circuit, as indicated in the diagram.

xxx Conditions under which Squegging Occurs

The mechanism of the cessation of oscillations may now be dealt with in greater detail. Suppose that the oscillations can be maintained at any chosen constant amplitude. The circuit is then equivalent to an amplifier being driven by a constant voltage generator. This generator will provide or absorb energy according

as $|m| < |a|$ or $|m| > |a|$ for this amplitude of signal voltage $\hat{v}_i$. For a given C-R network and constant input amplitude the bias developed across C will settle down to a steady value V_g depending on $\hat{v}_i$, C, R_i and R_g. Provided $CR_i \gg$ the duration of grid current flow for each cycle, and provided $CR_g \gg T$, the period of oscillations, the grid voltage will be approximately sinusoidal, as in Fig. 454, these being the conditions for non-distortion. The ratio $\frac{-V_g}{\hat{v}_i}$ then depends on the ratio $\frac{R_i}{R_g}$ only, to a close degree of approximation, and the relation between them is

$$\frac{-V_g}{\hat{v}_i} \doteq \sqrt{1 - \left(\frac{\pi R_i}{2R_g}\right)^2} \qquad \text{provided } R_i \ll R_g.$$

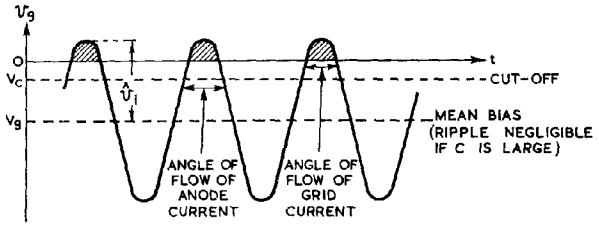

Fig. 454 - Steady state relation between $\hat{v}_i$, V_b and the angles of flow of grid and anode currents.

If we now plot the variation of $|m|$ and $|a|$ with amplitude $\hat{v}_i$, we obtain curves such as are shown in Fig. 455. The value of $|a|$ has been assumed constant, since the network is assumed linear, and the attenuation due to grid current is also linear under the assumed conditions.

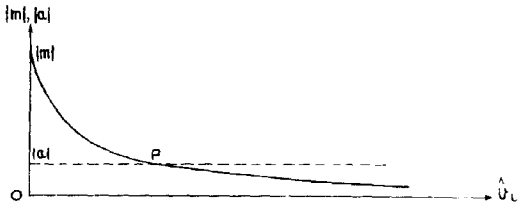

Fig. 455 - Variation of $|m|$ and $|a|$ with amplitude.

Provided the assumptions which have been made are justified, it follows that at the point P the controlling generator could be removed and oscillations would be maintained at the corresponding amplitude, where $|m| = |a|$. That this does not happen in the squegging oscillator is due to the delay which occurs in the build-up of bias, since, before the steady state operating point P is reached, the bias will be less than that for which the curves of Fig. 455 are drawn. The effect of this lag is indicated in Fig. 456. Both $|m|$ and $|a|$ are increased, since the angles of flow of both anode and grid currents are larger. In other words, the amplitude will be momentarily stabilised at the value for the point Q instead of P, towards which it must tend for stability.

Two cases arise, shown at (a) and (b) respectively. In (a), $\delta|m| > \delta|a|$, and the point Q is to the right of P.

This means that the amplitude of oscillation is larger than the value at which $|m| = |a|$. Oscillations continue until the bias has increased beyond the required value, since this value must be exceeded before the amplitude begins to decrease. Once the bias has exceeded the critical value it remains too large for oscillations to be maintained, due to the long time-constant CR_g. Hence the oscillations die away.

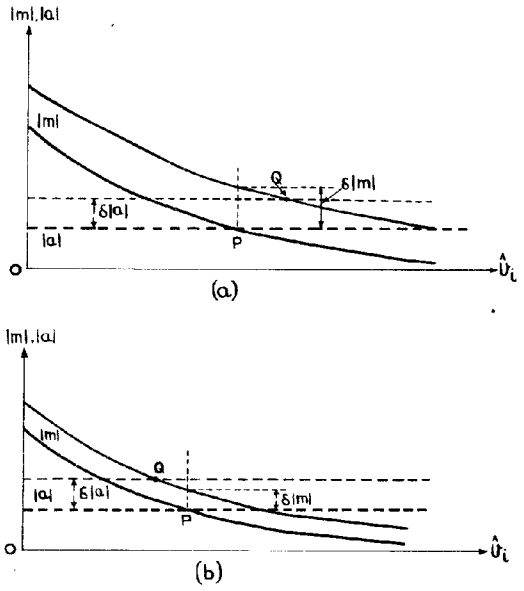

Fig. 456 - Effect of delay in build-up of bias.

In (b) $\delta|m| < \delta|a|$, so that the operating point Q is to the left of P. The amplitude of oscillations continues to build up with diminishing increases in bias, and the condition is stable, since each increase in bias makes $|a|$ increase with respect to $|m|$.

This is further illustrated in Fig. 457, where $|m|$ and $|a|$ are plotted against V_g for a fixed amplitude corresponding to the point P of Fig. 455. In the first figure (a) an increase in bias for a given amplitude leads to instability since $|a|$ becomes greater than $|m|$ and at the increased value of bias oscillations cannot be maintained. In (b), the increase in bias is accompanied by an increase in $|m|$ with respect to $|a|$, so that the amplitude is increased and the condition is stable.

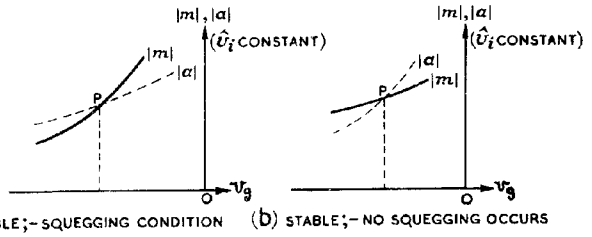

Fig. 457 - Squegging criteria.

The condition $\frac{\partial|m|}{\partial V_g} > \frac{\partial|a|}{\partial V_g}$ is the criterion for squegging to occur, under the conditions which have been assumed (long time-constants, sinusoidal oscillations, and $R_g \gg R_i$). This criterion depends on the relative values of $\hat{v}_i$, R_i, R_g, the cut-off voltage

$\hat{V}_c$ and the dynamic resistance of the tuned circuit. For a given $\hat{v}_i$ and V_c, and provided the dynamic resistance is not too large, squegging will occur if $\frac{R_g}{R_i}$ is sufficiently large.

Another method of making squegging more likely is to increase the damping of the tuned circuit. This causes the point P to occur at a steeper portion of the $|m| \sim \hat{v}_i$ curve (Fig. 456) and increases the likelihood of the point Q being to the right of P.

With triodes commonly used in low power radar oscillators employing high-Q circuits and Class C biasing, a grid leak of the order of 20 kΩ to 200 kΩ is usually sufficient to cause squegging.

Anode Self-Quenching Oscillators

In this form of self-quenching circuit the bias is held constant, but an effect similar to that of squegging is obtained by an automatic reduction in available HT potential. This reduces the angle of flow of grid current by shortening the grid base (Fig. 458(a)). A typical circuit is shown at (b). As in the grid self-quenching circuit, it is the value of the resistor R which is usually critical. If this is greater than a certain value quenching will ensue whatever the value of C. Pulse width is principally determined by the product of C and the mean DC resistance of the valve when conducting, whilst recurrence frequency depends chiefly on CR. The shape of the anode pulse is shown at (c).

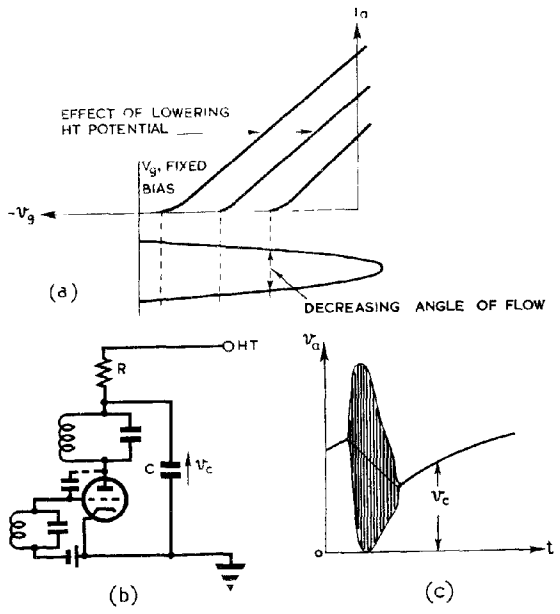

Fig. 458 - Anode self-quenching oscillator.

Anode self-quenching is normally employed as a protective device, rather than for regulating pulse width or recurrence frequency. Used in conjunction with grid self-quenching, the latter constituting the principal control, the anode network prevents damage to the valve should the grid circuit fail to prevent continuous oscillations.

48. The Super-Regenerative Receiver

Although the Super-Regenerative Receiver is more than an oscillator it is dealt with here since its operation depends on the build-up of oscillation in a modulated or quenched oscillator. The schematic arrangement of a separately-quenched circuit is shown in Fig. 459. (Self-quenched receivers are sometimes used in communications sets, but are not commonly used in radar and are not described here). Since the schematic arrangement resembles that of a modulated transmitter it is as well to indicate the essential differences between the two circuits. It is generally assumed that in a pulse-modulated transmitter the build-up and die-away intervals for each pulse are very much shorter than the pulse duration. When the oscillator is used in a super-regenerative receiver, on the other hand, feed-back conditions are so adjusted that in the absence of an applied signal the oscillations build up gradually and reach a maximum amplitude shortly before the end of the applied pulse; (Fig. 460). The oscillator is then quenched by the trailing edge of the modulation pulse and the oscillations die away rapidly.

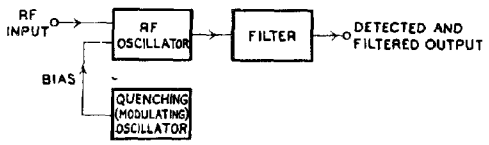

Fig. 459 - Schematic arrangement of super-regenerative receiver

The main difference between this action and that of the grid-modulated transmitter (Chap. 14) (or of the self-quenched oscillator described in Sec. 47) is that in the latter case the grid voltage rises sharply through cut-off so that the flow of valve current is sudden, initiating the main oscillation. In the case of the super-regenerative receiver, the applied pulse is less abrupt (being commonly sinusoidal) and the feed-back less vigorous, so that the random noise fluctuations in the input circuit, superimposed on the applied pulse, are largely effective in determining the initial grid voltages during each oscillation interval. When a signal of the correct frequency is applied to the input circuit the mean anode current is increased and a filter circuit in parallel with the anode load enables the increase in current to be detected as a negative-going pulse.

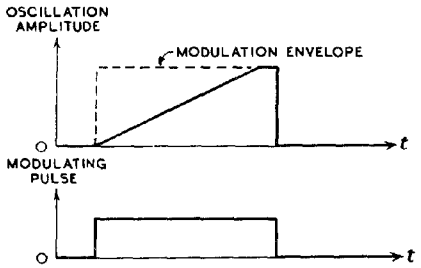

Fig. 460 - Build-up oscillations.

The effect of the super-regenerative circuit is that a given change of mean anode current can be produced by a very much smaller RF input signal than would be required, for example, by a reaction amplifier (Sec. 3, Fig. 385) used as an anode bend detector. Because of this a single valve stage used as a combined amplifier and detector in a super-regenerative circuit may provide an adequate output when the input signals are of the order of microvolts, whereas several hundred times this magnitude of signal would be required with a reaction amplifier-detector circuit.

The manner in which the much greater gain is obtained in the super-regenerative circuit may be explained with reference to the transformer-coupled circuit of Fig. 461. Suppose that the current and voltages in this circuit are zero when an EMF $v_i = \hat{v}_i \, \varepsilon^{j\omega t}$, is injected into the tuned circuit by the coupling loop. The equation giving the output voltage v_o may be shown to be

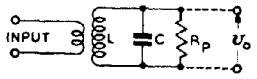

Fig.461 - Transformer-coupled tuned circuit.

$$\frac{d^2v_o}{dt^2} + \frac{1}{CR_p}\frac{dv_o}{dt} + \frac{v_o}{CL} = \frac{v_i}{CL} \quad \text{.....(1).}$$

The steady-state solution of this equation is the ordinary "AC solution", with $\hat{v}_o = Q\hat{v}_i$, where $Q = R_p\sqrt{\frac{C}{L}}$ (assumed large).

The manner in which the amplitude of the output voltage tends towards the steady state is illustrated in Fig. 462; the equation is:

$$\hat{v}_o = Q\hat{v}_i \left(1 - \varepsilon^{\frac{-t}{2CR_p}}\right) \quad \text{.....(2).}$$

Suppose now that the resistance R_p is replaced by the equivalent of a negative resistance, $-R_n$.

The solution of the corresponding equation:-

$$\frac{d^2v_o}{dt^2} - \frac{1}{CR_n}\frac{dv_o}{dt} + \frac{v_o}{CL} = \frac{v_i}{CL} \quad \text{.....(3),}$$

which is the same as (1) with $-R_n$ in place of R_p, is similar to that of the former equation, the amplitude growing according to the formula:

$$\hat{v}_o = Q\hat{v}_i \left(\varepsilon^{\frac{t}{2CR_n}} - 1\right); \quad \text{.....(4)}$$

(in this case $Q = R_n\sqrt{\frac{C}{L}}$).

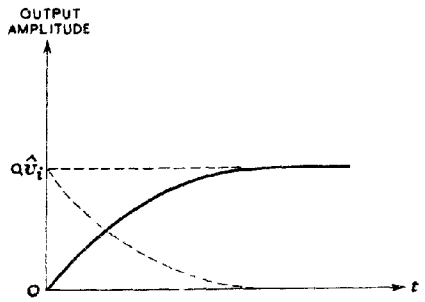

Fig. 462 - Build up of output voltage in transformer-coupled (non-oscillating) circuit.

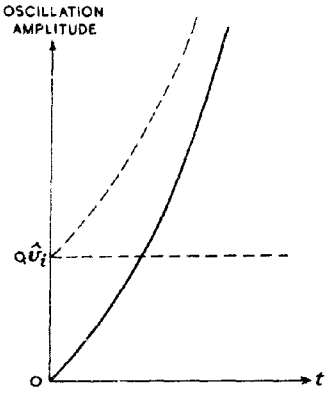

Fig. 463 - Build-up of oscillations in regenerative oscillating circuit.

This is illustrated in Fig. 463. Comparison of this figure with Fig. 462 shows that the former curve is the difference between the exponentially decreasing curve $Q\hat{v}_i\ \mathcal{E}^{\frac{-t}{2CR_p}}$ and $Q\hat{v}_i$, whereas the latter curve is the difference between $Q\hat{v}_i$ and the exponentially increasing curve $Q\hat{v}_i\ \mathcal{E}^{\frac{t}{2CR_n}}$.

If the amplitude of the applied signal is increased by an amount $\Delta\hat{v}_i$, the amplitudes of the curves of Figs. 462 and 463 are correspondingly increased. In the case of the regenerative (reaction) amplifier it is this increase in amplitude which provides the change in output current. In the super-regenerative circuit it is the time taken for the voltage v_e to reach a given amplitude which matters. When the oscillations have built up to a certain amplitude V_e the amplitude remains approximately constant at this value, due to the inherent non-linearity and limiting action of the valve characteristics, until the end of the modulation pulse. This cuts off the valve current, in effect replacing the resultant negative resistance by the natural damping resistance of the circuit, so that the oscillations are rapidly quenched. The whole process repeats with the next modulating pulse, by which time the RF input voltage will have changed in amplitude.

Consider the action during a single modulation pulse. The equation relating the time T for the oscillations to build up with V_e, the maximum amplitude, is

$$V_e = Q\hat{v}_i\ (\mathcal{E}^{\frac{T}{2CR_n}} - 1) \qquad \ldots\ldots\ldots\ldots\ldots\ldots\ldots\ldots(5).$$

Since we are concerned with values of T such that $\mathcal{E}^{\frac{T}{2CR_n}} \gg 1$, for RF voltages of small amplitude $\hat{v}_i$ this equation reduces to:

$$V_e \doteq Q\hat{v}_i\ \mathcal{E}^{\frac{T}{2CR_n}} \qquad \ldots\ldots\ldots\ldots\ldots\ldots\ldots\ldots(6).$$

If $\hat{v}_c$ is the amplitude of the carrier wave modulated by $(1 + A\cos\omega_m t)$, we have

$$\hat{v}_i = \hat{v}_c\ (1 + A\cos\omega_m t);$$

so that

$$\frac{T}{2CR_n} \doteq \log_{\mathcal{E}} V_e - \log_{\mathcal{E}} Q - \log_{\mathcal{E}} \hat{v}_c - \log_{\mathcal{E}}(1 + A\cos\omega_m t)$$
$$\ldots\ldots\ldots(8).$$

Since, for a given carrier level, the only quantity which varies in (8) is t, we have

$$\Delta T \doteq -2CR_n\ \Delta\left\{\log_{\mathcal{E}}\ (1 + A\cos\omega_m t)\right\} \qquad \ldots\ldots\ldots\ldots(9),$$

and this is independent of $\hat{v}_c$.

This decrease is illustrated in Fig. 464. t_p is the

duration of the modulating pulse. The two curves are identical except for the horizontal displacement ΔT. Hence, to a first approximation the average increase in amplitude of V_o due to the increase in the amplitude-modulated input is

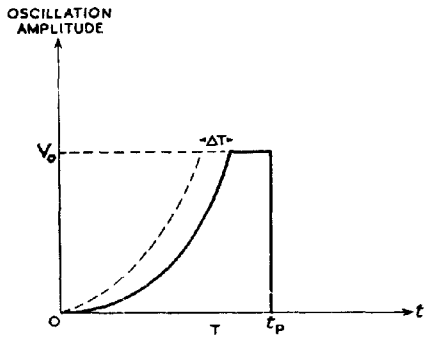

Fig. 464 - Decrease in time taken for oscillations to acquire a given amplitude (small signals).

$$\frac{\Delta T}{t_p} \quad V_e \ ;$$

i.e.

$$\frac{V_e}{t_p} \cdot 2CR_n \ \Delta \left\{ \ \log_\varepsilon (1 + A \cos\omega_m t) \right\} \quad \text{.....(10).}$$

We shall compare this with the increase for a reaction amplifier, given by

$$Q\hat{v}_c \cdot \Delta \left\{1 + A \cos\omega_m t\right\} \quad \text{.....(11).}$$

Suppose the input changes from its maximum value $\hat{v}_c (1 + A)$ to its minimum value $\hat{v}_c (1 - A)$. For the reaction amplifier equation (11) gives

$$\Delta \hat{v}_e = Q\hat{v}_c \left\{1 + A - \overline{1 - A} \right\} = 2AQ\hat{v}_c \ .$$

For the super-regenerative circuit the change in mean amplitude for the pulse interval t_p is given by equation (10):-

$$\frac{V_e \Delta T}{t_p} \doteq \frac{V_e \, 2CR_n}{t_p} \left\{\log_\varepsilon (1 + A) - \log_\varepsilon (1 - A)\right\}$$

$$\doteq \frac{2V_e CR_n}{t_p} \log_\varepsilon \left\{ \frac{1 + A}{1 - A} \right\}.$$

Provided A is small,

$$\log_\varepsilon \left(\frac{1 + A}{1 - A}\right) \doteq 2A.$$

Hence, for a lightly modulated carrier, the ratio between the change in mean amplitude in the super-regenerative circuit to the corresponding change in mean amplitude in the reaction-amplifier circuit is given approximately by:-

$$\frac{2V_o CR_n}{t_p} \cdot \frac{2A}{2AQ\hat{v}_o} = \frac{2V_o CR_n}{Q\hat{v}_c t_p}.$$

Since $Q = \omega_o CR_p$, this may be written

$$\frac{2V_o CR_n}{\hat{v}_c CR_p \omega_o t_p} = \frac{2 V_o R_n}{\omega_o t_p \hat{v}_c R_p}.$$

Suppose $t_p = 1\mu s$, $\omega_o = 2\pi\ 200.\ 10^6$ (corresponding to a frequency of 200 Mc/s); $V_o = 10$ volts and $\hat{v}_c = 10$ microvolts. Suppose also that $R_n = R_p$.

Then the ratio becomes

$$\frac{2.10}{2\pi.200.10^6.10^{-6}.10.10^{-6}} = \frac{10^6}{200\pi} \doteq 1690.$$

This ratio does not take into account the fact that the super-regenerative detector is operating for only a fraction of the quench period. However, even if the pulses fill only one-tenth of the reception time there is still an increase of more than 150:1 in the effective amplification provided by the super-regenerative circuit compared with the reaction amplifier.

The above simplified analysis has considered the action from the point of view of a sinusoidally modulated carrier -- the communications aspect. In radar, where RF pulses are received, a somewhat different approach is simpler. Here we are concerned with the amplitude of the actual output pulses, and not with any modulation component of these; and the result found to be approximately true for a sinusoidally modulated carrier, namely, that the amplitude of the modulation component is independent of the carrier amplitude, no longer applies. There is still however, an inherent AGC action, independent of this result. If the amplitude of the RF input is large, the approximation of equation (6) no longer holds, and the change in the rate of increase of oscillation amplitude following an increase in input amplitude is as shown in Fig. 465, rather than that shown in Fig. 464 for small signals. As the amplitude of the applied signal increases the increase in the mean amplitude of the output voltage does not increase proportionately, but is obviously limited. There is a maximum possible increase in the area under the modulation envelope of Fig. 460, occurring in theory when the envelope is entirely filled with RF oscillations. The result is that the super-regenerative receiver can detect, without ever overloading, signals varying in amplitude from a few microvolts to several volts.

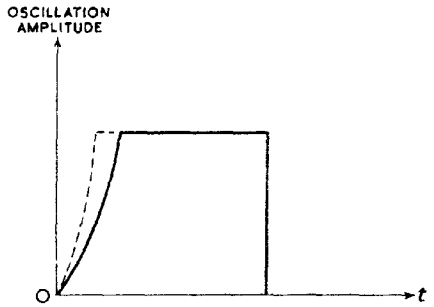

Fig. 465 - Decrease in time taken for oscillations to acquire a given amplitude (large signals).

When used for communications reception the region of variation of input amplitude over which distortion is not prohibitive is limited, and varies with the modulation depth. For radar purposes, where this type of circuit is used as a one-valve receiver for triggering radar beacons, distortion is not important. The output is of sufficient amplitude, even for very small input signals, to trigger a local transmitter, and because of the inherent AGC action no deleterious effects arise when much larger input signals are received. However, additional AGC circuits may be employed with advantage to limit the amplitude of the triggering pulse applied to the transmitter and to prevent valve saturation when very large signals are received.

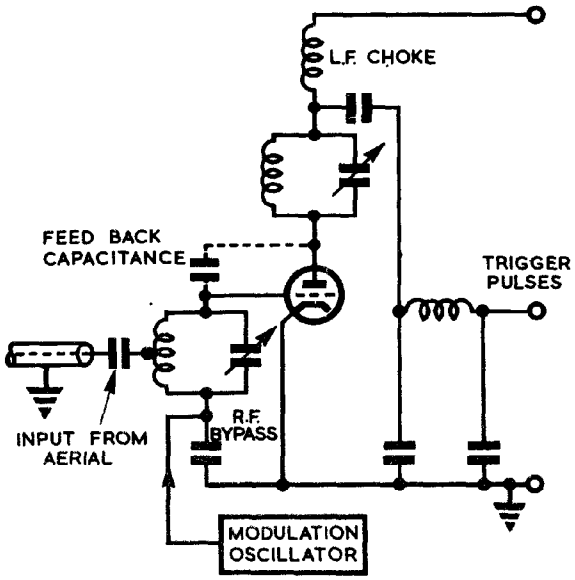

Fig. 466 - Typical radar super-regenerative circuit.

A typical arrangement of a super-regenerative receiver designed for RF pulse detection is shown in Fig. 466. The low-pass filter in the output side by-passes the fundamental and harmonic components of the quench frequency so that there is a constant steady voltage produced at the output terminals when no RF signal is applied to the grid. There is an inevitable noise fluctuation present. The width of the modulation pulse is made small and the quench frequency sufficiently high to ensure that several quench periods occur during a single input RF pulse.

When this arrives at the grid a negative-going pulse is produced at the output, slightly delayed by the filter circuit. This pulse is amplified and is used for triggering the local transmitter of a radar beacon.

AUTOMATIC FREQUENCY CONTROL

49. General

Like most automatic control systems, circuits which control the frequency of an oscillator are of the servo type (see Chap. 18). The frequency of oscillation is compared with some frequency standard in a suitable difference element, the output of which is used to adjust the oscillator so as to reduce the frequency

difference to zero.

The simplest requirement, namely to lock the oscillator frequency to that of an available transmitter or standard generator will not be dealt with here. In effect this converts the oscillator into an amplifier by increasing the coupling between the two generators. The more important practical requirement is to make automatic adjustments to the frequency of the local oscillator of a superheterodyne receiver so that the signal in the IF channel is kept in the middle of the preset IF band. This is necessary to prevent distortion and loss of signal strength. It is immaterial whether the changes in frequency are due to changes at the transmitter, which is more likely, or at the local oscillator. In either case, when such variations are detected, adjustments are made to the local oscillator to bring the IF signal back into the middle of the band.

The input quantity of the control system is therefore the setting of the IF tuned circuits, and the servo action is required to pull-in the IF signal by adjustments to the local oscillator. This may be done in the case of mechanically tuned oscillators by a servo motor turning the vanes of a variable condenser, altering the position of a tuning core or, in the case of a klystron, adjusting the tuning screws or diaphragm. Alternatively, if the frequency can be varied by altering one of the control voltages, such as the reflector potential of a Sutton tube, the motor can be dispensed with. In either case the chief problem in design is afforded by the difference element, usually called the Discriminator. This is required to convert a frequency difference into a voltage or current, indicative not only of the magnitude of the difference but also of the sense. Apart from the discriminator the remainder of the circuits involve nothing peculiar in servo construction.

50. The Discriminator

Two types of discriminator are employed, using amplitude and phase discrimination respectively. These are illustrated in Fig. 467. f_m is the mean intermediate frequency to which f_i, the IF signal frequency is to be aligned.

In both cases the reception of RF pulses within the bandwidth of the radio receiver develops corresponding pulses in the output of the discriminator which are either positive-going or negative-going according to whether the IF signal frequency is too high or too low. These pulses may either be rectified and applied as steady control voltages to the local oscillator or, as is more general, they may be incorporated with some automatic sweep circuit as described in Secs. 53 and 54.

51. Amplitude discrimination

In this method use is made of the variation in amplitude of the output from a high-Q circuit as the input frequency recedes from resonance. The circuit is tuned to $f_m \pm f_d$ where f_d is the maximum deviation allowed for. As f_i varies, so the output amplitude varies as indicated by the resonance curve (Fig. 467) and the detected output is thus indicative of the input frequency.

One method of incorporating this technique in a practical discriminator is shown in Fig. 468. Two high-Q rejector circuits, coupled to one of the IF stages, are tuned to $f_m + f_d$ and $f_m - f_d$ respectively. The output from each circuit is detected by the back-to-back diode circuits shown, and the voltage difference

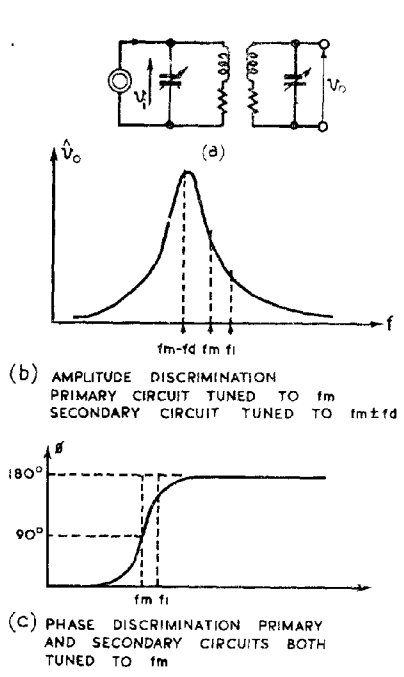

Fig. 467 - Fundamental principles of amplitude and phase discrimination.

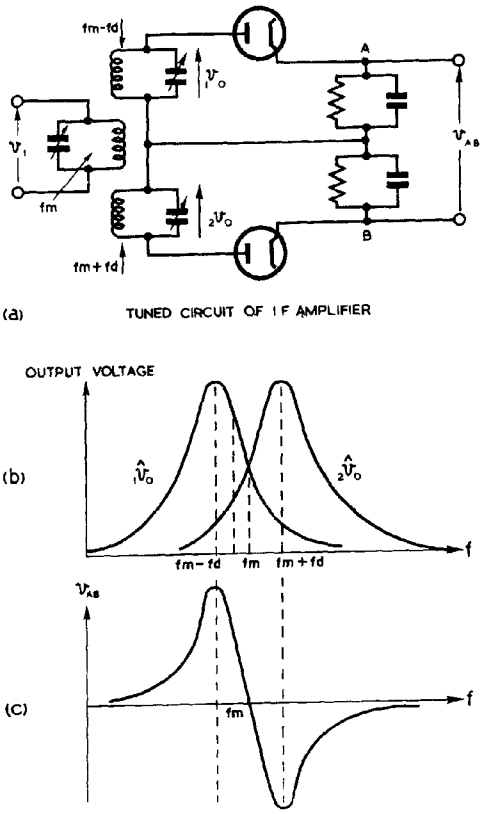

Fig. 468 - Amplitude discriminating circuit and response diagrams.

between A and B is indicative of the magnitude and sense of the error frequency $f_i - f_m$. The response diagrams for the two circuits are shown superimposed at (b). The detected output difference (c) is amplified if necessary and fed to the servo motor or other control device. This alters the frequency of the local oscillator so as to reduce the magnitude of the error.

52. Phase discrimination

As the title indicates, in this method it is the variation in the phase of the output of a tuned circuit as the input frequency varies which is used to provide the necessary frequency discrimination. It is necessary to compare this with a standard phase, normally the phase of the input. In the simple inductively coupled circuit shown in Fig. 467(a) the output and input voltages are in quadrature at resonance, the output phase being retarded as the frequency rises. If input and output signals are added together this change in phase is converted into a change in amplitude, as indicated by the vector diagrams of Fig. 469.

The resultant signal is detected and the magnitude of the rectified signal, varying with the input frequency, provides the discriminator output.

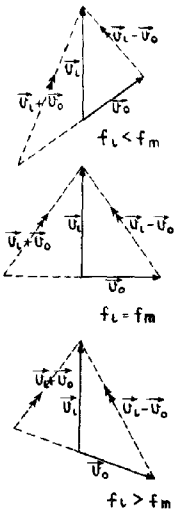

Fig. 469 - Phase discrimination: vector diagram.

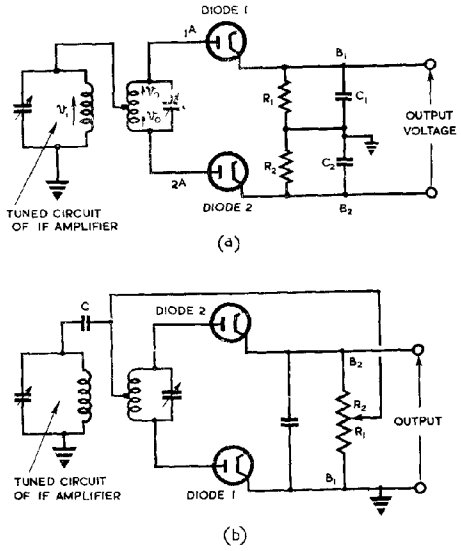

Fig. 470 - Phase discriminating circuits.

The simplified diagram of Fig. 470(a) shows how this method may be employed in a phase discriminator. v_i is the input voltage and v_e the voltage developed across each half of the secondary coil. As $_1A$ swings positive the RF potential $v_i + v_e$ is developed across diode 1 and it conducts, charging C_1 to a peak value $(v_i \hat{+} v_e)$. Similarly diode 2 conducts as $_2A$ swings positive so that C_2 charges to a peak value $(v_i \hat{-} v_e)$. R_1 and R_2 are the discharge resistors for the two condensers. The potential difference between B_1 and B_2 is $(v_1 \hat{+} v_e) - (v_1 \hat{-} v_e)$. In the circuit shown this is not usually in a convenient form for use as a control voltage, neither B_1 nor B_2 being earthed.

A practical form of this circuit is shown in Fig. 470(b). Here the coupling capacitance C takes the place of one of the rectifying condensers and the other is connected between the two cathodes. The direct connection from C to the junction of the resistors is necessary to discharge C through R_1 when diode 1 is not conducting. Also, if a variable potentiometer is substituted for the two resistors, this connection forms a convenient set-zero adjustment.

As in the simplified circuit, the output is developed across B_1B_2, and since B_1 is earthed this is in a convenient form to act as a control voltage, either direct or through a DC amplifier.

53. Automatic Sweep Circuit

Either of the methods described is restricted because of the narrow bandwidth of the high-Q circuits used. The twin-circuit method of amplitude discrimination gives a wider band, but this is compensated for by the relative intricacy of setting up the circuit. Unless the oscillator frequency is very close to its required value, the IF signal is outside the discriminator bandwidth and the AFC circuit fails to "pull-in". The difficulty is usually overcome by incorporating an automatic frequency sweep circuit in the control system. While there is no signal in the RF receiver the local oscillator frequency is swept continuously through a wide band.

When a signal does appear, the AFC circuit comes into operation as the oscillator frequency reaches its correct setting, and thereafter the latter is automatically adjusted and the sweep practically eliminated.

A circuit incorporating a phase discriminator and a low frequency sweep generator is illustrated in Fig. 471. The output from the sweep generator following the multivibrator is approximately sinusoidal. While there is no RF signal the anode voltage of the amplifier remains constant and the full sweep voltage is used to alter the Sutton tube frequency by varying its reflector potential.

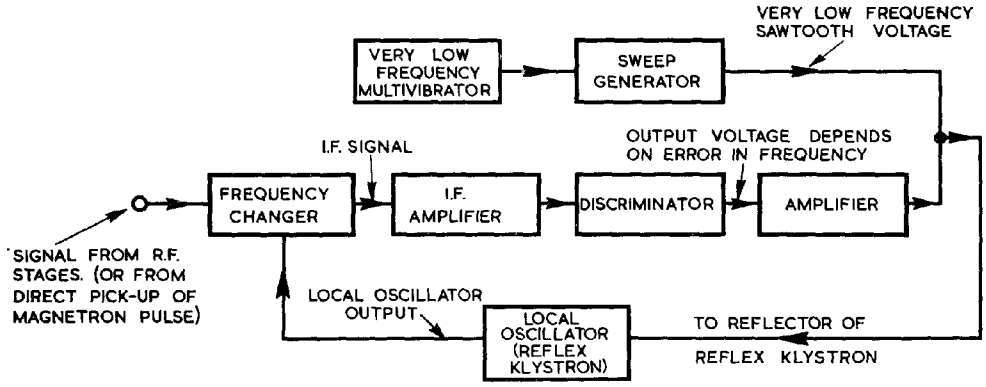

Fig. 471 - Circuit schematic for AFC of electrically tuned local oscillator.

When an RF signal appears the discriminator is brought into play and its amplified output nullifies the output from the sweep generator so that the reflector of the Sutton tube is maintained at an approximately constant potential. If the discriminator is sufficiently sensitive and the gain of the amplifier sufficiently large, only a very small frequency deviation is necessary to produce at the amplifier output sufficient amplitude to counteract the sweep voltage.

This method of searching for and locking onto a received signal is applicable to other local oscillator circuits in which variation of the potential of one of the control electrodes provides a sufficient degree of variation in the oscillation frequency.

54. Practical AFC circuits

Many different AFC circuits are in common use, most of which incorporate the principles of the foregoing paragraphs, differing only in the manner in which these principles are applied. A great

variety of automatic sweep circuits are available, some of which are much more economical of material than the relatively straightforward circuit shown in Fig. 471.

It is common practice to apply the positive-going or negative-going pulses from the discriminator to the sweep generator so that it is held inoperative, automatically providing the correct output voltage for the local oscillator reflector. This usually necessitates suppressing either the positive-going or the negative-going pulses, so that adjustments to pull in the oscillator frequency are made for frequency drifts in one direction only. For example when the discriminator output is weak, or consists of negative-going pulses, the sweep generator may continue to sweep the oscillator throughout a wide frequency range. When the discriminator output changes to a series of positive-going pulses the sweep generator is suppressed and the oscillator frequency automatically pulls in. Should the transmitter frequency drift so that negative-going pulses reappear in the discriminator output the AFC circuit fails to pull in, and the sweep generator comes into operation again until the discriminator output changes polarity. This mode of operation is particularly useful where economy of valve stages is important.

This file was downloaded
from the RTFM Library:

Link: www.scottbouch.com/rtfm

Please see site for usage terms,
and more aircraft documents.